1-1-1998

Isolation and characterization of a common nuclear matrix protein and other studies

Tracy Sue Schwab

ISOLATION AND CHARACTERIZATION OF A COMMON NUCLEAR MATRIX PROTEIN AND OTHER STUDIES

by

TRACY SUE SCHWAB

DISSERTATION

Submitted to the Graduate School

of Wayne State University,

Detroit, Michigan
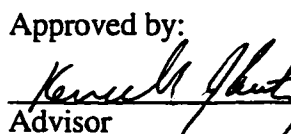
in partial fulfillment of the requirements
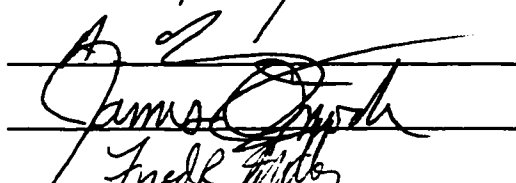
for the degree of

DOCTOR OF PHILOSOPHY

1998

MAJOR: CANCER BIOLOGY

Approved by:

_____ 7/2/98
Advisor   Date

Acknowledgements

I am forever grateful for the help and guidance of many individuals during my thesis work. First, my thesis advisor, Dr. Kenneth J. Pienta, who welcomed me into his laboratory as a graduate student. His constant support and encouragement during this time allowed me to continue and eventually finish my thesis. Secondly, I wish to thank Dr. Robert H. Getzenberg at The University of Pittsburgh for his time, support, and suggestions during my work. Thirdly, I would like to thank several members of my laboratory who contributed to my thesis work: Martha M. Quigley for her technical support of the two-dimensional gels and the initial screening of the libraries, Jeffrey E. Lehr for his technical work on the dual fluorescence studies, and Dr. Eric D. Schwab for his constant support in various aspects of my thesis work. I also wish to thank my family and friends for their constant support—especially my husband Eric who was continually by my side and offered any support that was necessary. Lastly, I wish to thank my members of my thesis committee: Dr. Samuel Brooks, Dr. Fred Miller, Dr. James Onoda, and Dr. A. Raz.

Table of Contents

List of Tables

List of Figures

Chapter Four

Chapter Six

Chapter One

Nuclear Matrix Proteins

Introduction

The mammalian nucleus contains approximately two centimeters of DNA which is packed into a nucleus that is ten microns in diameter. The packaging of DNA into the nucleus is organized by the nuclear matrix, the RNA-protein skeleton of the nucleus. The nuclear matrix is the scaffold that organizes DNA at a structural and functional level (Pienta et al., 1993A). By organizing DNA in both structural and functional manners, the nuclear matrix plays a critical role in normal cellular function. Several reports have demonstrated that the nuclear matrix is altered in cancer cells and is intimately involved in the function of several oncogenes. Defining how the nuclear matrix is involved in the process of cell transformation has implications not only for understanding malignancy but also for the development of new biomarkers for diagnosis and prognosis.

The concept of a residual nuclear structure, composed predominantly of protein, was proposed in 1942 by Mayer and Gulick when they noticed an insoluble protein which remained after extracting nuclei with high sodium chloride concentrations (Mayer and Gulick, 1942). In 1963, Smetana *et al.* reported the presence of a ribonucleoprotein network of fibers in nuclei after a series of extractions of soluble proteins and deoxy-ribo-nucleoproteins from Walker tumor and rat liver cells (Smetana et al., 1963). Eleven years later, the identification of a nuclear protein matrix was reported by Berezney and Coffey who used a variety of extractions of rat liver nuclei to remove the major components of the nucleus (Berezney and Coffey, 1974). Successive extractions using detergent and salt solutions were used to remove lipids, soluble proteins, intermediate filaments, DNA, and most of the RNA. The extractions revealed a non-chromatin framework that extended throughout the nucleus. Upon chemical analysis, it was found that the nuclear matrix contained 98.2% protein, 0.1% DNA, 0.5% phospholipid, and 1.2 % RNA (Berezney and

Coffey, 1974). A later report from the same laboratory stated that the structural components of the isolated matrix bear remarkable resemblance to well-defined structures of intact nuclei, suggesting the nuclear matrix network is not an artifact of the extraction and enzyme treatments (Berezney and Coffey, 1977). Berezney and Coffey went on to suggest that the nuclear matrix is a dynamically changing structure and therefore may play important roles in nuclear functions.

The nuclear matrix is defined as the RNA-protein skeleton of the nucleus which contributes to the structural and functional organization of DNA. In the last several decades, there has been a great deal of insight into the central role the nuclear matrix plays in cell biology. Five of the general functions of the nuclear matrix are listed in Table 1. They include nuclear morphology and regulation, DNA organization and replication, RNA synthesis and transport, and nuclear regulation.

Table 1.   Reported functions of the nuclear matrix

Function	Explanation
Nuclear morphology	The nuclear matrix contains structural elements of the pore complexes, lamina, internal network, and nucleoli which give the nucleus its overall 3-dimensional organization and shape.
DNA organization	DNA loop domains are attached to nuclear matrix at their bases and this organization is maintained during both interphase and metaphase. Nuclear matrix shares some proteins with the chromosome scaffold including topoisomerase II, an enzyme which modulates DNA topology.
DNA replication	The nuclear matrix has fixed sites for DNA replication and contains the replisome complex for DNA replication.
RNA synthesis	Actively transcribed genes are associated with the nuclear matrix. The nuclear matrix contains transcriptional complexes, newly synthesized heterogeneous nuclear RNA, and small nuclear RNA. RNA processing intermediates are bound to the nuclear matrix.
Nuclear regulation	The nuclear matrix has specific sites for steroid hormone receptor binding. DNA viruses are synthesized in association with the matrix. The nuclear matrix is a cellular target for transformation proteins, some retrovirus products like the large T antigen, and E1A protein. Many of the nuclear matrix proteins are phosphorylated at specific times in the cell cycle.

Nuclear shape is thought to reflect internal nuclear structures and processes and is determined, at least in part, by the nuclear matrix. The nuclear matrix contains structural

elements of the pore complexes, lamina, internal network, and nucleoli that give the nucleus its overall three-dimensional organization and shape. The lamina forms the periphery of the matrix while the nuclear matrix extends inward from the lamina (Hancock and Boulikas, 1982). The nucleolus, which is composed of RNA and proteins, is responsible for RNA synthesis and processing of pre-ribosomal RNA within the cell and assembly of ribosomal proteins (Verheijen et al., 1988). However, how the nuclear matrix is involved in the organization of DNA was largely unexplored. It is now known that chromosomes are not free floating in the nucleus but instead have a specific three-dimensional spatial organization, hence, emphasis turned to the role of the nuclear matrix in DNA organization. Vogelstein *et al.* were the first to visualize DNA loop structures attached to the nuclear matrix by releasing the normally supercoiled loops of DNA in the presence of a low concentration of ethidium bromide (Vogelstein et al., 1980). Using fluorescence microscopy, 3T3 nuclei, devoid of soluble proteins and histones, were placed in various concentrations of ethidium bromide and viewed. A halo, representing DNA intercalated with ethidium bromide, was seen surrounding the nuclear matrix skeleton. Intercalation of low concentrations of ethidium bromide into DNA caused positive supercoiling which was manifested as an enlargement of the halo. At higher concentrations of ethidium bromide, the DNA continued to supercoil which was represented by a decrease in halo size. Nicking the DNA resulted in uniform halos regardless of the concentration of the ethidium bromide used. The results of this study implicated DNA loop domains as an important component of DNA organization. It is now recognized that DNA is organized into functional loop domains of approximately 60 kilobases and that these loops are attached at their bases to the nuclear matrix. The points of attachments of DNA sequences to the matrix have been studied and are termed matrix attachment regions (MARs) or scaffold attachment regions (SARs) (Ludérus et al., 1992). The MARs generally contain AT-rich DNA sequences, as well as sequences that are similar to topoisomerase II consensus sequences (Hakes and Berezney et al., 1991). To date, no conserved consensus sequences are known for MARs. MARs, however, have been found to be closely

associated with actively transcribed genes and thus may control their expression. Romig *et all.* identified four novel DNA binding proteins that specifically bind to MARs (Romig et al., 1992). One of which (SAF-A) was found to specifically bind to several MAR elements from different species. Other MARs have been purified and functionally characterized that bind lamins A and C (Hakes and Berezney, 1991). Dickinson *et al* . cloned a DNA-binding protein that binds to MARs called SATB1 (Dickinson et al., 1992). SATB1 appears to recognize a particular type of AT-rich sequence in the minor groove of DNA. Most recently, Durfee *et al* . have isolated a 84-kD nuclear matrix protein (p84) that localizes to an area in the nucleus associated with RNA processing (Durfee et al., 1994). In particular, p84 was found to specifically interact with the amino-terminal region of the retinoblastoma susceptibility gene.

The nuclear matrix has also been implicated in the replication of DNA. Vogelstein *et al.* demonstrated the rate of movement of newly synthesized DNA by autoradiography using ^{3}H-thymidine (Vogelstein et al., 1980). Using pulse-chase experiments, Pardoll *et al.* provided further evidence that the nuclear matrix provides fixed sites for the attachment of replication complexes (Pardoll et al., 1980). These investigators demonstrated that after short pulses with ^{3} H-thymidine given to rats, the matrix DNA had a very high specific activity when compared to the total DNA. This indicated that newly synthesized DNA is associated with the nuclear matrix, which had been shown by other investigators (Van der Velden et al., 1984). Berezney and Coffey also reported that DNA which was labeled rapidly during DNA synthesis appeared to be associated with the nuclear matrix (Berezney and Coffey, 1975). These replication sites which contain the enzymes needed to duplicate DNA were named "replicases" by Reddy and Pardee (Reddy and Pardee, 1980). Earnshaw and Heck demonstrated that topoisomerase II, an enzyme known to regulate DNA topology, is also a component of the DNA loops in mitotic chromosomes and is associated with the nuclear matrix (Earnshaw and Heck, 1985). Berezney and Buchholtz provided further evidence to support the role of the nuclear matrix in eukaryotic DNA

replication by examining the process of replication of DNA which occurs discontinuously in subunits on chromosomal DNA called replicons (Berezney and Buchholtz, 1981). They proposed that DNA replication complexes remain bound to the nuclear matrix while DNA is reeled through during replication. Further evidence came from Valenzuela et al. when HeLa nuclei were shown to have an enrichment of replication forks (i.e., branched DNA) associated with the nuclear matrix (Valenzuela et al., 1983). Tubo et al. demonstrated that nuclear matrix prepared from labeled nuclei was associated with the DNA (Tubo et al., 1985). In addition, Younghusband observed that the nuclear matrix is the site of adenovirus DNA replication in infected HeLa cells (Younghusband, 1985), while Smith and Berezney reported a significant portion of DNA polymerase α bound to isolated nuclear matrices during active replication in regenerating liver cells (Smith and Berezney, 1980).

The nuclear matrix has also been implicated in transcription. The nuclear matrix consists not only of protein, but also RNA which was shown to be an essential component (Nickerson et al., 1989). Herlan et al. found that labeled RNAs associated tightly with the nuclear matrix, and the majority of the RNA included in the RNA-protein matrix consisted of pre-rRNA (Herlan et al., 1979). Small nuclear RNAs complexed with proteins (snRNP) have also been localized to the nuclear matrix (Nakayasu et al., 1982). Heterogeneous nuclear RNA (hnRNA), which is the precursor to messenger RNA, was shown to be associated with the nuclear skeleton after the removal of most of the chromatin, suggesting that the hnRNA is associated with nonchromatin structures within the nucleus (Herman et al., 1978). This association was shown to be specific when labeled hnRNA was added to isolated nuclei and very little hnRNA became associated with the nuclear structure of both intact and chromatin-depleted nuclei (Herman et al., 1978; Miller et al., 1978). Van Eekelen and Van Venrooij reported a specific set of proteins that were associated with the hnRNA and nuclear matrix complex and concluded that proteins are involved in the binding of hnRNA to the nuclear matrix (Van Eekelen and Van Venrooij,

1982). This association of hnRNA to the nuclear matrix led to the idea that the nuclear matrix may play a role in transcription. Further evidence came when it was shown that all precursors of RNA were found to be exclusively associated with chick oviduct nuclear matrix, supporting the notion that the nuclear matrix may be the structural site for RNA processing (Ciejek et al., 1982). In a series of experiments using HeLa nuclei, Jackson *et al.* demonstrated that RNA is synthesized at the nuclear cage (i.e., nuclear matrix) (Jackson et al., 1981). They observed, along with prior investigators, that RNA is attached in a specific manner to the nuclear matrix (Jackson et al., 1981; Cook et al., 1982). In addition, transcribed sequences were found to be closely associated with the nuclear cage. This latter observation has been demonstrated in active viral genes using nine cell lines transformed with viral sequences of polyoma and/or avian sarcoma virus (Cook et al. 1982). Using HeLa cells infected with adenovirus type 2, Marimam *et al..* provided additional evidence that adenoviral-specific nuclear matrix RNA contains precursors, intermediates, and products of RNA processing (Marimam et al., 1982). Other investigators have reported similar results (Long and Ochs, 1983A; Long and Schrier, 1983B; Ben-Zeev and Aloni, 1983). Smith *et al.*, using a previously-isolated rat liver nuclear matrix protein and its corresponding antibody, provided evidence that the nuclear matrix plays a role in RNA splicing *in vitro* (Smith et al., 1989). In addition, Buckler-White *et al.* isolated nuclear matrix from mouse 3T3 cells infected with polyoma virus and showed there is a fixed number of sites for T antigen on the matrix (Buckler-White et al., 1980). Additional evidence for the interaction of the nuclear matrix with transcriptionally active genes came from studies involving the chick oviduct (Robinson et al., 1983; Ciejek et al., 1983), SV40-infected cells (Abulafia et al., 1984), chicken liver (Jost and Seldran, 1984), and chicken erythrocytes (Hentzen et al., 1984). Bidwell *et al.* examined nuclear matrix DNA-binding proteins that interacted with the osteocalcin gene promoter (Bidwell et al., 1993). Lastly, transcription factors have been reported to be localized to the nuclear matrix (Merriman et al., 1995; Nardozza et al., 1996; Kim et al., 1996;). All of these studies are consistent with the involvement of the nuclear matrix in gene transcription.

From the above studies, it is easy to see why it was proposed that the nuclear matrix is involved in gene regulation and expression. Gene expression can best be demonstrated by steroid hormones, which are thought to be involved in the transcriptional control of some genes. Barrack and Coffey used the induction of vitellogenin synthesis, which is a well characterized model used in studying the regulation of specific gene expression by steroid hormones (Barrack and Coffey, 1980). They found nuclear matrix of an estrogen-responsive tissue (chicken liver) and of an androgen target tissue (rat ventral prostate) contained specific binding sites for both estradiol and dihydroxytestosterone, respectively. In addition, the levels of these matrix-associated steroid binding sites vary in response to changes of the hormonal status of the animal. In a later study, Barrack demonstrated the presence of specific acceptors for the androgen receptor in nuclear matrix of the prostate (Barrack, 1983). In addition, the majority of these acceptors were found in the internal network components of the matrix while only 17% were found to be in the peripheral lamina. Kumara-Siri *et al.* reported that the T$_3$-nuclear receptor is associated with the nuclear matrix suggesting that this association may help to regulate thyroid hormone action (Kumara-Siri et al., 1986). Since the nuclear matrix plays crucial roles in the normal cell, it seems obvious to conclude that the nuclear matrix may play a role in the development of cancer, perhaps as the result of protein alterations during transformation. Several laboratories, therefore, have undertaken the task to identify and characterize specific nuclear matrix proteins from various cell lines and tissues. To date, there have been few nuclear matrix proteins that have been characterized and their possible functions investigated. Several of these have been previously mentioned. Numatrin, a nuclear matrix protein that was first identified when stimulation of B lymphocytes with various mitogens was associated with a predominant increase in the synthesis of this protein (Feuerstein and Mond, 1987). Later studies revealed numatrin might play a role in early transduction of mitogenic signals at the G1 phase of the cell cycle (Feuerstein et al., 1988) and in DNA associated processes (Feuerstein et al., 1990). NuMA, another characterized nuclear matrix protein, was found to be associated with the spindle poles during mitosis,

suggesting that NuMA may play a role in nuclear reorganization during division (Lydersen and Pettijohn, 1980; Compton et al., 1992; Saredi et al., 1996). Other laboratories have specifically characterized nuclear matrix proteins that are cancer specific (i.e., only found in cancer and not in normal tissues or cells). Such cancer specific nuclear matrix proteins, which will be discussed in later chapters, may be utilized in the clinical diagnosis and prognosis of cancer.

My thesis work primarily focused on studies involving differential expression of nuclear matrix proteins. Chapter two investigates the changes in nuclear matrix protein expression when prostate cells are injected into various organ sites within the rat. Chapter three examines alterations in nuclear matrix expression among various human lung cancer cell lines. Chapter four details the identification and characterization of several nuclear matrix proteins that were found to be common in breast tissue and in various cell lines while chapter five encompasses a broad discussion of all of the nuclear matrix protein chapters. Lastly, chapter six describes the multidrug resistance analysis of human and rat prostate cancer cell lines in addition to the development of several multidrug resistant rat prostate cancer cell lines that was undertaken as a separate project during my thesis tenure.

Chapter Two

The Effect of Organ Site on Nuclear Matrix Protein Composition

Introduction

Cells require an extensive series of networks that enable the cell to grow and survive in its particular environment. The structures and functions of a cell are dependent on a cell matrix system which extends from the cell periphery to the DNA (Getzenberg et al., 1990). Electron micrographs provided the experimental evidence of a cellular matrix system which clearly demonstrated the linkages of the cellular periphery, cytoskeleton, and the nuclear matrix (Fey et al., 1984). Figure 1 is an electron micrograph demonstrating the cell matrix system showing the linkages of the cytoskeleton components from the cell periphery to the nuclear matrix. The system of networks do not end at the border of the cell, but continue into the surrounding milieu. How cells respond to their environment, therefore, can be explained by the tissue matrix system which involves the linkages of the cell matrix to the extracellular matrix (ECM) (Getzenberg et al., 1990). Extracellular signals within the ECM, when exposed to the appropriate receptor(s) on a cell membrane, can transverse into the cytoplasm and/or nucleus by utilizing these matrix networks. Therefore, what a cell touches (i.e., ECM) helps determine what the cell will do.

Several studies demonstrate that the ECM can alter cell morphology and affect DNA synthesis and gene expression (Hay, 1977; Ben-Zeev, 1980; Wittelsberger et al., 1981; Ingber, 1980; Pienta and Coffey, 1991). Gospodarowicz *et al.* reported that the regulation of the shape of a cell, when grown on different substrata, dictates its response to different mitogenic hormones (Gospodarowicz et al., 1978). Folkman and Moscona also demonstrated that cell shape could be manipulated by altering the tissue culture plastic adhesivity upon which the cells were grown (Folkman and Moscona, 1978). Later

9

experiments revealed that DNA synthesis is also regulated by cell shape and that DNA

metabolism appears to be linked with the physical expansion of the cell and nucleus
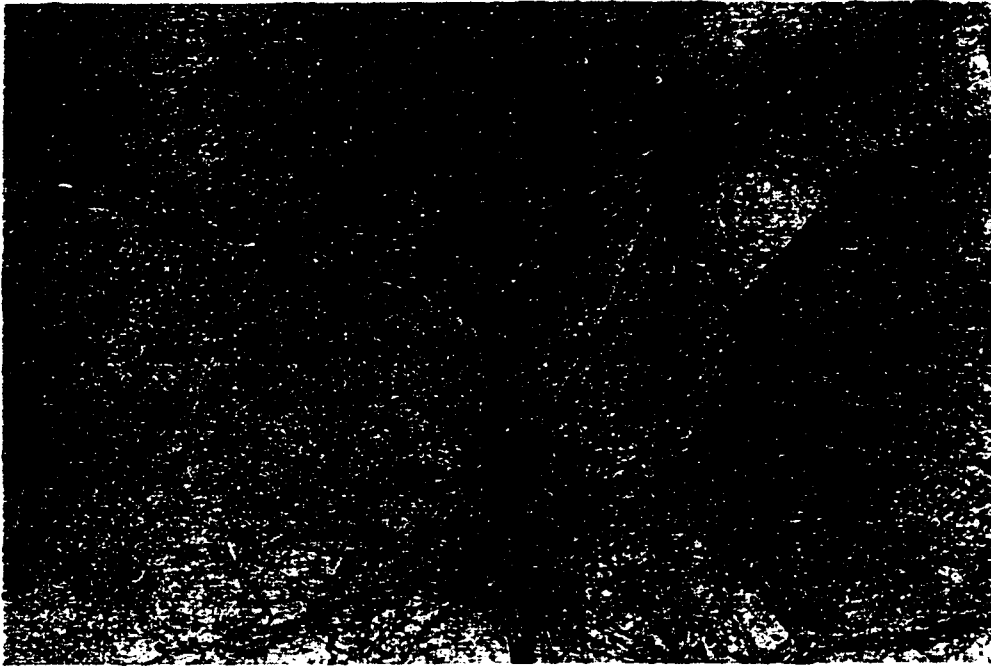
Figure 1. Electron micrograph demonstrating the tissue matrix system. Photo courtesy of Drs. Fey and Penman.

(Folkman and Moscona, 1978; Ingber et al., 1987). Specifically, altered gene expression

of a cell was shown to be affected by the ECM. Primary rat hepatocytes, when grown on

different extracellular matrices, have been demonstrated to exhibit altered gene expression

(Hansen et al., 1994). In addition, the amount of insulin mRNA present in cultured

hepatocytes was shown to be dependent upon the ECM used (Muschel et al., 1986). A

cell's interaction with the ECM and neighboring cells are an important determinant in the

final location and differentiation status of the cell. Cunha *et al.* reported that urogenital

sinus mesenchyme induces adult urinary bladder epithelial cells to remodel to form prostatic

epithelial cells providing evidence that the ECM can play a role in differentiation (Cunha et

al., 1980). Reddi *et al* . reported that the mature fibroblasts undergo redifferentiation to

form new chondroblasts and chondrocytes when they came into contact with a

demineralized bone collagen matrix (Reddi and Andersen, 1976).

Later studies examined the ECM's role in transformation since it was known that one of the hallmarks of transformation involves an alteration in cellular and nuclear morphology. Several studies demonstrated that the ECM could directly alter cellular shape and function. Pienta *et al.* examined the effect of normal rat kidney epithelial cells when exposed to ECMs secreted from both normal and tumor cells (Pienta et al., 1991). These normal cells, when plated on a tumor secreted basement membrane, adopted a morphology and phenotype consistent with transformed cells. These observations were further studied by the same laboratory using high resolution two-dimensional electrophoresis analysis (Getzenberg et al., 1991A). Distinct protein differences were found between normal rat kidney cells and K-ras transfected rat kidney cells when grown on different extracellular matrices. These data represent the first report that modification of the ECM environment can have an effect on the nuclear matrix protein composition. These studies, however, examined the *in vitro* effects of the ECM on nuclear matrix proteins. The purpose of this study, therefore, was to examine the differences of nuclear matrix protein composition *in vivo* by comparing nuclear matrix protein compositions of tumors grown at different organ sites in the rat by injections of the MAT–LyLu (MLL) rat prostate cancer cell line.

Materials and Methods

Cell Lines

MAT–LyLu (MLL, Metastatic, Anaplastic, Tumor to Lymph nodes and Lungs) cell line was maintained in RPMI 1640 supplemented with 10% fetal bovine serum and 1% penicillin/streptomycin solution. Cells were grown in a monolayer and maintained at 37°C, 5% CO_2, and 90% humidity. Cell culture reagents were obtained from Sigma (St. Louis, MO).

Tumor Samples

Cells growing in culture were detached using 1X trypsin followed by neutralization with

media. Cells were pelleted, counted by a hemacytometer, and resuspended in Hanks

Buffered Salt Solution (HBSS). One million cells (100μL) were injected intramuscularly,

directly into the tail vein, heart, lung, or into the prostate of male Copenhagen rats

(200–250g) (Harlan, Indianapolis, IN). One injection was given per rat. Two to four rats

were injected per organ site. Tumors were allowed to grow for two to four weeks to

ensure ample tumor size. All tumors produced at each site were used for nuclear matrix

isolation and tumors were not mixed between groups or within each group. Tumors were

removed from the rats and immediately placed into 1X phosphate buffered saline (PBS)

containing 1.2 mM phenylmethlsulfonyl fluoride (PMSF) on ice to inhibit protease activity.

Tissue was homogenized on ice followed by filtration through a mesh and centrifuged at

780 rpm for ten minutes. Supernatant was removed and the remaining pellet underwent

nuclear matrix isolation.

Analysis of Nuclear Matrix Proteins

Nuclear Matrix Preparation

Nuclear matrix proteins were prepared using published methodologies (Fey and Penman,

1988; Getzenberg et al., 1990). Pellets were suspended in cytoskeletal buffer containing

100mM NaCl, 300mM sucrose, 10mM piperazine-N,N'-bis-[2-ethanesulfonic acid]

(Pipes) (pH 6.8), 5mM $MgCl_2$, 0.5% Triton X–100, 1.2mM phenylmethylsulfonyl

fluoride (PMSF), and 2mM vanadyl adenosine and placed on ice for 20 minutes. The

solution was spun at 2,200 rpm for ten minutes at 4°C followed by the addition of an

extraction buffer containing 250mM $(NH_4)_4SO_2$, 300mM sucrose, 10mM Pipes (pH 6.8),

5mM $MgCl_2$, 0.5% Triton X–100, 1.2mM PMSF, and 2mM vanadyl adenosine. The

solution was incubated for ten minutes on ice. The pellet was resuspended in chromatin

buffer [50mM NaCl, 300mM sucrose, 10mM Pipes (pH 6.8), 5mM $MgCl_2$, 0.5% Triton

X–100, 1.2mM PMSF, and 100μg/mL DNaseI] and incubated for 20 minutes at 20°C.

Samples were centrifuged at 2,200 rpm for ten minutes and resuspended in cytoskeleton

buffer containing RNase A (100mM NaCl, 300mM sucrose, 10mM Pipes (pH 6.8), 5mM

MgCl$_2$, 0.5% Triton X–100, 1.2mM PMSF, and 25 µg/mL RNase A) for ten minutes at

20°C. After centrifugation at 2,200 rpm for ten minutes, the pellet was dissolved in

disassembly buffer (8M urea, 20mM (2-[N-morpholino]ethanesulfonic acid) (MES) (pH

6.6), 1mM ethyleneglycol bis (b-aminoethyl ether)-N,N,N'N'-tetraacetic acid (EGTA),

0.1mM MgCl$_2$, 1% β-mercaptoethanol, and 1.2mM PMSF) and spun at 50,000 rpm for

one hour at 15°C. The supernatant was collected and placed into Spectra/Por dialysis

tubing (Spectrum Medical Industries, Houston, Texas) and dialyzed for at least 16 hours in

a buffer (pH 7.1) containing 0.15M KCl, 25mM imidazole hydrochloride, 5mM MgCl$_2$, 2

mM dithiothreitol, 0.125 mM EGTA, and 0.2mM PMSF. The collected supernatant was

centrifuged at 45,000 rpm for 1.5 hours at 25°C. The soluble nuclear matrix proteins were

ethanol precipitated at –20°C overnight. All solutions contained freshly prepared PMSF to

inhibit serine proteases. The protein was resuspended in 20µL of sample buffer (9M urea,

65mM CHAPS, 140 mM dithiothreitol, and 2.2% ampholytes). Coomassie Plus assay

(Pierce, Rockford, Il) was used for protein determination using bovine serum albumin as a

standard. Vanadyl adenosine was purchased from Gibco Life Sciences, (Grand Island,

New York). All other chemicals were purchased from Sigma (St. Louis, MO).

High Resolution Two-Dimensional Electrophoresis

High resolution two-dimensional electrophoresis was carried out using the Investigator

2–D Electrophoresis System from Oxford Glycosystems (Bedford, MA). One millimeter

diameter tube gels [9.5M urea, 2.0% (v/v) Triton X–100, 4.1% acrylamide solution, 5mM

CHAPS, ampholytes, and ammonium persulfate] were cast followed by pre-focusing until

the maximum voltage reached 1500 volts. 40µg of nuclear matrix protein sample was

loaded onto the tube gels and isoelectric focused for 18,000 volt-hours. The isoelectric

focusing was carried out using pH 3–10 ampholytes which have been optimized for

separation of cellular proteins. Tube gels were extruded and incubated in gel equilibration buffer (0.3M Tris base, 0.075M Tris-HCl, 3.0% sodium dodecyl sulfate, 50mM dithiothreitol, and 0.01% bromophenol blue) for two minutes at room temperature. Each tube gel was placed on top of a 10% polyacrylamide gel and run for approximately five hours at 20,000 mW per gel. Gels were fixed overnight in 50% methanol/10% acetic acid, enhanced with 5% gluteraldeyde followed by silver staining using an Accurate Chemical silver staining kit (Accurate Chemical Co., Inc., Westbury, NY) as described elsewhere (Wray et al., 1981). Protein molecular weight standards were obtained from Diversified Biotechnology (Boston, MA). Isoelectric points were determined using BDH carbamylated standards (Gallard-Schlesinger, Carle Place, NY) and Sigma Chemical Co. (St. Louis, MO). Multiple gels were run for each sample. Only protein spots clearly and reproducibly observed in all the gels of a sample type were counted as actually representing the nuclear matrix components. The gels were analyzed using the BioImage 2D Electrophoresis Analysis System (BioImage, Ann Arbor, MI) which matches protein spots between gels and databases the gels and protein spots. Organ sites were compared to the gel produced by MLL cells injected into the orthotopic site of the prostate.

Results and Conclusions

The interaction of the ECM with neighboring cells has been implicated in various changes within the cell. In order to see if the nuclear matrix protein pattern of MLL cells are altered when grown at different organ sites, MLL prostate cancer cells were injected into the prostate, lung, heart, intramuscular, and tail vein producing tumors which were used for the isolation of nuclear matrix. Nuclear matrix samples were analyzed by their protein pattern revealed by high resolution two-dimensional electrophoresis. The MLL tumors from the heart, lung, intramuscular, and tail vein nuclear matrix protein compositions were compared only to the prostate tumor nuclear matrix pattern. This comparison was chosen since the MLL cell line was originally derived from a rat prostate

tumor. Upon analysis, there were distinct protein differences, as well as common proteins, seen in all of the organ nuclear matrix protein compositions when compared to the prostate derived nuclear matrix. Figure 2 shows the two-dimensional nuclear matrix pattern of the prostate derived tumor by which all other gels were compared. Approximately 150 nuclear matrix proteins spots were identified ranging in size from 10–200 kD and pIs from 5.0–9.3. The majority of the nuclear matrix proteins were common between the various organ sites agreeing with the findings in other laboratories (Partin et al., 1993; Chew et al., 1997; Getzenberg et al., 1996). When compared to the prostate protein pattern, fourteen proteins were identified as being present only in the lung (L–1 through L–14) (Figure 3). The proteins ranged from approximately 18kD–95kD while the pIs ranged from 6.2–7.0. Seven proteins (L5 through L–11) were present in a cluster of 30–36 kD with pIs 6.6–6.9. Six proteins were found that were only present in the intramuscular tumor tissue (IM–1 through IM–6) (Figure 4). These proteins ranged from approximately 14kD–40kD with

pIs from 6.9–9.4. Seventeen proteins (H–1 through H–17) were found only in the heart tumor tissue when compared to the prostate nuclear matrix pattern (Figure 5) and ranged from 14kD–89kD with pIs from 6.0–8.8. H2–H8 were identified as a distinct group of proteins of 55–70kD and pIs 6.1–6.3. Five proteins (TV–1 through TV–5) were present in tail vein tumor tissue and not in the prostate tumor tissue (Figure 6). These proteins ranged from approximately 19kD–36kD with pIs from 6.0–6.4. Table 2 lists all of the nuclear matrix proteins that were found in the various tumor tissues and not in the prostate. Figure 7 is a schematic representation of these proteins in a two-dimensional gel format.

In conclusion, these data demonstrate that MLL cells, when grown outside of the prostate, contain alterations in the nuclear matrix protein composition *in vivo*. Such alterations may be the result of different environments (i.e., ECM, hormones, etc.) in which the cells grew. This study has been published (Replogle-Schwab et al., 1996B).
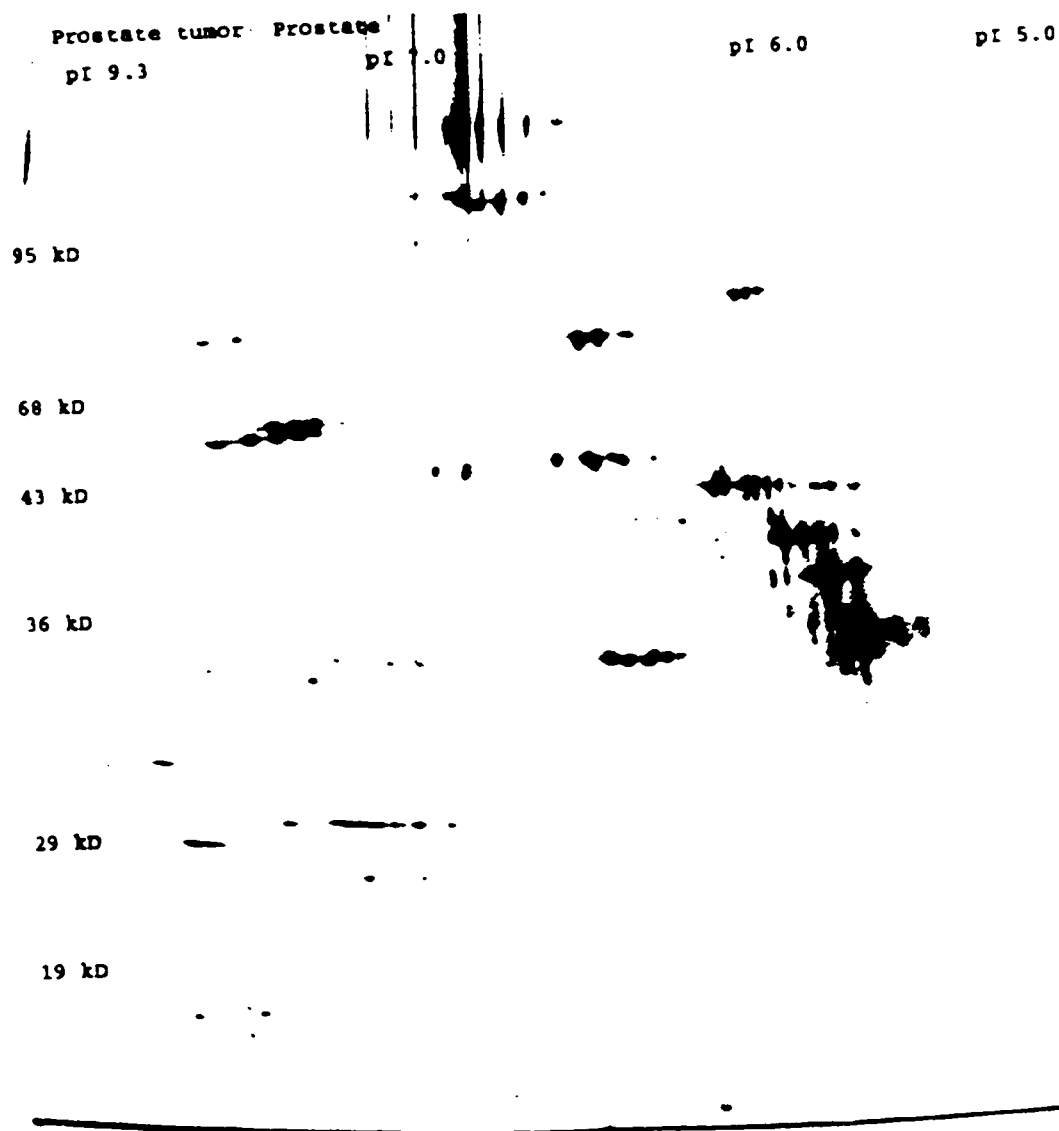
Figure 2. High resolution two-dimensional gel electrophoresis of a prostate tumor derived from an injection of MLL cells. This gel was used to compare the remaining nuclear matrix tumor protein compositions.
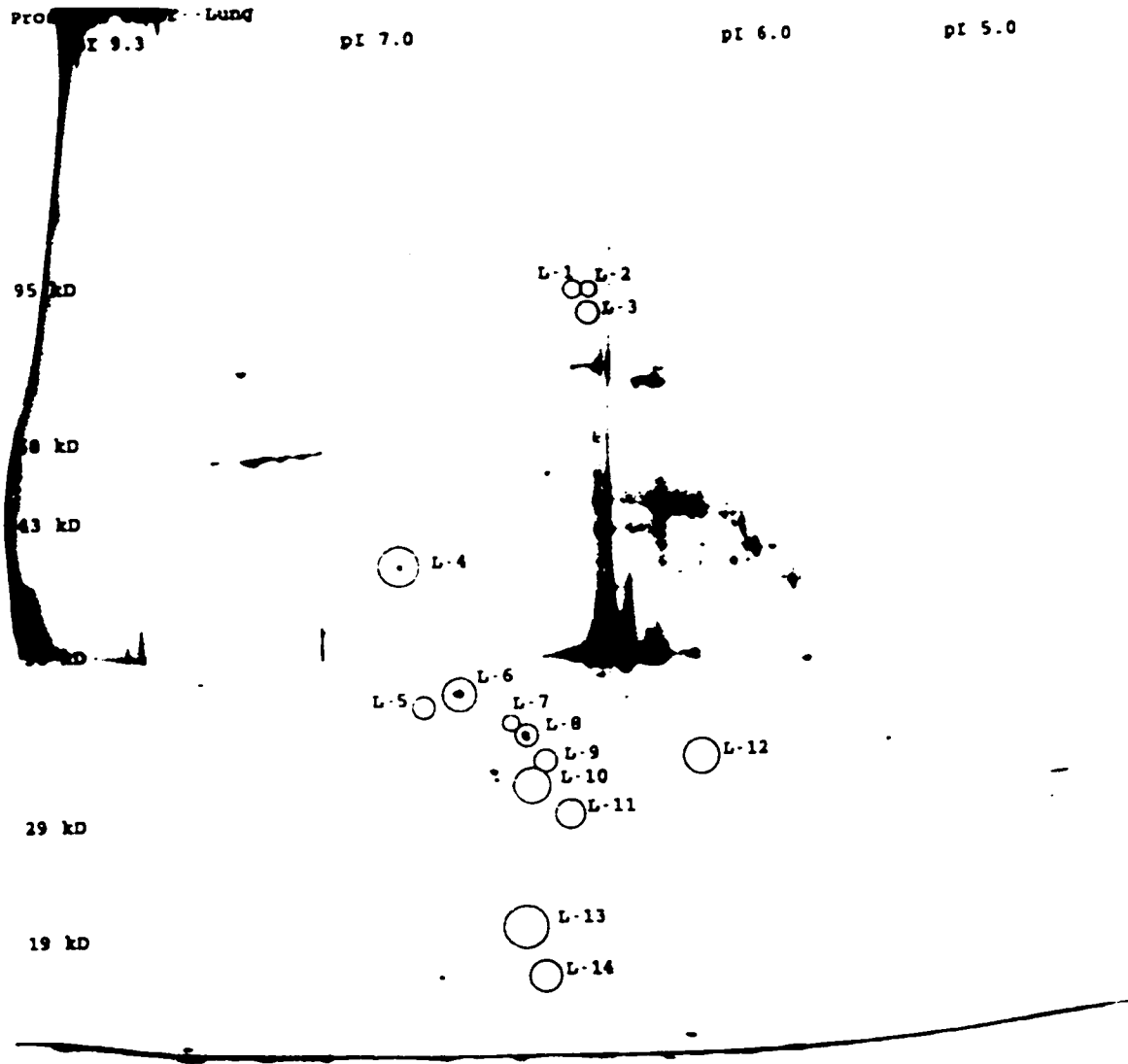
Figure 3. High resolution two-dimensional gel electrophoresis of a lung tumor derived from an injection of MLL cells. L–1 through L–14 represent nuclear matrix proteins that were not found in the prostate tumor nuclear matrix composition.
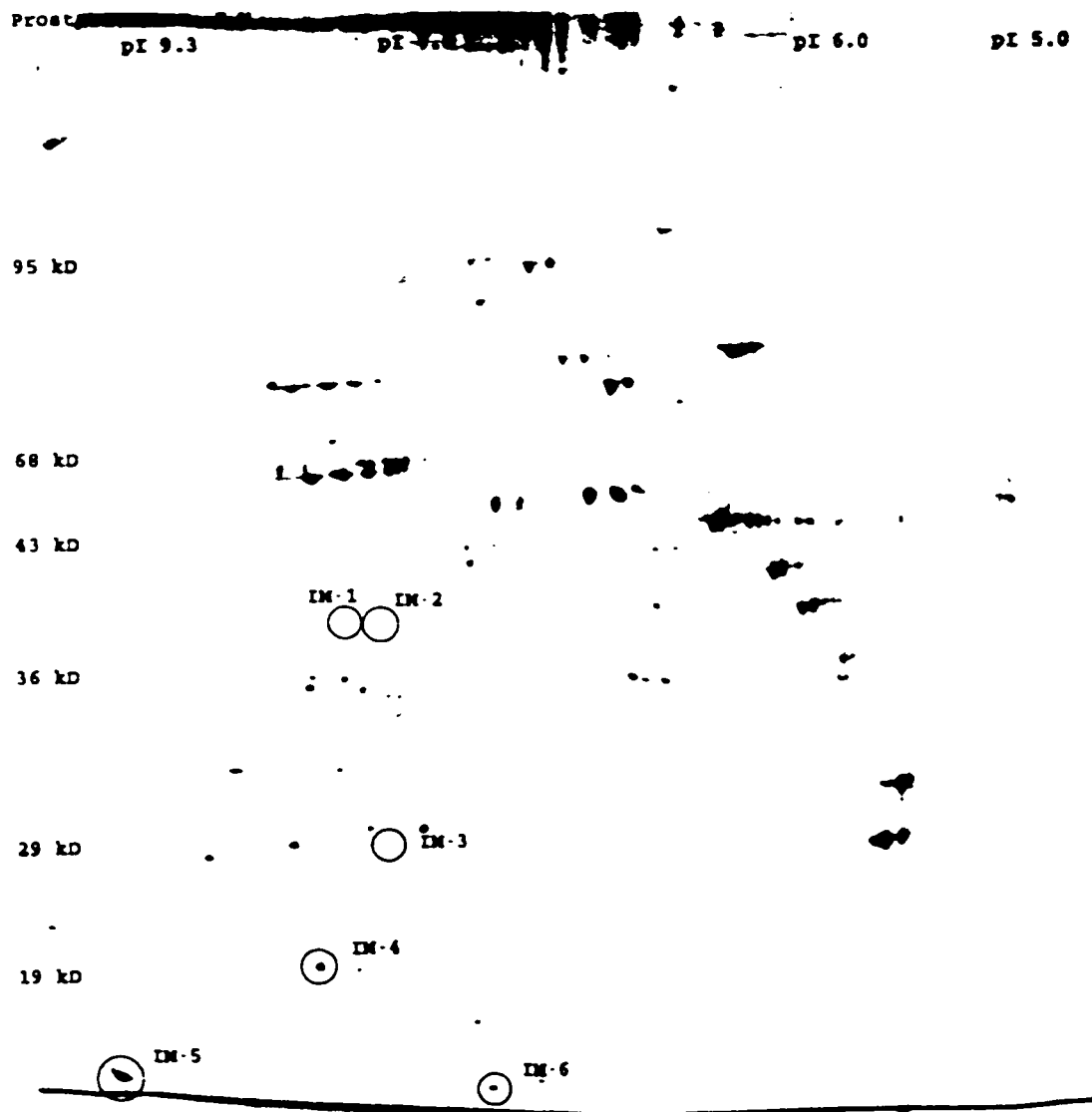
Figure 4. High resolution two-dimensional gel electrophoresis of an intramuscular tumor derived from an injection of MLL cells. IM–1 through IM–6 represent nuclear matrix proteins that were not found in the prostate tumor nuclear matrix composition.

Prostate tumor · Heart
pI 9.3   pI 7.0   pI 6.0   pI 5.0

95 kD   H-1

68 kD   H-9   H-2 H-3   H-4 H-5   H-6   H-7 H-8

43 kD   H-10

36 kD

29 kD   H-16   H-15 H-17   H-11 H-12

19 kD   H-13

H-14
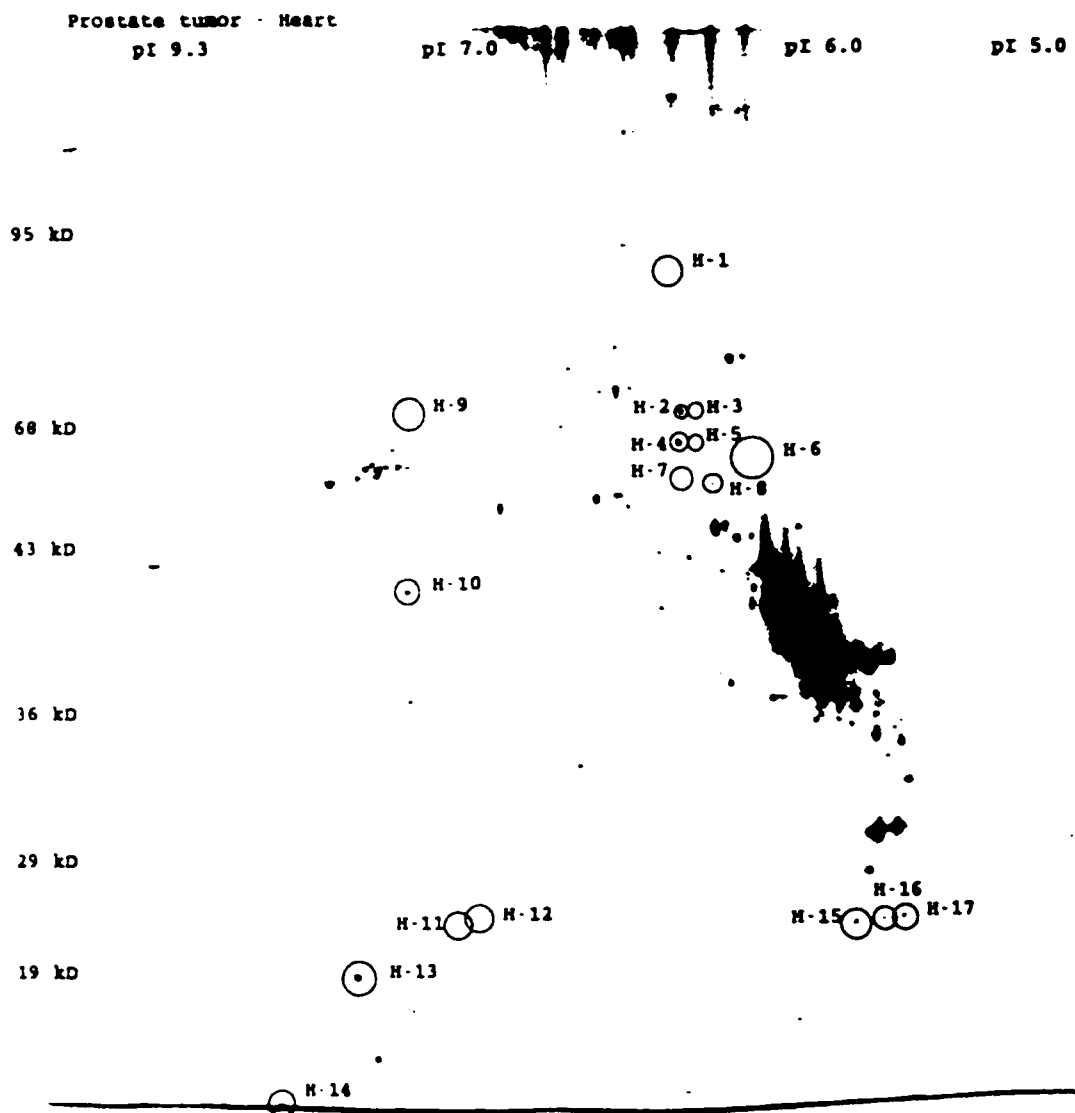
Figure 5. High resolution two-dimensional gel electrophoresis of a heart tumor derived from an injection of MLL cells. H–1 through H–17 represent nuclear matrix proteins that were not found in the prostate tumor nuclear matrix composition.

Prostate tumor
pI 9.3   pI 6.0   pI 5.0

95 kD

68 kD

43 kD

TV-1
TV-2   TV-3
36 kD

29 kD   TV-4

19 kD   TV-5
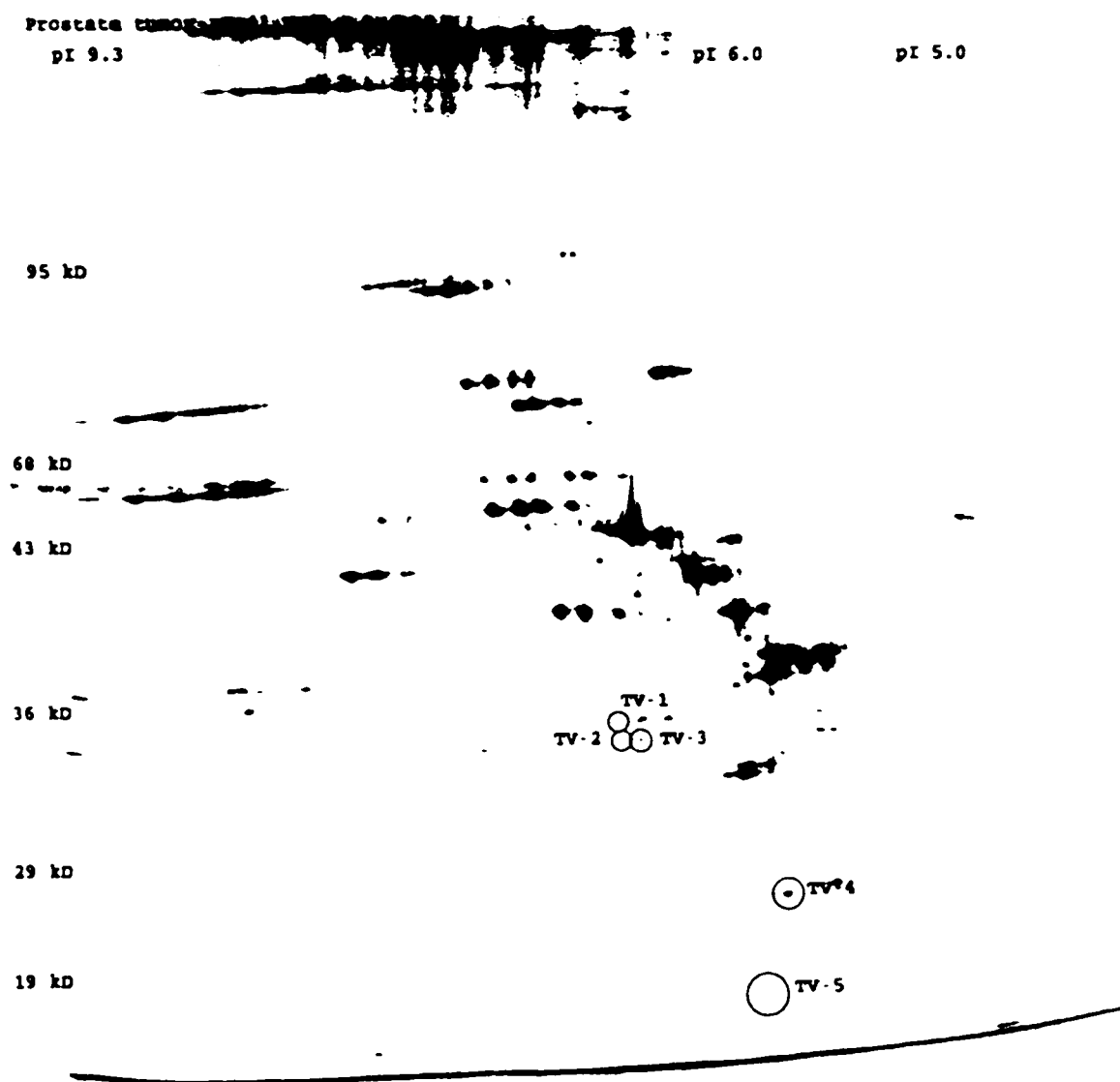
Figure 6. High resolution two-dimensional gel electrophoresis of a tail vein tumor derived from an injection of MLL cells. TV–1 through TV–5 represent nuclear matrix proteins that were not found in the prostate tumor nuclear matrix composition.

Table 2. Proteins present in heart (H-1 through H-17), intramuscular (IM-1 through IM-6), lung (L-1 through L-14), and tail vein (TV-1 through TV-5) not found in the prostate.

Designation	Molecular Mass	Isoelectric Point	Designation	Molecular Mass	Isoelectric Point
H-1	89kD	6.4	IM-5	14kD	9.4
H-2	70kD	6.3	IM-6	14kD	6.9
H-3	70kD	6.2	L-1	95kD	6.6
H-4	66kD	6.3	L-2	95kD	6.5
H-5	66kD	6.2	L-3	89kD	6.5
H-6	60kD	6.1	L-4	41kD	7.0
H-7	58kD	6.3	L-5	34kD	6.9
H-8	55kD	6.2	L-6	35kD	6.8
H-9	70kD	7.6	L-7	33kD	6.7
H-10	41kD	7.6	L-8	33kD	6.7
H-11	23kD	7.1	L-9	32kD	6.6
H-12	24kD	7.0	L-10	31kD	6.6
H-13	19kD	8.1	L-11	30kD	6.6
H-14	14kD	8.8	L-12	32kD	6.2
H-15	24kD	6.0	L-13	20kD	6.7
H-16	24kD	6.1	L-14	18kD	6.6
H-17	24kD	6.1	TV-1	36kD	6.4
IM-1	40kD	7.6	TV-2	35kD	6.4
IM-2	40kD	7.3	TV-3	35kD	6.3
IM-3	29kD	7.2	TV-4	28kD	6.1
IM-4	20kD	7.9	TV-5	19kD	6.0
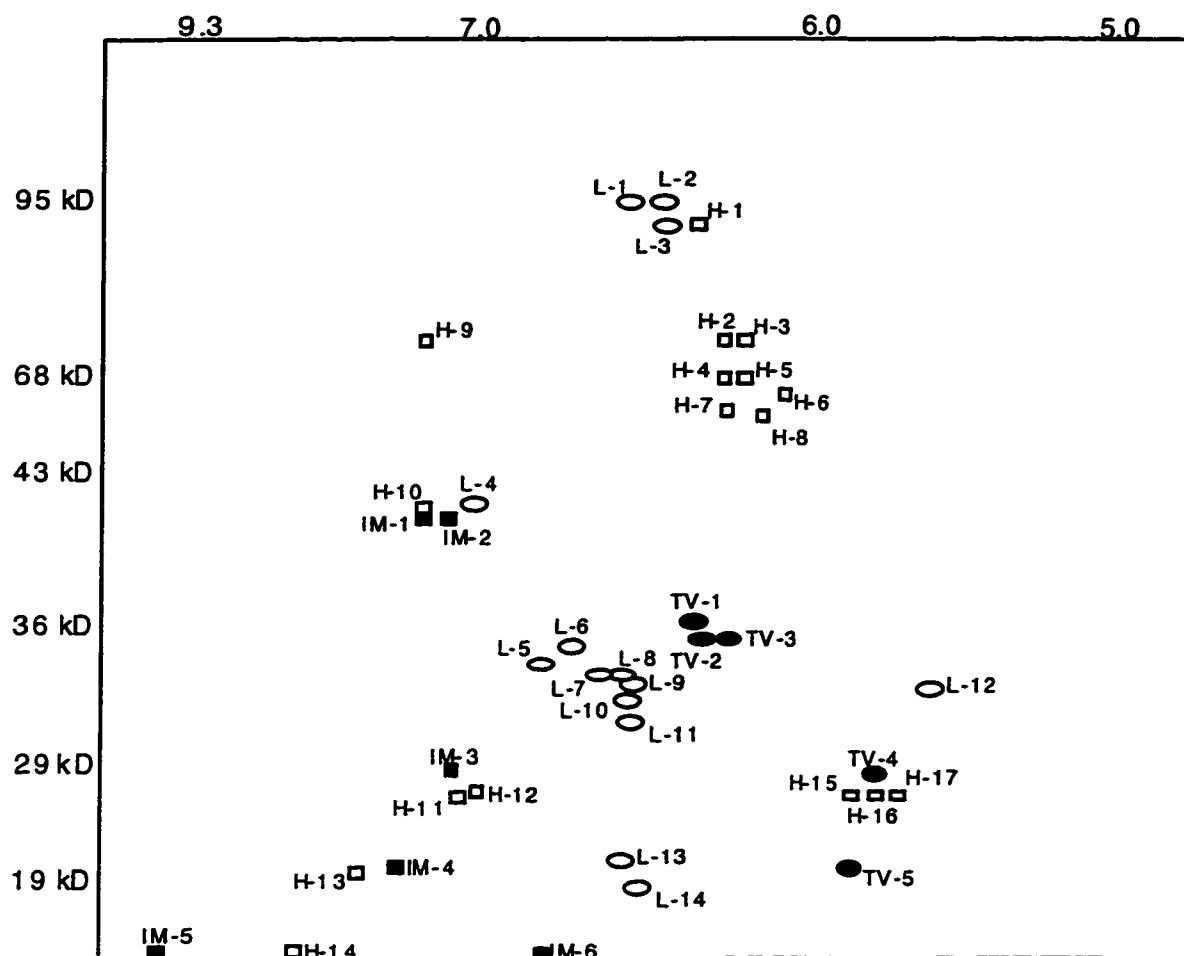
Figure 7. A schematic representation of the high-resolution two-dimensional electrophoresis of the nuclear matrix proteins from MLL-producing tumors in the lung O (L–1 through L–14), intramuscular ■ (IM–1 through IM–6), tail vein ● (TV–1 through TV–5), and heart □ (H–1 through H–17) when compared to the prostate tumor. Only protein differences are shown.

Chapter Three

Nuclear Matrix Protein Composition of Human Lung Carcinoma Cell Lines

Introduction

Lung cancer is the leading cause of death in the United States, as well as many countries throughout the world (Minna et al., 1989). Although there has been much effort in delineating more effective diagnostic techniques as well as better therapies, the incidence of lung cancer continues to increase. One area of clinical therapy that has received a great amount of attention is the utilization of cancer specific biomarkers. Such biomarkers could prove extremely helpful in the area of diagnosis and disease progression. Nuclear matrix proteins, in particular, are a relatively untapped resource for novel cancer specific biomarkers. Nuclear matrix proteins, as described in previous chapters, have been shown to be involved in many critical processes within the cell. Specifically, gene expression components such as steroid receptors and several transcription factors, have been reported to be associated with the nuclear matrix (Barrack and Coffey, 1980; Nardozza et al., 1996). These lines of evidence suggest that the nuclear matrix protein composition within the cell may be partly responsible for controlling gene expression. Hence, alterations of the nuclear matrix proteins within a cell may lead to alterations in gene expression and function. Therefore, investigators began to examine nuclear matrix proteins in cell lines and tissues in various differentiation and transformation states.

Since it was known that the differentiation process alters the pattern of gene expression dramatically, interest in whether differentiation is accompanied by alterations in nuclear matrix composition began to grow. In one of the first studies to examine this issue, Stuurman *et al.* compared the nuclear matrix protein composition of an undifferentiated murine embryonal carcinoma cell line with the same cell line that had undergone

differentiation by the exposure to all-trans-retinoic acid (Stuurman et al., 1989). Upon analysis, dramatic differences in nuclear matrix protein composition were found when the undifferentiated cells were compared to their differentiated derivatives suggesting that the nuclear matrix has a cell-type-specific composition that is closely related to the differentiation status of the cell.

In other studies, high resolution two-dimensional electrophoresis of nuclear matrix compositions of cancer cells compared to their normal counterparts where found to contain altered protein expression. Differences in nuclear matrix proteins were found to be altered in hepatoma cancer cells compared to their normal counterparts (Berezney et al., 1979), bladder cancer vs normal cells (Gordon et al., 1993; Getzenberg et al., 1996), rat prostate cancer vs normal tissue (Getzenberg et al., 1991B), breast cancer tissue compared to normal breast tissue (Khanuja et al., 1993), colon cancer tissue vs normal colon tissue (Keesee et al., 1994), human prostate cancer tissue compared to benign prostate hyperplastic tissue (Partin et al., 1993), and squamous cell carcinoma of the head and neck vs normal tissue (Donat et al., 1996). To our knowledge, the nuclear matrix protein composition of large cell lung carcinoma, small cell lung carcinoma (SCLC), squamous cell lines, and adenocarcinoma cell lines of the lung has not been investigated. The purpose of this study was to compare the nuclear matrix protein composition of various cell types of human lung cancer cell lines.

Materials and Methods

Cell Culture

Two human large cell carcinoma cell lines (NCI–H460, NCI–H661), five human SCLC cell lines (NCI–H69, NCI–H82, NCI–H128, NCI–H146, NCI–H446), three human squamous cell carcinoma cell lines (NCI–520, SK–MES–1, and SW 900), and three human adenocarcinoma cell lines of the lung (A–427, CALU–3, and SK–LU–1) were obtained from the American Type Culture Collection (Rockville, MD). SK–MES–1,

A–427, CALU–3, and SK–LU–1 lines were cultured in MEM media containing 10% fetal bovine serum (FBS) and 1% antibiotics while SW 900 cells were grown in Leibovitz's L–15 media supplemented with 10% FBS and 1% antibiotics. All other cell lines were grown in RPMI 1640 media with 10% FBS and 1% antibiotics. All cell culture reagents were obtained from GIBCO-BRL (Grand Island, NY).

Nuclear Matrix Protein Isolation

Nuclear Matrix Preparation. Nuclear matrix proteins were prepared using published methodologies (Fey and Penman, 1988; Getzenberg et al., 1990). Pellets were suspended in cytoskeletal buffer containing 100mM NaCl, 300mM sucrose, 10mM piperazine-N,N'-bis-[2-ethanesulfonic acid] (Pipes) (pH 6.8), 5mM MgCl$_2$, 0.5% Triton X–100, 1.2mM phenylmethylsulfonyl fluoride (PMSF), and 2mM vanadyl adensoine and placed on ice for 20 minutes. The solution was spun at 2,200 rpm for ten minutes at 4°C followed by the addition of an extraction buffer containing 250mM (NH$_4$)$_4$SO$_2$, 300mM sucrose, 10mM Pipes (pH 6.8), 5mM MgCl$_2$, 0.5% Triton X–100, 1.2mM PMSF, and 2mM vanadyl adenosine. The solution was incubated for ten minutes on ice. The pellet was resuspended in chromatin buffer [50mM NaCl, 300mM sucrose, 10mM Pipes (pH 6.8), 5mM MgCl$_2$, 0.5% Triton X–100, 1.2mM PMSF, and 100μg/mL DNaseI] and incubated for 20 minutes at 20°C. Samples were centrifuged at 2,200 rpm for ten minutes and resuspended in cytoskeleton buffer containing RNase A [100mM NaCl, 300mM sucrose, 10mM Pipes (pH 6.8), 5mM MgCl$_2$, 0.5% Triton X–100, 1.2mM PMSF, and 25 μg/mL RNAse A] for ten minutes at 20°C. After centrifugation at 2,200 rpm for ten minutes, the pellet was dissolved in disassembly buffer [8M urea, 20mM (2-[N-morpholino]ethanesulfonic acid) (MES) (pH 6.6), 1mM ethyleneglycol bis (b-aminoethyl ether)-N,N,N'N'-tetraacetic acid (EGTA), 0.1mM MgCl$_2$, 1% β-mercaptoethanol, and 1.2mM PMSF] and spun at 50,000 rpm for one hour at 15°C. The supernatant was collected and placed into Spectra/Por dialysis tubing (Spectrum Medical Industries,

Houston, Texas) and dialyzed for at least 16 hours in a buffer (pH 7.1) containing 0.15M

KCl, 25mM imidazole hydrochloride, 5mM $MgCl_2$, 2 mM dithiothreitol, 0.125 mM

EGTA, and 0.2mM PMSF. The collected supernatant was centrifuged at 45,000 rpm for

1.5 hours at 25°C. The soluble nuclear matrix proteins were ethanol precipitated at $-20°C$

overnight. All solutions contained freshly prepared PMSF to inhibit serine proteases. The

protein was resuspended in 20μL of sample buffer (9M urea, 65mM CHAPS, 140 mM

dithiothreitol, and 2.2% ampholytes). Coomassie Plus assay (Pierce, Rockford, Il) was

used for protein determination using bovine serum albumin as a standard. Vanadyl

adenosine was purchased from Gibco Life Sciences, (Grand Island, New York). All other

chemicals were purchased from Sigma (St. Louis, MO).

High Resolution Two-Dimensional Electrophoresis

High resolution two-dimensional electrophoresis was carried out using the

Investigator 2–D Electrophoresis System from Oxford Glycosystems (Bedford, MA).

Tube gels (9.5M urea, 2.0% (v/v) Triton X–100, 4.1% acrylamide solution, 5mM

CHAPS, ampholytes, and ammonium persulfate) were cast followed by pre-focusing until

the maximum voltage reached 1500 volts. 40μg of nuclear matrix protein sample was

loaded onto glass tubes with a one millimeter inner diameter and isoelectric focusing was

carried out using pH 3–10 ampholytes optimized for separation of cellular proteins for

18,000 volt hours. Tube gels were extruded and incubated in gel equilibration buffer

(0.3M Tris base, 0.075M Tris-HCl, 3.0% sodium dodecyl sulfate, 50mM dithiothreitol,

and 0.01% bromophenol blue) for two minutes at room temperature. Each tube gel was

placed on top of a 10% polyacrylamide gel and run for approximately five hours at 20,000

mW per gel. Gels were fixed overnight in 50% methanol/10% acetic acid, enhanced with

5% gluteraldeyde followed by silver staining using an Accurate Chemical silver staining kit

(Accurate Chemical Co., Inc., Westbury, NY) as described elsewhere (Wray et al., 1981).

Proteins molecular weight standards were obtained from Diversified Biotechnology

(Boston, MA). Isoelectric points were determined using 2–D protein standards from Sigma Chemical Co. (St. Louis, MO). All samples were run in triplicate. Only protein spots clearly and reproducibly observed in all the gels of a sample type were counted as actually representing the nuclear matrix components. The 2–D gels were compared only in their designated lung type classification (large cell carcinoma, SCLC, squamous cell carcinoma, and adenocarcinoma).

Results

This study investigated the nuclear matrix composition of various cell lines from the four major cell types of lung cancer: squamous cell carcinoma, SCLC, adenocarcinoma, and large cell carcinoma. Cells were collected, nuclear matrix proteins were isolated and separated on high resolution two-dimensional electrophoresis. Following silver staining, the gels were visually compared according to the lung classification to which the sample belonged (i.e. squamous cell carcinomas were compared to other squamous cell samples). Figures 8A–8C reveal the nuclear matrix protein compositions of the three adenocarcinoma cell lines SK–LU–1, A–427, and CALU–3 respectively. The nuclear matrix protein patterns of the large cell carcinoma cell lines H–460 and H-661 are shown in Figures 9A and 9B. The squamous cell carcinoma nuclear matrix protein patterns are shown in Figures 10A–10C for SW900, H520, and SK–MES–1. Lastly, Figures 11A–11E represent the small cell carcinoma lung carcinoma cell lines H–128, H146, H82, H69, and H446 respectively. Approximately 150 protein spots were identified ranging in size from 10–200kD and pIs 4.5–9.7. Upon comparison, there were distinct protein differences, as well as common proteins, seen in all four lung carcinoma categories. Common proteins were identified of which ten common proteins were selected in each lung cancer classification which were visible in every cell line within their category. Table 3 lists the ten common proteins from each category of lung carcinoma cell lines. All of the common proteins in all four categories were below 35kD in size and ranged from pIs 4.9–9.5.

Table 4 lists the different proteins found within each category that were different from gel to gel (i.e., SK–LU–1–A is a protein found only in SK–LU–1, but not in A–427 and Calu–3). The molecular mass and pI range of the different proteins are as follows: adenocarcinoma (13–28kD; pIs 6.0–9.3); large cell carcinoma (13–27kD; pIs 6.0–8.3); squamous cell carcinoma (10–31kD; pIs 5.4–9.4), and SCLC (11–33kD; pIs 4.9–9.3). While the analysis intended to compare gels only within a single classification, common and different proteins were also observed between gels of different classifications. In conclusion, common nuclear matrix proteins, as well as distinct differences, were observed in the four major types of lung cancer. This work has previously been published (Yamazaki et al., 1996).
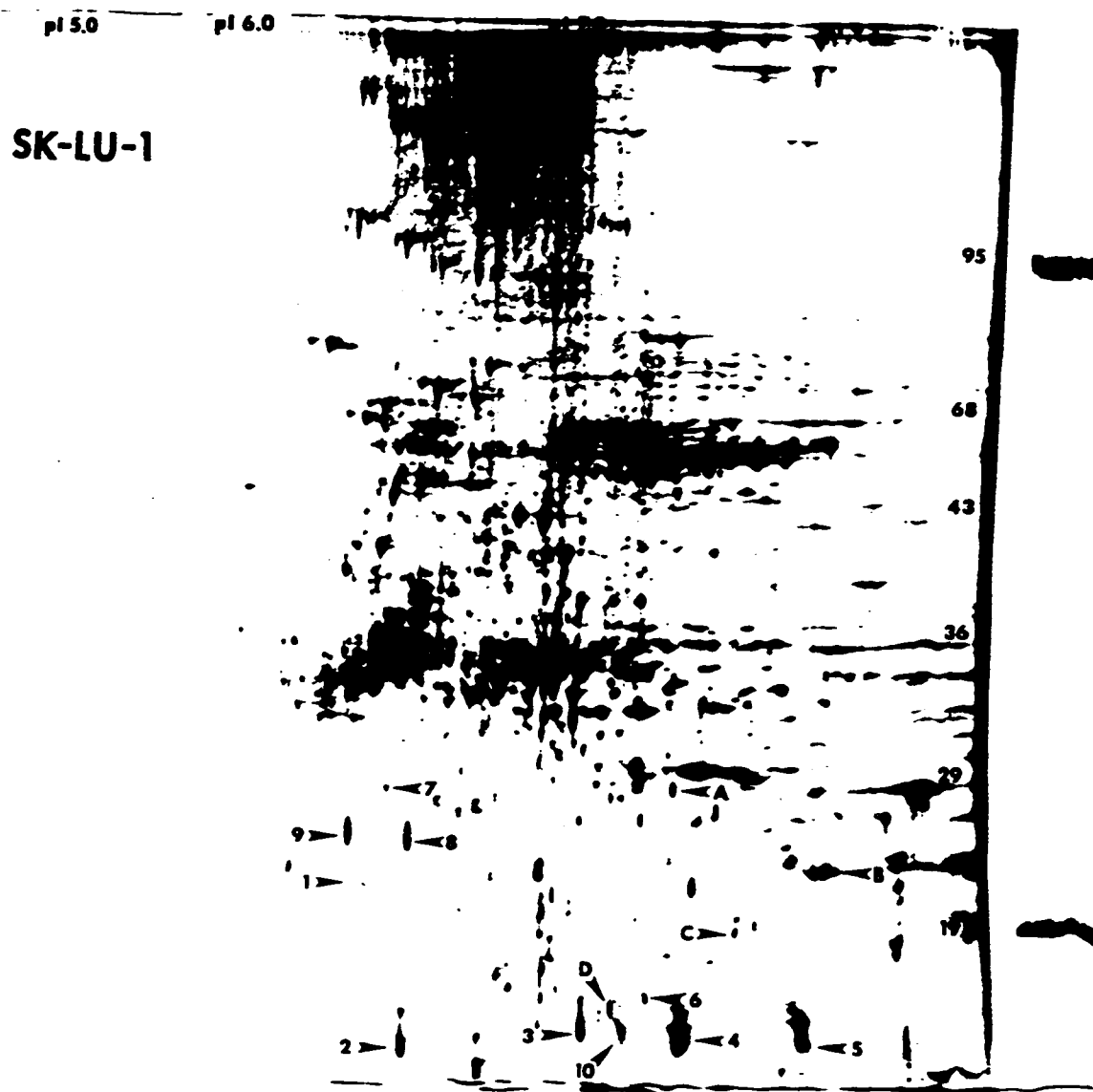
Figure 8A: The human lung adenocarcinoma cell line SK-LU-1 two-dimensional gel. The common adenocarcinoma nuclear matrix proteins are labeled 1-10 while the distinct SK-LU-1 nuclear matrix proteins are labeled A-D.
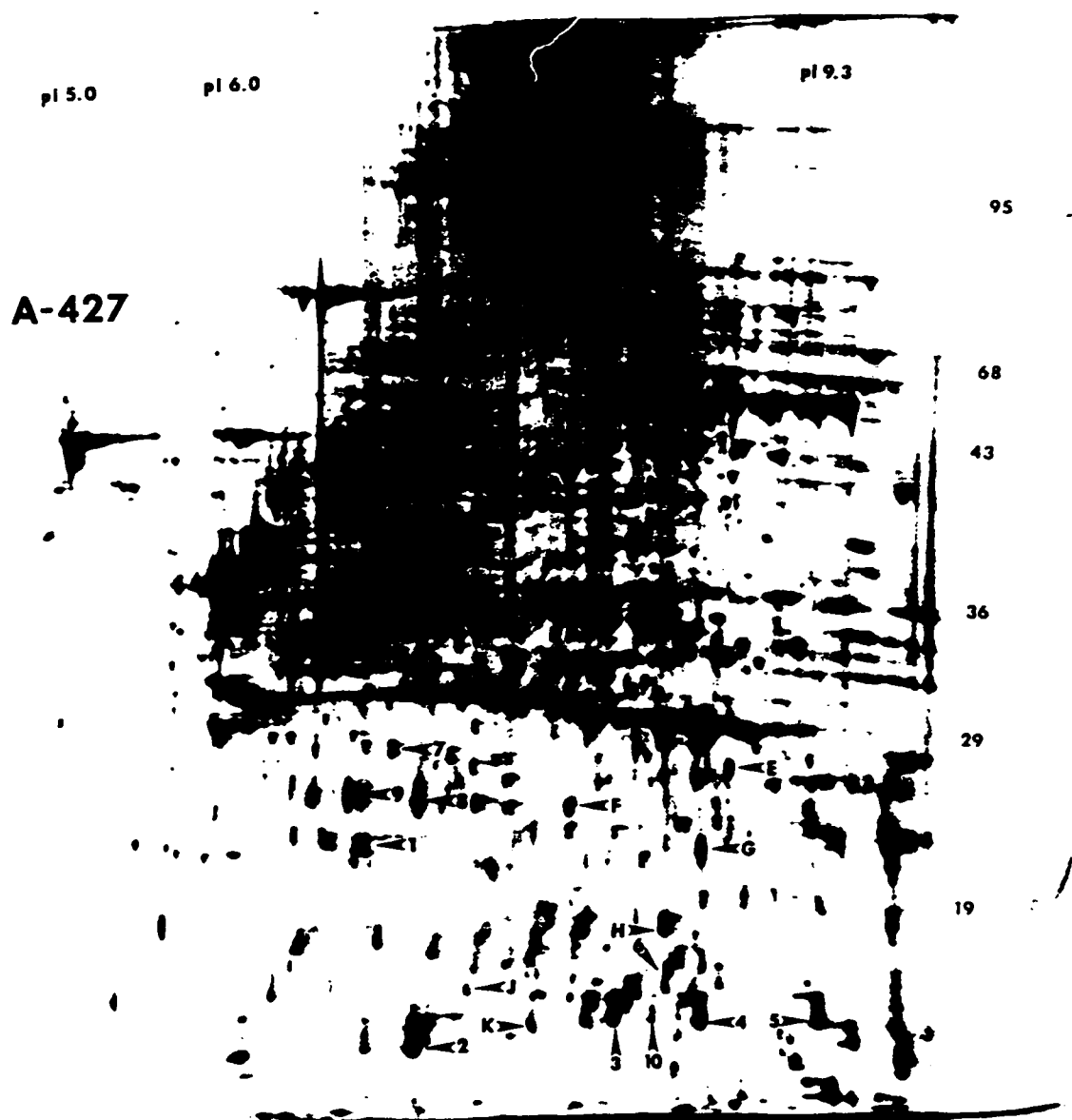
Figure 8B: The human lung adenocarcinoma cell line A-427 two-dimensional gel. The common adenocarcinoma nuclear matrix proteins are labeled 1-10 while the distinct A-427 nuclear matrix proteins are labeled E-K.
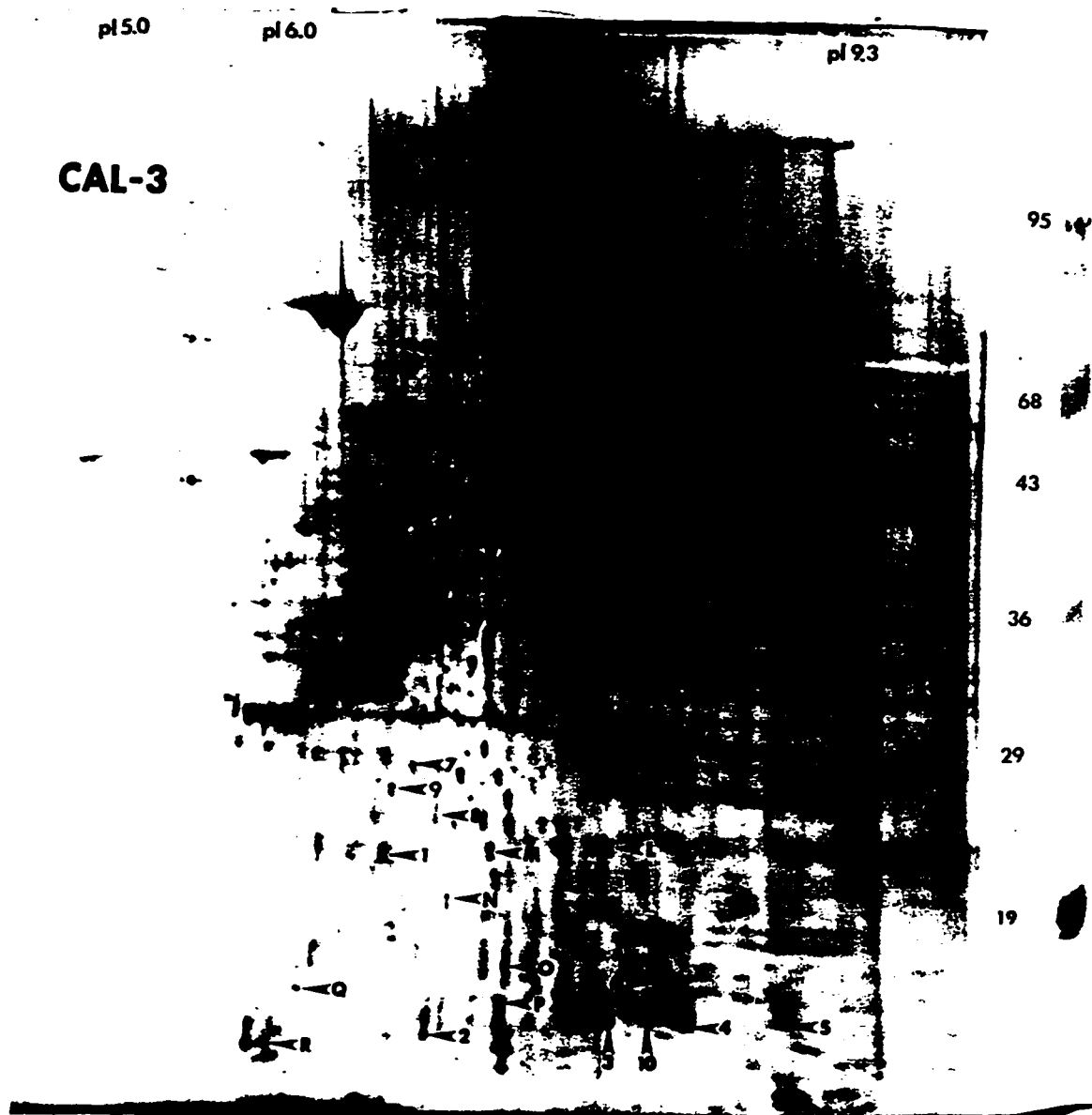
Figure 8C: The human lung adenocarcinoma cell line CAL-3 two-dimensional gel. The common adenocarcinoma nuclear matrix proteins are labeled 1-10 while the distinct CAL-3 nuclear matrix proteins are labeled L-R.
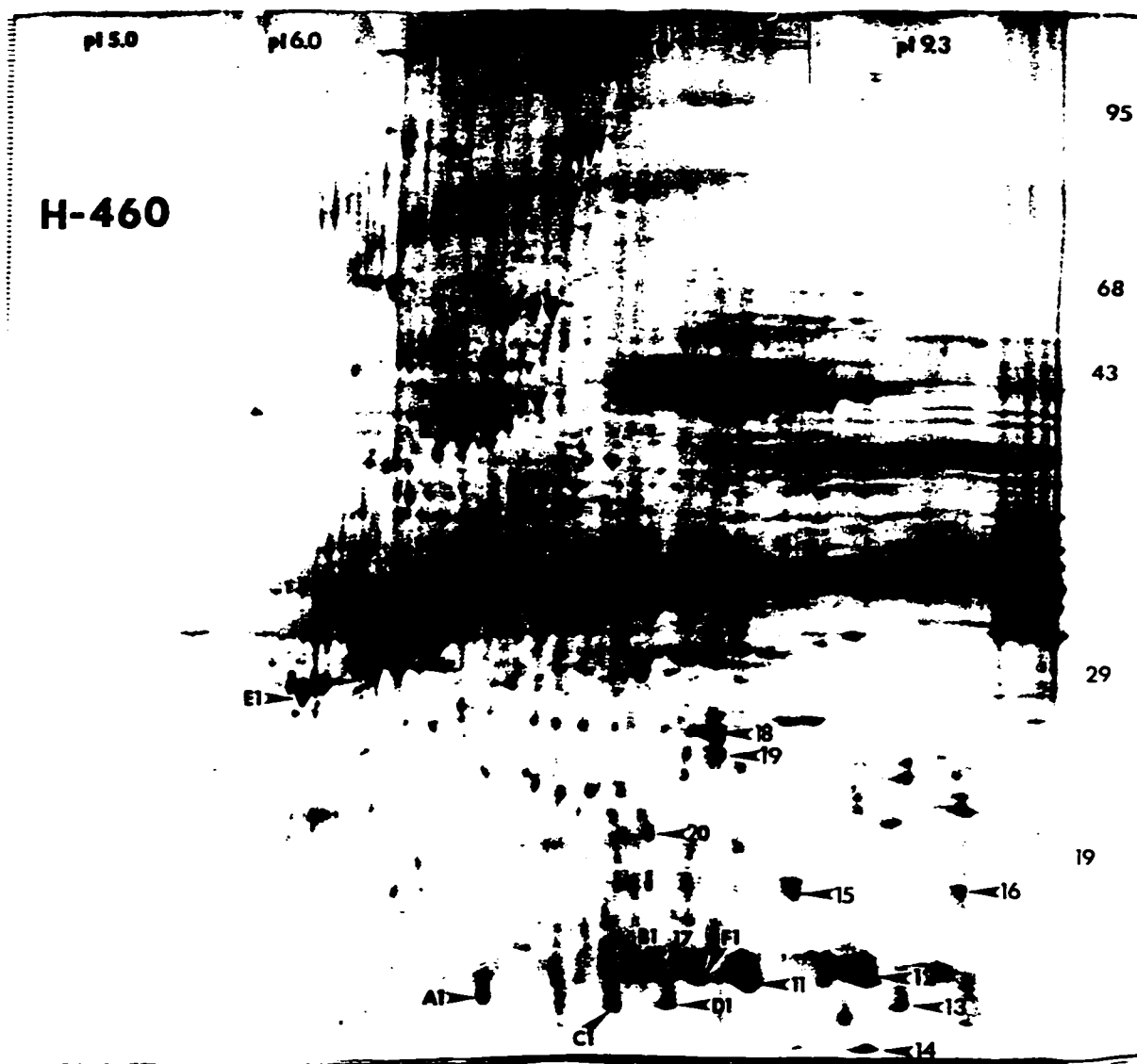
Figure 9A: The human large cell carcinoma cell line H-460 two-dimensional gel. The common large cell carcinoma nuclear matrix proteins are labeled 11-20 while the distinct H-460 nuclear matrix proteins are labeled A1-F1..
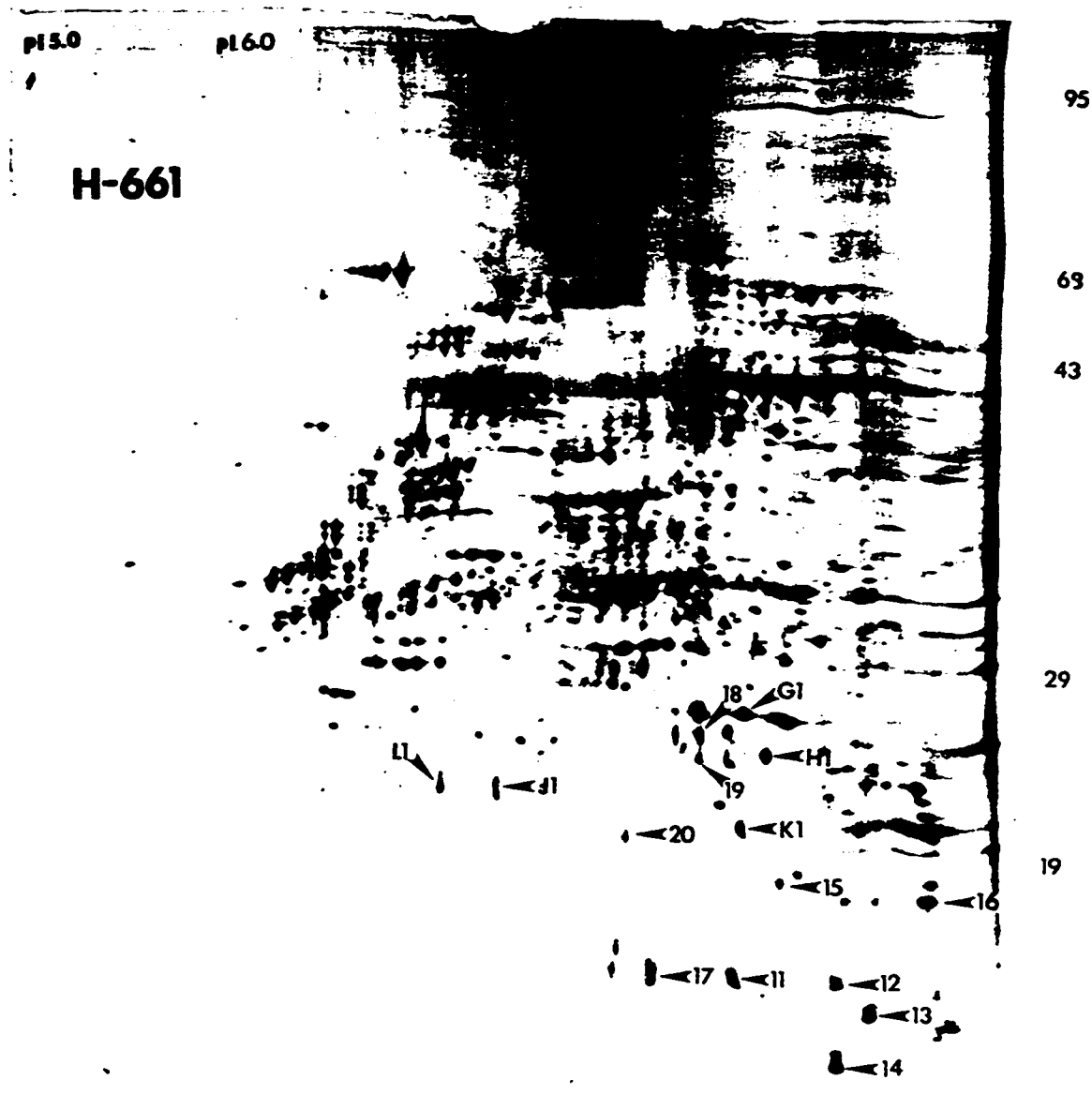
Figure 9B: The human large cell carcinoma cell line H-661 two-dimensional gel. The common large cell carcinoma nuclear matrix proteins are labeled 11-20 while the distinct H-460 nuclear matrix proteins are labeled G1-L1.
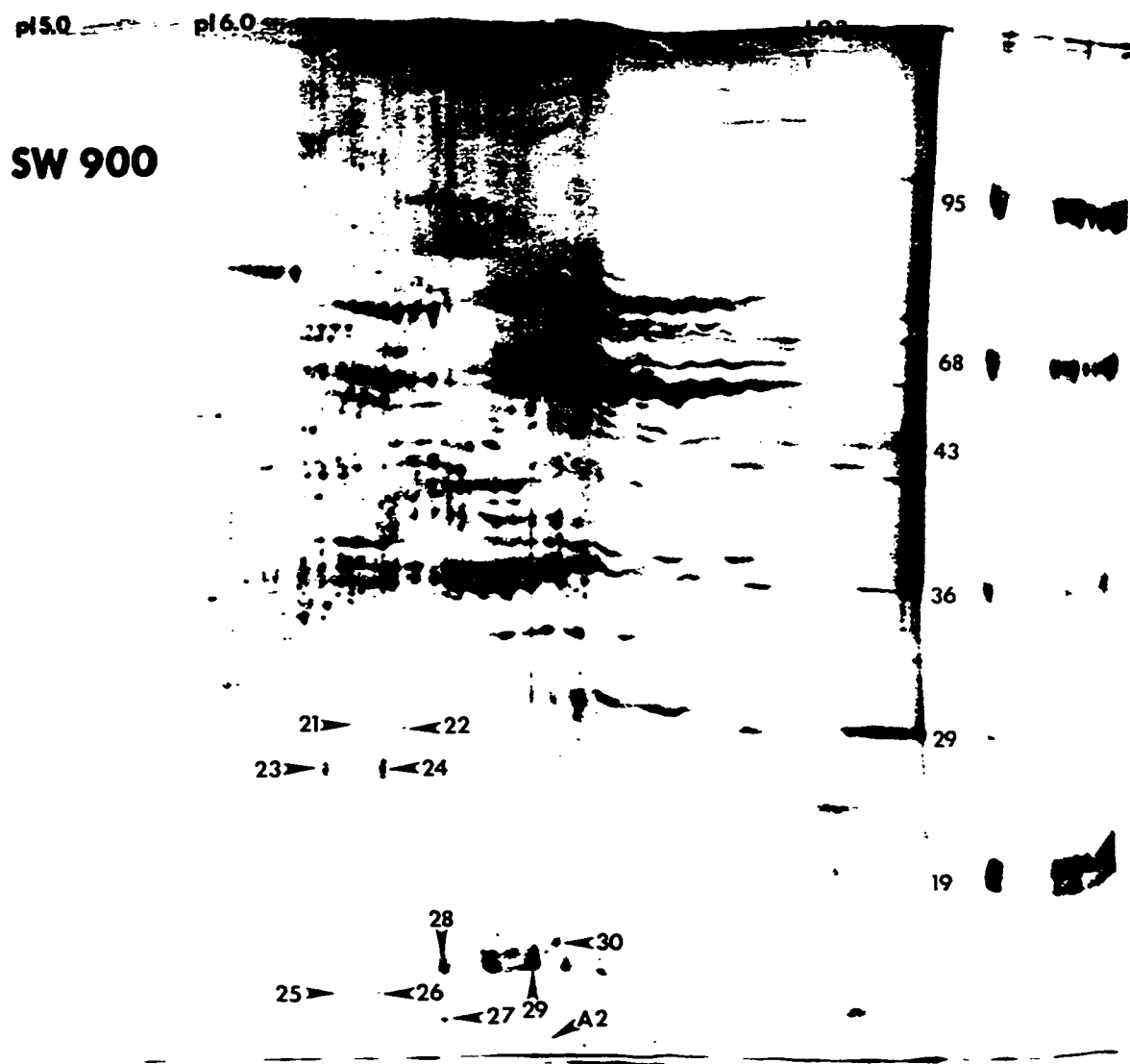
Figure 10A: The human squamous carcinoma cell line SW900 two-dimensional gel. The common squamous cell carcinoma nuclear matrix proteins are labeled 21-30 while the distinct SW900 nuclear matrix proteins is labeled A2.
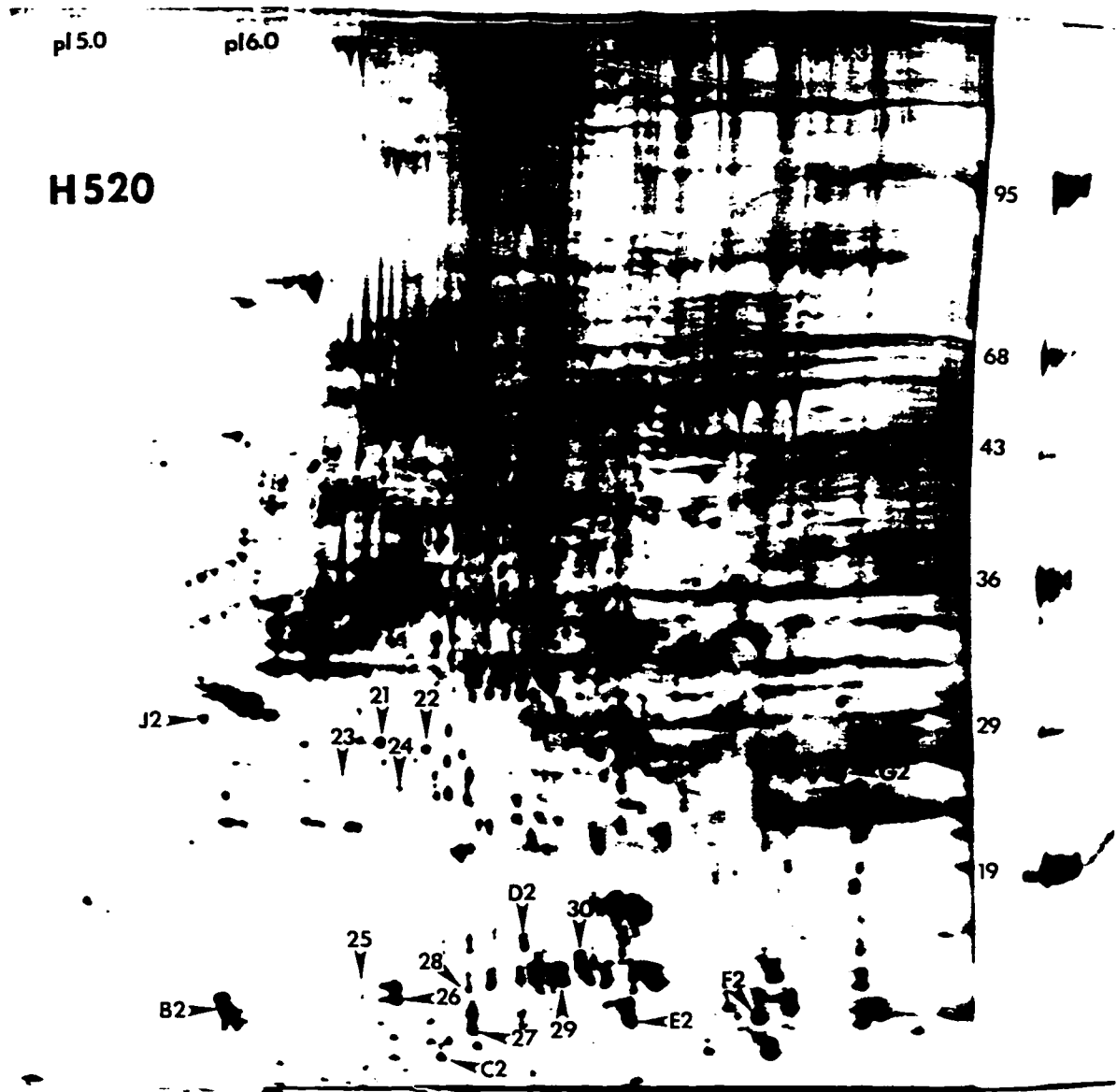
Figure 10B: The human squamous carcinoma cell line H520 two-dimensional gel. The common squamous cell carcinoma nuclear matrix proteins are labeled 21-30 while the distinct H520 nuclear matrix proteins are labeled B2-G2, and J2.
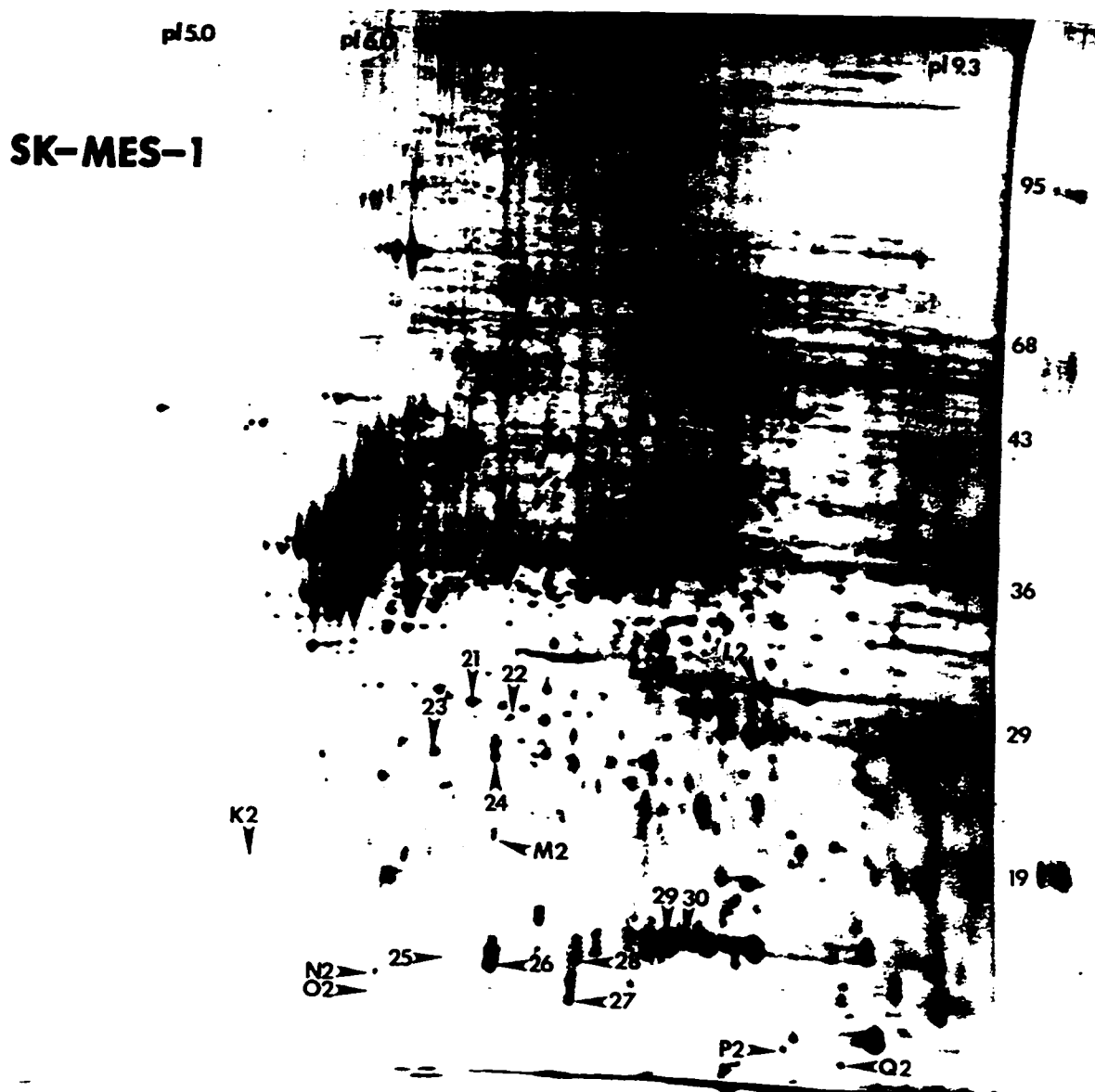
Figure 10C: The human squamous carcinoma cell line SK-MES-1 two-dimensional gel. The common squamous cell carcinoma nuclear matrix proteins are labeled 21-30 while the distinct SK-MES-1 nuclear matrix proteins are labeled K2-Q2.
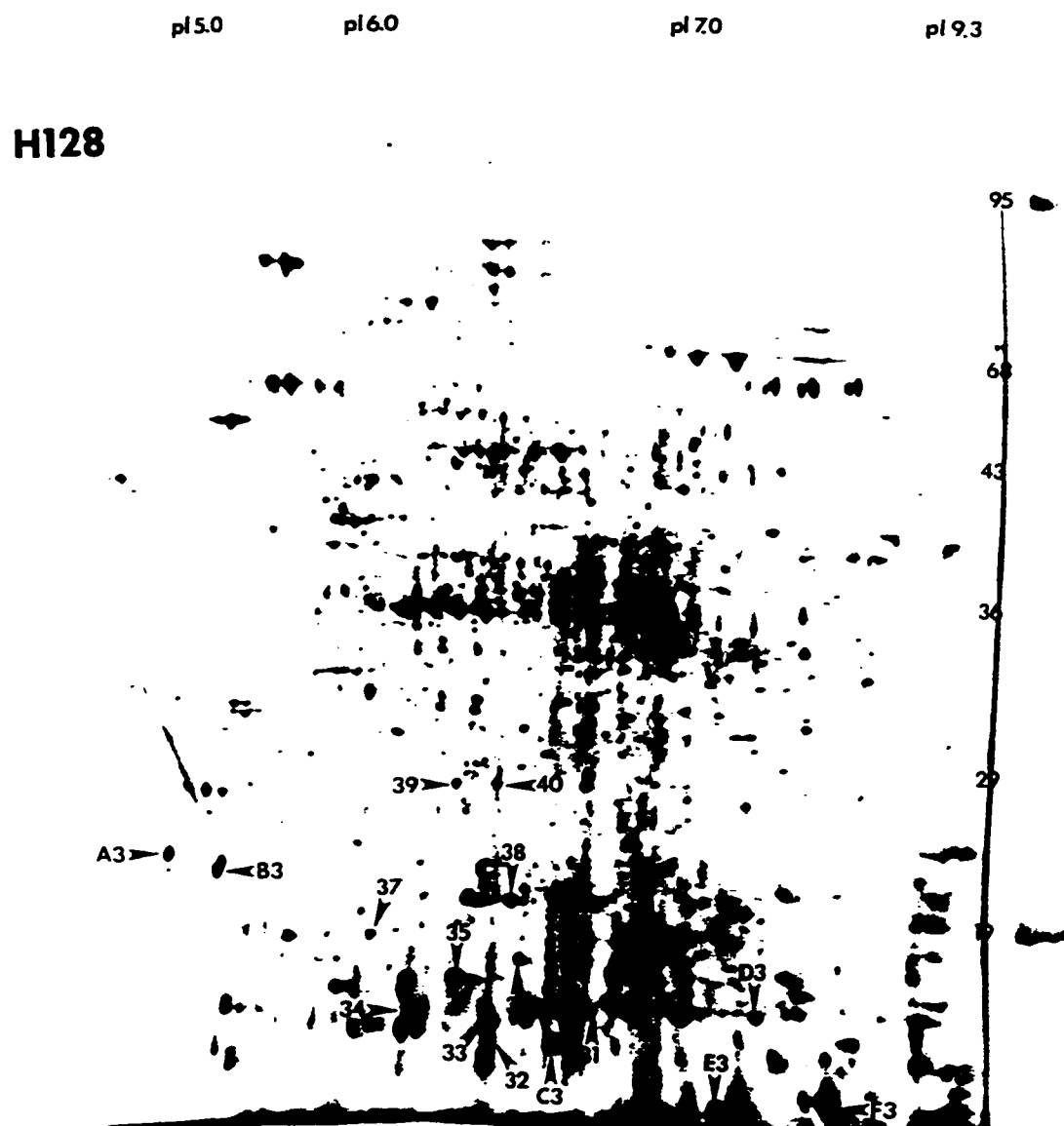
Figure 11A: The human SCLC cell line H128 two-dimensional gel. The common SCLC nuclear matrix proteins are labeled 31-40 while the distinct H128 nuclear matrix proteins are labeled A3-F3.
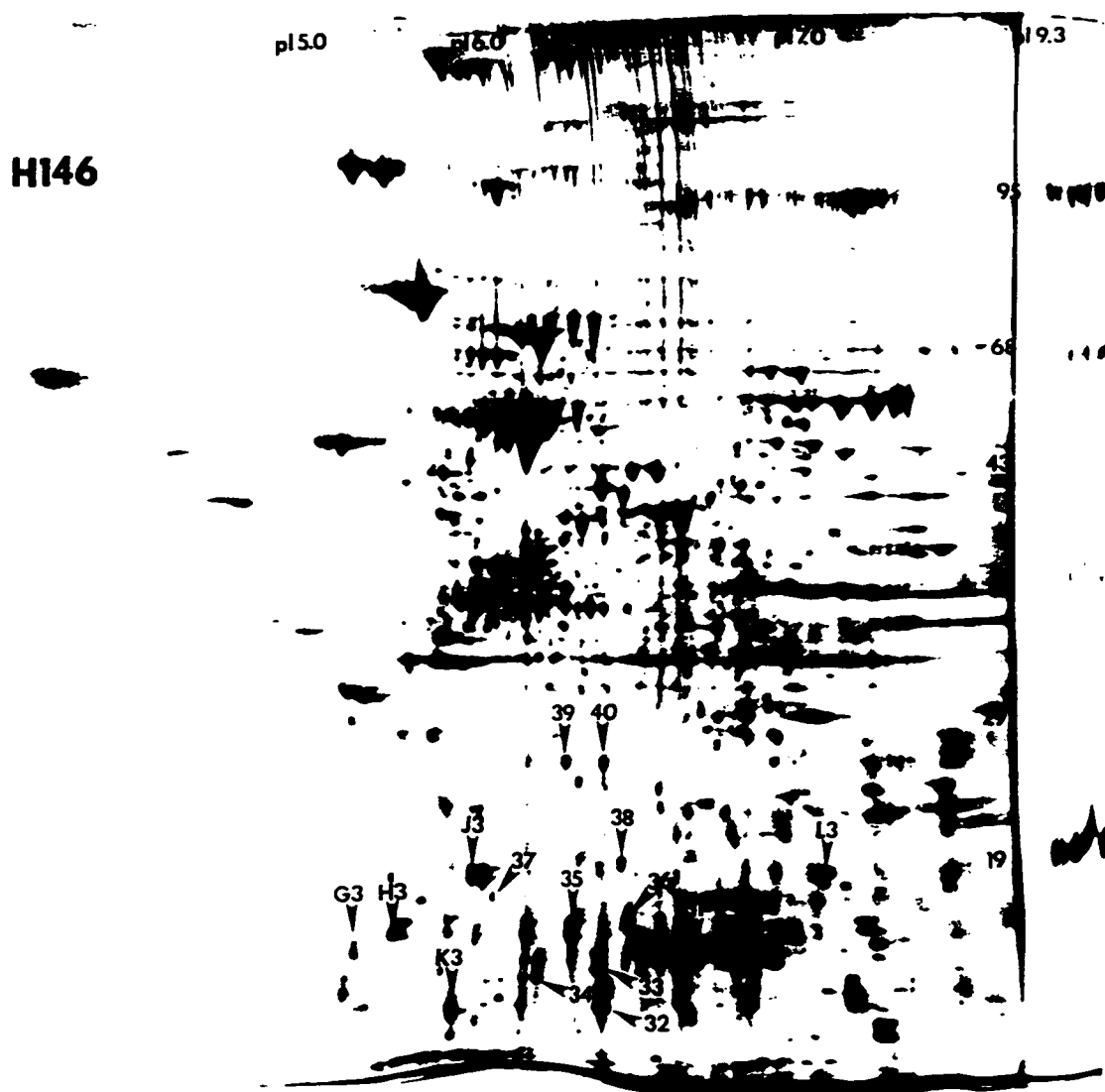
Figure 11B: The human SCLC cell line H146 two-dimensional gel. The common SCLC nuclear matrix proteins are labeled 31-40 while the distinct H146 nuclear matrix proteins are labeled G3, H3, and J3-L3.

Figure 11C: The human SCLC cell line H82 two-dimensional gel. The common SCLC nuclear matrix proteins are labeled 31-40 while the distinct H82 nuclear matrix proteins are labeled M3 and N3.
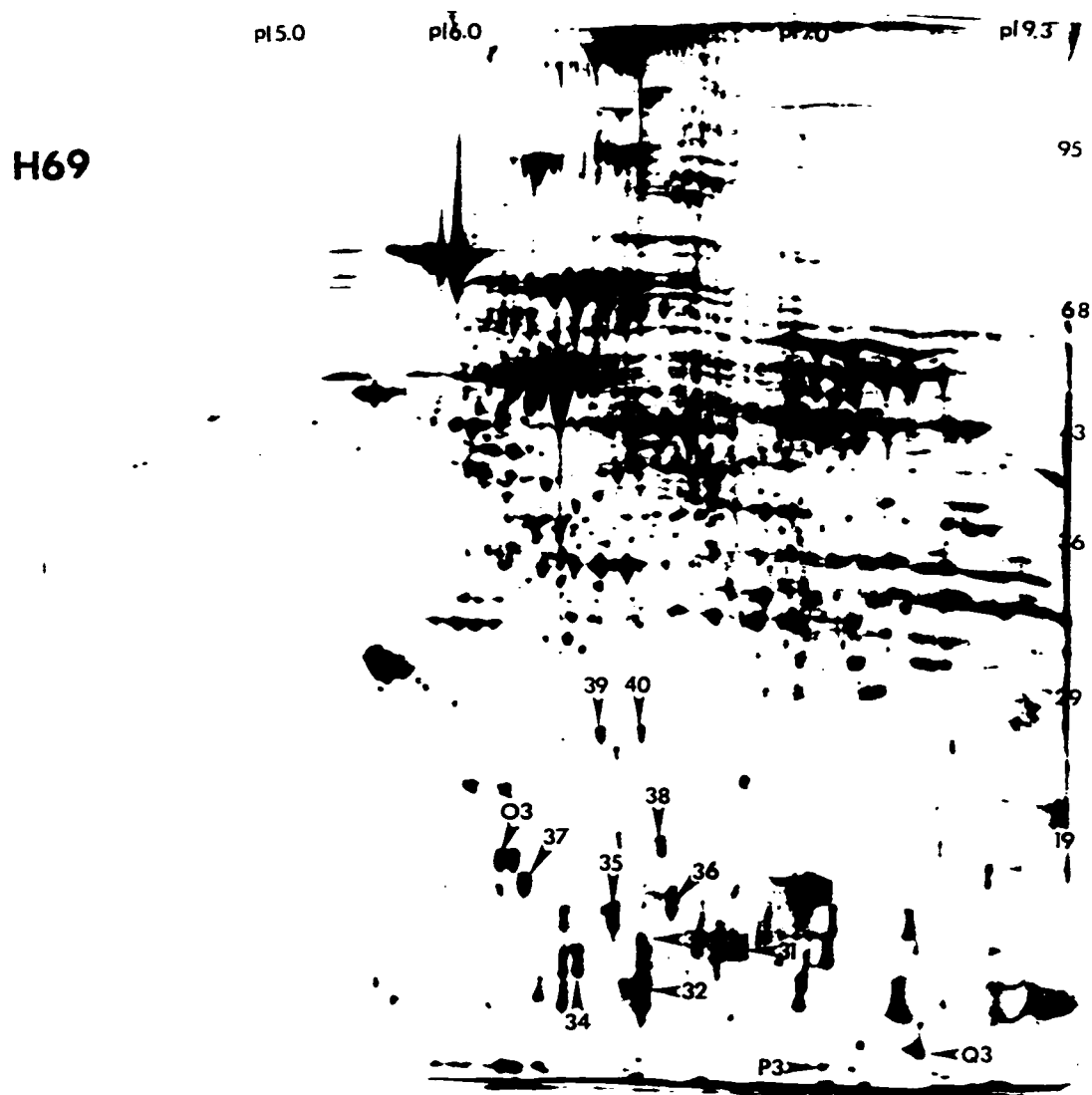
Figure 11D: The human SCLC cell line H69 two-dimensional gel. The common SCLC nuclear matrix proteins are labeled 31-40 while the distinct H69 nuclear matrix proteins are labeled O3-Q3.

pl 5.0   pl 6.0   7.0   pl 9.3

H446

95

68

43

36

R3

39 40   S3

29

T3

U3

V3

38

W3

19

37

36

35

X3

34   33   Y3   Z3

32   31
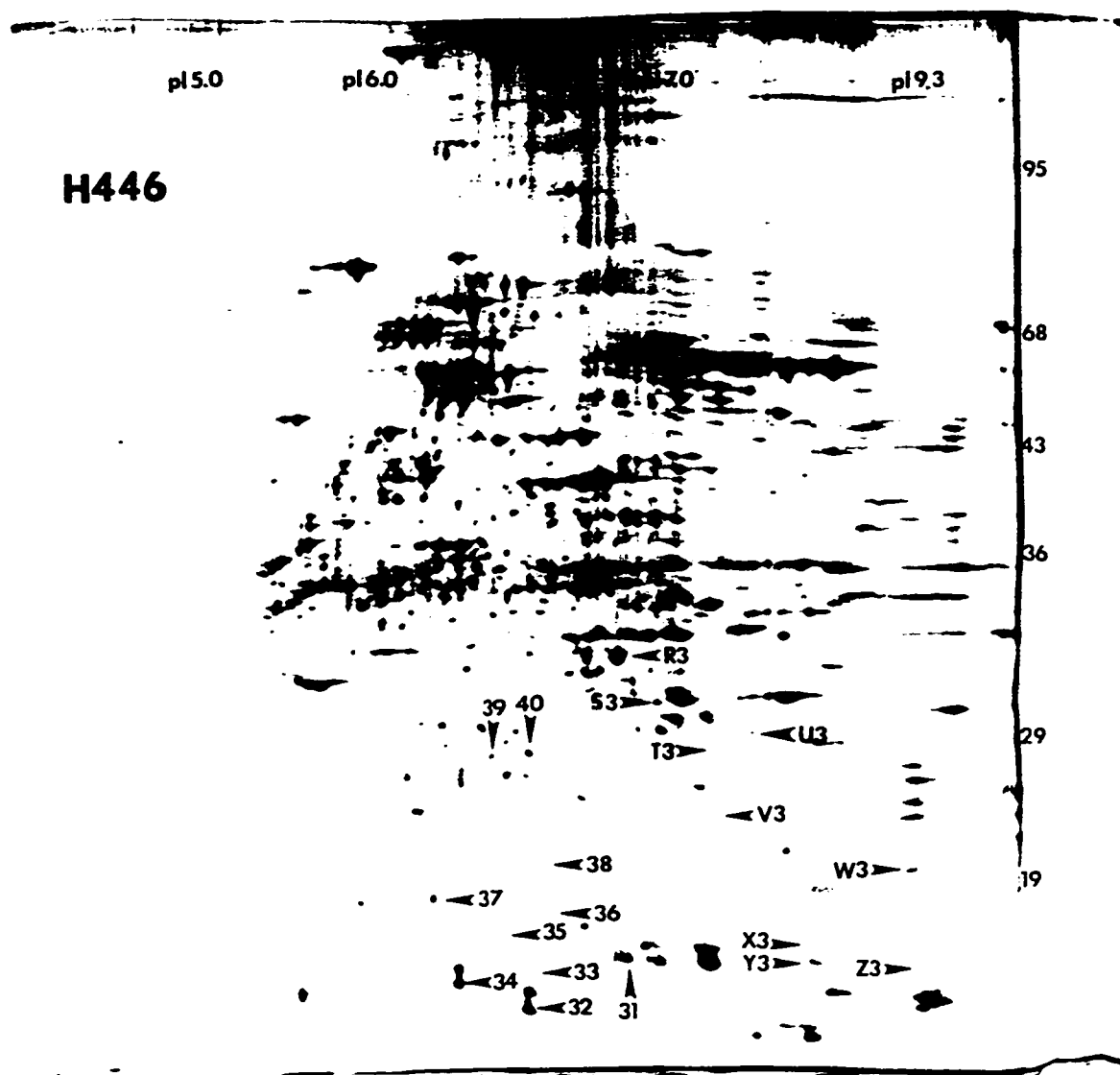
Figure 11E: The human SCLC cell line H446 two-dimensional gel. The common SCLC nuclear matrix proteins are labeled 31-40 while the distinct H446 nuclear matrix proteins are labeled R3-Z3.

Table 3.   Common nuclear matrix proteins identified in the four classes of lung cancer.

Protein	Mass	pI	Protein	Mass	pI
Adenocarcinoma			*Squamous*		
1	22	6.3	21	30	6.4
2	13	6.5	22	29	6.5
3	14	7.2	23	27	6.3
4	14	8.1	24	27	6.4
5	14	9.1	25	15	6.3
6	16	7.5	26	15	6.5
7	28	6.4	27	13	6.7
8	24	6.5	28	15	6.7
9	26	6.3	29	16	7.0
10	14	7.5	30	16	7.0
Large Cell			*SCLC*		
11	15	8.1	31	15	6.6
12	15	9.0	32	13	6.4
13	14	9.3	33	15	6.4
14	12	9.0	34	15	6.2
15	18	8.3	35	16	6.3
16	18	9.5	36	16	6.4
17	15	7.3	37	19	6.0
18	26	8.0	38	19	6.4
19	24	8.0	39	26	6.3
20	20	7.2	40	26	6.4

Table 4. Different nuclear matrix proteins found within each category of lung cancer.

Protein	Mass	pI	Protein	Mass	pI	Protein	Mass	pI	Protein	Mass	pI
Adenocarcinoma			*Large Cell*			H520: F2	13	8.7	H-146: H3	16	5.5
SK-LU-1: A	27	8.0	H-460: A1	13	6.5	H520: G2	24	9.4	H-146: J3	19	6.0
SK-LU-1: B	23	9.3	H-460: B1	14	6.9	H520: J2	28	5.8	H-146: K3	13	5.7
SK-LU-1: C	19	8.3	H-460: C1	13	6.9	SK-MES-1: K2	19	5.4	H-146: L3	19	7.0
SK-LU-1: D	15	7.6	H-460: D1	13	7.1	SK-MES-1: L2	31	7.8	H82: M3	13	5.9
A-427: E	28	9.0	H-460: E1	27	6.0	SK-MES-1: M2	20	6.4	H82: N3	19	8.5
A-427: F	24	7.0	H-460: F1	14	7.9	SK-MES-1: N2	14	6.1	H69: 03	18	6.1
A-427: G	22	8.9	H661: G1	27	8.1	SK-MES-1: O2	13	6.1	H69: P3	11	7.4
A-427: H	18	7.9	H661: H1	24	8.3	SK-MES-1: P2	13	8.0	H69: Q3	12	8.1
A-427: J	16	6.9	H661: J1	23	6.7	SK-MES-1: Q2	12	8.5	H446: R3	33	6.9
A-427: K	15	7.0	H661: K1	20	8.1	*SCLC*			H446: S3	31	7.0
CALU-3: L	22	7.2	H661: L1	23	6.5	H-128: A3	24	4.9	H446: T3	28	7.6
CALU-3: M	22	6.7	*Squamous*			H-128: B3	23	5.0	H446: U3	29	7.8
CALU-2: N	19	6.5	SW 900: A2	10	7.0	H-128: C3	14	6.6	H446: V3	23	7.6
CALU-3: O	16	6.7	H520: B2	15	6.0	H-128: D3	15	7.6	H446: W3	19	9.3
CALU-3: P	15	6.7	H520: C2	12	6.6	H-128: E3	12	7.4	H446: X3	16	8.2
CALU-3: Q	15	6.0	H520: D2	16	6.9	H-128: F3	12	8.2	H446: Y3	15	8.2
CALU-3: R	13	6.0	H520: E2	13	7.9	H-146: G3	15	5.2	H446: Z3	15	9.3

Chapter Four

Identification and Characterization of A Common Nuclear Matrix Protein

Introduction

The nuclear matrix has been suggested to play many roles in the daily functions of the cell. Of the approximately 150 nuclear matrix proteins that can be visualized using high resolution two-dimensional gel electrophoresis, only a small percentage have been characterized. As previously mentioned, analysis of nuclear matrix proteins between normal and cancer cells have been shown to be altered in bladder (Gordon et al., 1993; Getzenberg et al., 1996), prostate (Getzenberg et al., 1991B; Partin et al., 1993), colon (Keesee et al., 1994), breast (Khanuja et al., 1993), lung (Yamazaki et al., 1996), and squamous cell carcinoma of the head and neck (Donat et al., 1996). The majority of investigators have pursued the characterization of nuclear matrix proteins that are present in cancer cells and not in the normal cells. Originally, this was our interest as well. Our laboratory was the first to report that nuclear matrix proteins were altered in normal and breast cancer cells by examining various cell lines as well as human breast tissue (Khanuja et al., 1993). In that publication, four proteins were identified that were found only in the tumor samples. Therefore, it was our intent to characterize one of those four proteins for my thesis work. However, it became obvious that due to differences in the high resolution two-dimensional gel electrophoresis procedures used, I was unable to identify these proteins with absolute certainty. Therefore, it was decided to identify and characterize nuclear matrix proteins that were found to be reproducible in the MCF10A cell line. This chapter describes the analysis of several of these nuclear matrix proteins.

Materials and Methods

Cell Culture

MCF10A cells were a gift from Dr. Herbert Soule (Michigan Cancer Foundation, Detroit, Michigan). The MCF10A cells were grown in 1:1 DMEM/F12 media supplemented with 5% horse donor serum, 1X antibiotic/antimycotic, 10μg/mL insulin, 20ng/mL epidermal growth factor, 100ng/mL cholera toxin, and 0.5μg/mL hydrocortisone. TSU, PC-3, and H661 cells were maintained in RPMI 1640, 10% FBS, and 1X antibiotic/antimycotic. WiDr and A–498 cells were maintained in DMEM, 10% FBS, and 1X antibiotic/antimycotic. All cells were grown at 37°C in 5% CO_2. All cell culture reagents were supplied from Sigma (St. Louis, MO).

Nuclear Matrix Isolation

Nuclear matrix proteins were prepared using published methodologies (Fey and Penman, 1988; Getzenberg et al., 1990). All tissue culture cells were trypsinized and pelleted at 800rpm at 4°C for ten minutes. The dura tumor was removed from a CB17 SCID mouse (Harlan, Indianapolis, IN) while normal human liver tissue had been previously removed from a patient and immediately frozen and stored at –80°C until use. Tissues were immediately placed into 1X phosphate buffered saline (PBS) containing 1.2 mM phenylmethlsulfonyl fluoride (PMSF) on ice to inhibit protease activity. Tissue was homogenized on ice using a douncer followed by filtration through a mesh and centrifuged at 780rpm for ten minutes. Supernatant was removed and the remaining pellets underwent nuclear matrix isolation. Tumor or cell pellets were suspended in cytoskeletal buffer containing 100mM NaCl, 300mM sucrose, 10mM piperazine-N,N'-bis-[2-ethanesulfonic acid] (Pipes) (pH 6.8), 5mM $MgCl_2$, 0.5% Triton X–100, 1.2mM phenylmethylsulfonyl fluoride (PMSF), and 2mM vanadyl adenosine and placed on ice for 20 minutes. The solution was spun at 2,200 rpm for ten minutes at 4°C followed by the addition of an extraction buffer containing 250mM $(NH_4)_2SO_4$, 300mM sucrose, 10mM Pipes (pH 6.8),

5mM MgCl$_2$, 0.5% Triton X-100, 1.2mM PMSF, and 2mM vanadyl adenosine. The solution was incubated for ten minutes on ice. The pellet was resuspended in chromatin buffer [50mM NaCl, 300mM sucrose, 10mM Pipes (pH 6.8), 5mM MgCl$_2$, 0.5% Triton X-100, 1.2mM PMSF, and 100μg/mL DNase I] and incubated for 20 minutes at 20°C.

Samples were centrifuged at 2,200 rpm for ten minutes and resuspended in cytoskeleton buffer containing RNase A [100mM NaCl, 300mM sucrose, 10mM Pipes (pH 6.8), 5mM MgCl$_2$, 0.5% Triton X-100, 1.2mM PMSF, and 25 μg/mL RNase A] for ten minutes at 20°C. After centrifugation at 2,200 rpm for ten minutes, the pellet was dissolved in disassembly buffer [8M urea, 20mM (2-[N-morpholino]ethanesulfonic acid) (MES) (pH 6.6), 1mM ethyleneglycol bis (b-aminoethyl ether)-N,N,N'N'-tetraacetic acid (EGTA), 0.1mM MgCl$_2$, 1% β-mercaptoethanol, and 1.2mM PMSF] and spun at 50,000 rpm for one hour at 15°C. The supernatant was collected and placed into Spectra/Por dialysis tubing (Spectrum Medical Industries, Houston, Texas) and dialyzed for at least 16 hours in a buffer (pH 7.1) containing 0.15M KCl, 25mM imidazole hydrochloride, 5mM MgCl$_2$, 2 mM dithiothreitol, 0.125 mM EGTA, and 0.2mM PMSF. The collected supernatant was centrifuged at 45,000 rpm for 1.5 hours at 25°C. The soluble nuclear matrix proteins were ethanol precipitated at -20°C overnight. All solutions contained freshly prepared PMSF to inhibit serine proteases. The nuclear matrix protein used for two-dimensional electrophoresis was resuspended in 20μL of sample buffer (9M urea, 65mM CHAPS, 140 mM dithiothreitol, and 2.2% ampholytes). The nuclear matrix proteins that were to be run on one-dimensional Western analysis were resuspended in 100-200μL of 1X PBS.

Coomassie Plus assay (Pierce, Rockford, Il) was used for protein determination using bovine serum albumin as a standard. Vanadyl adenosine was purchased from Gibco Life Sciences, (Grand Island, New York). All other chemicals were purchased from Sigma (St. Louis, MO).

High Resolution Two-Dimensional Electrophoresis

High resolution two-dimensional electrophoresis was carried out using the

Investigator 2–D Electrophoresis System from Oxford Glycosystems (Bedford, MA). One

millimeter diameter tube gels [9.5M urea, 2.0% (v/v) Triton X–100, 4.1% acrylamide

solution, 5mM CHAPS, ampholytes, and ammonium persulfate] were cast followed by

pre-focusing until the maximum voltage reached 1500 volts. For gels that were to be silver

stained, 40µg of nuclear matrix protein sample was loaded onto the tube gels and isoelectric

focused for 18,000 volt-hours. For microsequencing and antibody production, 100µg of

nuclear matrix protein sample was loaded onto the tube gels. The isoelectric focusing was

carried out using pH 3–10 ampholytes which have been optimized for separation of cellular

proteins. Tube gels were extruded and incubated in gel equilibration buffer (0.3M Tris

base, 0.075M Tris-HCl, 3.0% sodium dodecyl sulfate, 50mM dithiothreitol, and 0.01%

bromophenol blue) for two minutes at room temperature. Each tube gel was placed on top

of a 10% polyacrylamide gel and run for approximately five hours at 20,000 mW per gel

for gels that were to be silver stained or approximately six to seven hours at 14,000mW for

gels used for microsequencing or antibody production (14,000mW is the recommended

power setting when six or more gels are run simultaneously). Gels that were to be silver

stained were fixed overnight in 50% methanol/10% acetic acid, enhanced with 5%

gluteraldeyde followed by silver staining using an Accurate Chemical silver staining kit

(Accurate Chemical Co., Inc., Westbury, NY) as described elsewhere (Wray et al., 1981).

Gels that were to be used for microsequencing or antibody production were stained using

the technique reverse staining described below. Protein molecular weight standards were

obtained from Diversified Biotechnology (Boston, MA). Isoelectric points were

determined using BDH carbamylated standards (Gallard-Schlesinger, Carle Place, NY) and

Sigma Chemical Co. (St. Louis, MO). Only protein spots clearly and reproducibly

observed in all gels were counted as actually representing the nuclear matrix components.

Reverse Staining of Two-Dimensional Gels

Two-dimensional gels that were used for microsequencing or antibody production underwent a reverse staining procedure for visualization of the nuclear matrix proteins. Reverse staining of the gels have been described elsewhere (Fernandez-Patron et al., 1992). Briefly, gels were rinsed for ten minutes in distilled water, followed by the addition of 0.2M imidazole for 10–15 minutes and slowly agitated. The imidazole was removed and 0.3M $ZnCl_2$ was added for 10–15 seconds and poured off. Protein spots remained clear while gel containing no protein turned opaque. Gels were than stored in water until the nuclear matrix proteins were excised from the gels.

Microsequencing and Peptide Synthesis

Approximately 200 two-dimensional gels were run and reverse stained in order to see the individual nuclear matrix proteins. The proteins KP1–KP5 were extracted from the gel, placed into tubes, and stored at –80°C. All proteins were concentrated onto a 10% vertical gel and blotted onto PVDF nitrocellulose (Bio Rad, Hercules, CA). Several gels were run in order to accommodate all of the protein spots. Membranes were Coomassie Blue stained by wetting the membrane in methanol followed by addition of 0.1% Coomassie R–250 (Sigma, St. Louis, MO) in 40% methanol for no longer than one minute and immediately destained with 50% methanol. Blots were rinsed with distilled water and the appropriate bands cut out of the membranes and sent to the Michigan State University Microsequencing Core Facility (Lansing, MI). Using the microsequencing information, synthetic peptides (KP2A and KP3A) were generated by the Protein Sequencing Core Facility at The University of Michigan (Ann Arbor, MI). In addition, λgt11 peptide fragments were also generated with the same lengths and the approximate dissociation temperatures (Tm) as the KP2A and KP3A peptides.

Northern Analysis

MCF10A total RNA was isolated using Trizol reagent by the manufacturer's protocol

(Gibco BRL Life Science, Grand Island, NY). 500μg of total RNA was further isolated using a PolyAT Tract mRNA Isolation System kit from Promega (Madison, WI) to yield mRNA. 5μg of MCF10A mRNA was diluted to 11μL with formaldehyde loading buffer (0.25% w/v bromophenol blue, 0.25% w/v xylene cyanole, 40% w/v sucrose in water, and ethidium bromide). The mRNA was separated on a 1.2% agarose gel containing 1X MOPS buffer and 2.2M formaldehyde. The running buffer used was 1X MOPS. The gel was run at constant voltage until the bromophenol blue traveled approximately two inches. After washing the gel four times with double-deionized water, the RNA was transferred overnight to a nylon membrane using the TurboBlotter System (Schleicher & Schuell,Keene, NH) following the manufacturer's protocol. The membranes were UV cross-linked and dried for 30 minutes at 80°C in a vacuum oven.

Northern analyses were performed according to standardized protocols. Briefly, membranes were saturated with 10mL of 5X SSC for several minutes at 37°C. The 5X SSC was poured out and replaced with 10mL of prehybridization/hybridization solution (50% formamide, 5X SSC, 1X modified Denhardt's solution, and 250μL of 125μg/mL denatured sheared salmon sperm). The membranes were prehybridized at 37°C for four to six hours. Purified end labeled probes (described later) was added directly to the prehybridization solution and the membranes were hybridized overnight at 37°C. Membranes were washed using buffer A (2X SSC, 0.1% sodium pyrophosphate, and 0.1% SDS) and buffer B (0.2X SSC, 0.1% sodium pyrophosphate, and 0.1% SDS). Membranes were placed on film and exposed at −80°C.

Antibody Production

Polyclonal antibodies were generated by Bethyl Laboratories, Inc (Montgomery, TX). Antibodies were generated against the whole proteins (KP2 and KP3) and the synthetic peptides (KP2A and KP3A) in New Zealand rabbits. Over 200 high resolution two-dimensional gels were run and reverse stained in order to provide adequate amounts of

the KP2 and KP3 proteins for the immunization protocol. The KP2A and KP3A peptides were conjugated to hemocyanin (KHL) to enhance immunoreactivity. All of the antigens were mixed with Freund's adjuvant and injected subcutaneously. 100μg of peptide-carrier peptide was used for each immunization while approximately 50–100μg of whole protein was utilized for each injection. The following immunization protocol was used: Pre-bleeds (control sera) were drawn followed by the first immunization of the whole proteins or carrier peptides (Day 0). The whole proteins KP2 and KP3 were used for the second and third immunizations on days 14 and 28 and the terminal bleeds (TB) collected on day 42. The peptides KP2A and KP3A were injected on Days 14, 28, 42, and 56 followed by terminal bleed collection on day 70. Two rabbits per antigen were immunized due to the genetic variability in response to the antigens or in the case of a rabbit death. The sera underwent immunoglobulin purification using Protein G Hiltrap Columns (Pharmacia Biotech, Pisxataway, NJ) according to the manufacturers' instructions. Briefly, columns were equilibrated with water followed by binding buffer. Sera was loaded onto the columns followed by washing with binding buffer. Material was eluted from the columns by using elution buffer and fractions were collected. Antibodies were then stored at 4°C.

cDNA Libraries

MCF10A cells were grown and cell pellets isolated. Cells were stored at –80°C and sent on dry ice to Clontech Laboratories, Inc (Palto, Alto, CA) where the unamplified and amplified λgtll cDNA libraries were constructed using a modified Gubler and Hoffman procedure (Gubler and Hoffman, 1983). The unamplified library was prepared from mRNA using unique oligo(dT) primers. EcoR1 adaptors were ligated prior to the cloning into the λgt11 vector. The insert range size varied from 0.5–3.0kb with the average insert size of 1.9kb. The unamplified library was divided into two tubes with the titers 2.0×10^5 pfu/mL (120μL) and 1.5×10^6pfu/μL (160μL) while the amplified library titer was

>10^9pfu/mL. The libraries were maintained under proper conditions suggested by Clontech to in order to maintain the titers. Specifically, working library aliquots were kept at 4°C and are stable for six months. Long term storage involved the removal of 50μL aliquots, addition of dimethyl sulfoxide to a final concentration of 7%, followed by storage at –70°C which can maintain the library titer constant for years. The bacterial host strain utilized with the λgt11 phage was the *E. coli* strain Y1090r⁻.

Y1090r⁻ Bacterial Culture Plating

The Y1090r⁻ stock was stored at –20°C in 25% glycerol until use. 5μL of the Y1090r⁻ strain was streaked onto a $MgSO_4$-free LB agar plate containing 50μg/mL ampicillin which was added to the LB agar after the solution had cooled to below 50°C (master plate). The agar plates were made several days prior to streaking and checked for contamination by allowing the inverted plates to incubate at 37°C overnight. Streaked Y1090r⁻ plates could be used for up to two weeks. After streaking, the plates were incubated in a 37°C incubator overnight to allow growth of the colonies. A single isolated colony from the master plate was streaked onto another $MgSO_4$-free LB agar plate containing 50μg/mL ampicillin and incubated inverted at 37°C overnight (primary working plate). Bacterial plates were stored at 4°C wrapped in parafilm when not in use.

Library Titering

A single, isolated colony from the Y1090r⁻ primary working plate was used to inoculate a flask containing LB broth supplemented with 10mM $MgSO_4$ and 0.2% maltose. The flask was incubated on a shaker at 200rpm overnight at 37°C with proper aeration. The cultures were analyzed to ensure that the bacteria was in the log phase of growth by measuring the optical density (OD) on a spectrophotometer. 1X lambda dilution buffer was used for all library lysate dilutions. 10X lambda dilution buffer contained 1.0M NaCl, 0.1 $MgSO_4$•7H_2O, and 0.35M Tris-HCl (pH 7.5). The 10X lambda dilution buffer was

autoclaved and stored at 4°C. The 10X buffer was diluted by ten-fold and sterile gelatin

(0.01%) was added to make the 1X lambda dilution buffer which was also stored at 4°C.

2μL of the library lysate was diluted into one mL of 1X lambda dilution buffer (dilution 1).

2μL of dilution 1 was diluted into a second tube containing 1 mL of 1X lambda dilution

buffer (dilution 2). Preparation of the titering dilutions of phage lysate were divided into

four tubes: tube one (100μL 1X lambda dilution buffer, 200μL of Y1090r⁻ culture, and

2μL of phage dilution 2); tube two (100μL 1X lambda dilution buffer, 200μL of Y1090r⁻

culture, and 5μL of phage dilution 2); tube three (100μL 1X lambda dilution buffer, 200μL

Y1090r⁻ culture, and 10μL phage dilution 2); and tube four (control) (100μL 1X lambda

dilution buffer, 200μL Y1090r⁻ culture, and 0μL phage dilution 2). Tubes were mixed and

incubated at 37°C for 15 minutes. Seven mLs of melted LB soft top agarose + 10mM

MgSO₄ was added to each tube and mixed well. LB soft top agarose contained LB broth,

7.2g/L agarose, and 10mM MgSO₄ which was then autoclaved and stored at 4°C. This

solution was melted in a microwave oven and cooled in a water bath to below 45°C prior to

use. After the 15 minute incubation, the contents of the tubes were poured onto 150mm

LB-agar + 10mM MgSO₄ plates, which were previously warmed to 37°C. Plates were

swirled quickly to ensure even spreading of the agar. Plates were cooled at room

temperature for approximately ten minutes to allow the agar to harden. Plates were inverted

and incubated at 42°C for five to eight hours. Plaques were counted and the titer

determined using the following equation:

$$pfu/mL = \frac{no.\ of\ plaques}{\mu L\ used} \times Dilution\ Factor \times 10^3 \mu L/mL$$

Library Screening

The library screening methods used were provided by Clontech, Inc. A single,

isolated Y1090r⁻ colony from the primary working plate was used to inoculate LB broth +

MgSO₄ + 0.2% maltose. Flasks were incubated with good aeration at 37°C at 200rpm

overnight. Based on the calculated titer, dilutions of the library stock were made yielding

approximately 30,000pfu for each 150mm plate. Dilutions were gently mixed with 200μL

of Y1090r⁻ culture and incubated at 37°C for 15 minutes. Seven mLs of melted soft top

agarose + 10mM MgSO₄ were added to the tubes, mixed, and poured onto prewarmed LB

agar + MgSO₄ plates. Plates were allowed to set followed by inversion and incubation at

42°C until the plaques reached a diameter not exceeding 1.5mm or were just beginning to

make contact with one another (five to eight hours). Plates were placed at 4°C for at least

one hour to allow the LB soft top agarose to harden. Plates could then be stored at 4°C

overnight wrapped in parafilm. Protran nitrocellulose membranes (Schleicher and Schuell,

Keene, NH) were labeled with a pencil and placed onto the plates using sterile forceps

taking care not to trap any air bubbles. The membranes and plates were marked in three

asymmetrical locations by stabbing through the filter and into the agar with an 18-gauge

needle. After two minutes, the membranes were carefully peeled off of the plates and

floated on top of DNA denaturing solution (1.5M NaCl and 0.5N NaOH), plaque-side up,

for 30 seconds. The membranes were then immersed into the denaturing solution for five

minutes. The membranes were then placed into neutralizing solution [1.5M NaCl and

0.5M Tris-HCl (pH 8.0)] for five minutes. Membranes were briefly rinsed in 2X SSC

(0.3M NaCl, 0.03M sodium citrate•2H₂O, pH 7.4) and placed onto Whatman 3M paper

plaque side-up to dry. A second membrane was placed onto the same plate using the same

procedure as described above except that the membrane remained on the plate for three

minutes. A Stratalinker UV crosslinker (Stratagene, La Jolla, CA) was used to fix the

DNA to the membranes. If necessary, membranes were stored at 4°C wrapped in saran

wrap. Membranes were then incubated in prehybridization solution (6X SSPE, 5X

Denhardt's solution, 0.25% sodium dodecyl sulfate, and 100 μg/mL denatured salmon

sperm DNA) at 42°C overnight in Belco Glass Inc. hybridization ovens (Vineland, NJ).

Stock solutions of SSPE and Denhardt's solution were made as follows: 20X SSPE (3M NaCl, 0.2M NaH$_2$PO$_4$•H$_2$O, 0.02M EDTA; pH 7.4) and 50X Denhardt's solution [5g ficoll, 5g polyvinylpyrrolidone, and 5g BSA (Pentax-fraction V) dissolved in 500mL of water]. The 50X Denhardt's solution was aliquoted and stored at –20°C. Up to five membranes could be placed into each bottle. Individual membranes were separated by mesh (Belco Glass Inc., Vineland, NJ) and great care was taken to avoid air bubbles to ensure that all membranes came in direct contact with the prehybridization solution. Labeled KP2 or KP3 probes (one million cpm/mL prehybidization solution) were added to the bottles and incubated at 42°C overnight. The radioactive hybridization solution was carefully discarded and the membranes were washed with buffer A (2X SSC and 0.5% SDS) and buffer B (1X SSC and 0.1% SDS). Once the appropriate background was reached, the membranes were sealed in plastic bags, and exposed to film overnight at –80°C. Developed films were examined for positive plaques. If a positive plaque was seen, the primary plaque was picked and placed into 1mL of 1X lambda dilution buffer and stored at 4°C. The primary plaques were re-plated, hybridized, and washed using the same protocols described above. Positive plaques were selected and stored in 1mL of lambda dilution buffer (secondary plaques). The secondary plaques were then re-screened and positive plaques were picked (tertiary plaques) and stored at 1X lambda dilution buffer at 4°C.

Preparation of Y1090r⁻ Lysates and Isolation of Phage DNA

In order to verify the validity of the tertiary clones, all tertiary clones underwent Southern analysis. A Y1090r⁻ culture was grown overnight, pelleted, and resuspended in 0.5X volume of 10mM MgSO$_4$. 100μL of the tertiary plaque elute was combined with 1.0mL of Y1090r– cells, inverted 10–15X, and incubated at 42°C for 15 minutes. 30mL of LB broth + 5mM CaCl$_2$ (prewarmed to 37°C) was added to 125mL polypropylene screw-cap bacterial culture flasks followed by the addition of the 1.1mL of the Y1090r⁻ and tertiary phage solution. Flasks were incubated at 37°C for approximately three hours at

200rpm. If after three hours, there is no evidence of lysis (i.e., LB broth is clearing while white debris is accumulating in the broth), 10mL of the culture was removed and added to a new 125mL screw-cap flask and 20mL of warmed LB broth + 5mM $CaCl_2$ (1:3 dilution) and incubated for approximately two hours at 37°C at 200rpm. If there is still no lysis seen after two hours, the 1:3 dilution was repeated and the flask was incubated at 37°C at 200rpm for an additional two hours. After the lysis was complete, the solution was placed into a 50mL polypropylene centrifuge tube, 100µL chloroform was added, the tubes mixed, and centrifuged at 3500rpm at 4°C for 12 minutes to pellet the bacterial debris. 25mL of the lysate was removed to a 50mL polypropylene centrifuge tube while 1.5mL of the lysate was added to 2.2mL eppendorf tubes for storage at 4°C. 25µL of DNase I (10,000 units/mL), 25µL of RNase A (1mg/mL), and 25mL of 20% PEG+2M NaCl in 1X lambda dilution buffer was added to the 25mL lysate. Tubes were mixed, incubated on ice for 1.5 hours, and centrifuged at 7500rpm at 4°C for 1.25 hours to form phage/PEG pellets. The supernatant was discarded and the tubes were allowed to dry for five minutes followed by the addition of 350µL of 1X lambda dilution buffer to resuspend the pellets. The solution was transferred to a 1.5mL eppendorf tube and centrifuged at 12,000rpm for 30 seconds. The aqueous phase was placed into a 1.5mL eppendorf tube followed by the addition of 18µL of 0.5M EDTA and 45µL of 10% SDS + 5mg/mL proteinase K. Tubes were vortexed and incubated at 48°C overnight. Samples were extracted twice with phenol/chloroform, once with chloroform, then ethanol precipitated by using 1/3 volume of 10M NH_4OAc combined with 3 volumes of 100% ethanol. DNA was pelleted at 12,000rpm for 15 minutes. The pellets were washed with 70% ethanol and resuspended in 50–100µL sterile water and stored at –20°C. DNA concentrations were measured using a spectrophotometer.

Isolation and Amplification of cDNA Insert

Polymerase chain reaction (PCR) using primers flanking the cloning site was used

to quickly characterize positive clones [λgt11 LD-insert screening amplimer sets from

Clontech (Palo Alto, CA)] following the manufactor's protocol. Specifically, 36μL of

PCR-grade water, 5μL 10X KlenTaq PCR reaction buffer, 1μL 5' LD amplimer, 1μL 3'

LD amplimer, 1μL 50X dNTP mix, 1μL 50X Advantage KlenTaq polymerase mix, and

5μL of phage DNA were added to a tube, vortexed, spun briefly, and a few drops of

mineral oil added. (5μL of control template used for the positive control, while 5μL of

sterile water was used for the negative control). Thermal cycling was commenced using a

Perkin Elmer Cetus DNA thermal cycler (Norwalk, CT) using the following cycle

parameters: 94°C for one minute followed by 35 cycles of 94°C for 30 seconds and 68°C

for three minutes, ending with 68°C for three minutes. Samples were combined with a gel

loading solution (Sigma, St. Louis, MO) and immediately loaded onto a 1% agarose gel for

Southern analysis.

Southern Analysis

PCR amplified samples were loaded onto a 1% agaraose gel (2g agarose, 4mL 50X TAE,

200mL sterile water, and 5μL ethidium bromide) and separated using 1X TAE running

buffer at 100 volts. Gels were placed into denaturing buffer (0.5M NaOH and 1.5M NaCl)

for 30 minutes at room temperature with gentle agitation. Gels were rinsed with distilled

water and transferred to neutralizing buffer (3M NaCl, 0.3 $Na_3C_6H_5O_7 \cdot 2H_2O$, pH 7.0) and

slowly agitated for 30 minutes at room temperature. Gels were soaked in 20X SSC (0.5M

Tris-HCl, pH 7.0 and 1.5M NaCl) for 30 minutes at room temperature with gentle

agitation. Transfer of the DNA onto nitrocellulose membranes was accomplished by using

the TURBOBLOTTER Rapid Downward Transfer System (Schleicher & Schuell, Keene,

NH) using the manufacturers' instructions. Specifically, Nytran nitrocellulose membranes were immersed in distilled water followed by immersion in 20X SSC for five minutes. The blotting assembly was assembled and the transfer was accomplished overnight at room temperature using 20X SSC as the transfer buffer. Membranes were washed in 2X SSC for five minutes, followed by UV crosslinking and baking at 80°C for 30 minutes. Membranes were placed into prehybidization solution (6X SSPE, 5X Denhardt's solution, 0.25% sodium dodecyl sulfate, and 100µg/mL denatured salmon sperm DNA) and incubated at 42°C overnight. Probes were then added and allowed to hybridize overnight at 42°C. Membranes were washed with buffers A and B until the proper level of background was reached. Membranes were sealed and exposed to film at –80°C overnight. Films were developed and analyzed.

Labeling of the probes

All probes were end labeled by T4 polynucleotide kinase in the same manner. The following contents were combined into a tube: 100ng unlabeled DNA, 1.5µL T4 Polynucleotide Kinase (10,000U/mL), 1.5 µL of 10X T4 Polynucleotide Kinase buffer (New England Biolabs, Beverly, MA), and 100µCi γ-^{32}P (NEN Life Science Products, Boston, MA). Sterile water was used to bring the final volume up to 15µL. Tubes were place into a thermocycler and incubated at 37°C for one hour. In order to eliminate unincorporated radionucleotides, labeling reactions were loaded onto SELECT G-25 spin columns (5 Prime-3 Prime Inc., Boulder, CO) and utilized according to the manufacturers' instructions. Probes were counted using a scintillation counter, and used immediately or stored at –20°C.

Western Analysis

Ethanol precipitated nuclear matrix proteins were resuspended into 1X PBS and the

concentrations determined using bovine serum albumin as a standard. 10μg of the nuclear

matrix samples mixed with a SDS reducing sample buffer were loaded onto a Mini-

PROTEAN II electrophoresis system (Bio Rad, Hercules, CA) utilizing 10%

polyacrylamide gels [5mL 30% acrylamide/0.8% bisacrylamide, 3.75 mL 1.5M Tris-

HCl/0.4% SDS (pH 8.8), and 6.25mL sterile water]. The gel solution was degassed

followed by the addition of ammonium persulfate (APS) and TEMED to initiate

polymerization. The stacking gel was composed of 650μL 30% acrylamide/0.8%

bisacrylamide, 1.25mL of 0.5M Tris-HCl/0.4% SDS (pH 6.8), and 3.05mL sterile water.

The solution was degassed and APS and TEMED were added. Nuclear matrix samples

were boiled for four minutes prior to loading. BENCHMARK prestained protein ladder

standards (GibcoBRL Life Sciences, CA) were also loaded in order to follow the

electrophoretic and blotting processes. Gels were run at 100 volts followed by incubation

in blotting buffer (25mM Tris, 192mM glycine, and 20% v/v methanol, pH 8.3) for 30

minutes with gentle agitation. Gels were than transferred onto Hybond ECL nitrocellulose

membrane (Amersham Life Science, Buckinghamshire, England) using the Mini Trans-

Blot Electrophoretic Transfer Cell (Bio Rad, Hercules, CA). The blotting apparatus was

assembled according to the manufacturers' protocols and blotted for one hour at 100 volts.

Membranes were immediately placed into blocking solution [10% nonfat dried milk in 1X

TBS-T (20mM Tris base, 137mM sodium chloride, pH 7.6, and 0.1% Tween-20)]

overnight at 4°C with gentle agitation. All antibodies generated by Bethyl Labs were used

at a 1:10,000 dilution in 1X TBS-T and incubated with the membranes for one hour at

room temperature with gentle agitation. Membranes were extensively washed with 1X

TBS-T followed by a one hour incubation with a 1:22,000 dilution of a goat anti-rabbit IgG

conjugated to horseradish peroxidase (Pierce, Rockford, Il). Membranes were extensively

washed and developed using the ECL Western blotting detection system (Amersham Life

Science, Buckinghamshire, England) following the manufacturers' instructions.

Membranes were exposed to Hyperfilm-ECL (Amersham Life Science, Buckinghamshire,

England) and developed.

Immuocytology

Immunocytology was performed using the UniTect Immunohistochemistry Detection Systems from Oncogene Science Inc (Uniondale, NY) following the manufacturers' instructions. This system employs an amplified biotin-streptavidin technology which is visualized using an avidin-biotinylated horseradish peroxidase complex followed by localization by a DAB (diaminobenzidine tetrahydrochloride) substrate. Cells were plated onto LAB-TEK II glass chamber slides (Nalge Nunc Int., Naperville, Il) and grown for several days. Cells were fixed using a 50:50 solution of acetic acid and methanol for 15 minutes at 4°C. Slides were rinsed with several washes of 1X PBS followed by incubation with normal goat serum in 1X PBS for 20 minutes at room temperature with gentle agitation to suppress non-specific binding of IgG. Slides were washed with 1X PBS and incubated with 1:5,000 dilutions of the KP3A antibodies (terminal bleeds or prebleeds) diluted in 1% (w/v) bovine serum albumin in 1X PBS for one hour at room temperature with gentle agitation. Slides were rinsed with three changes of 1X PBS for five minutes each followed by incubation with a biotinylated affinity-purified secondary IgG for 30 minutes at room temperature with gentle agitation. Slides were rinsed with three changes of 1X PBS for five minutes each and incubated with an avidin-biotinylated horseradish peroxidase macromolecular complex (ABC reagent) for 30 minutes at room temperature with gentle agitation. Slides were washed extensively with 1X PBS and incubated with DAB substrate (Sigma, St. Louis, MO) for approximately five minutes and rinsed in distilled water. Slides were counterstained in hematoxylin (Sigma, St. Louis, MO) for five minutes and rinsed in distilled water. Slides were mounted with coverslips and examined using light microscopy using a Zeiss Axioskop Microscope (Germany).

Dual Fluorescence Studies

Cells were plated onto chamber slides and allowed to grow. Cells were fixed with

a 50/50 solution of acetic acid and methanol for 15 minutes at 4°C. Slides were rinsed and

blocked in 10% goat serum for 20 minutes at room temperature. Slides were rinsed in 1X

PBS and incubated in a 1:5,000 dilution of KP3A antibodies (pre-bleed and terminal bleed)

and coincubated with a 1:1,000 dilution of one of the following antibodies: mouse IgG_{2A}

PCNA (proliferating cell nuclear antigen) (PharmMingen, San Diego, CA), mouse IgG_1

Ki-67 (PharmMingen, San Diego, CA), or mouse IgG_1 NuMA (Oncogene Research

Products, Cambridge, MA). These primary antibodies were diluted in 1% (w/v) bovine

serum albumin in 1X PBS for one hour at room temperature with gentle agitation. Slides

were rinsed with 1X PBS several times followed by incubation in a 1:250 dilution of either

sheep anti-mouse IgG2a antibody conjugated to rhodamine or goat anti-mouse IgG1

antibody conjugated to FITC (Nordic Immunology, Tilberg, Netherlands) in 1% (w/v)

BSA in 1X PBS for one hour at room temperature with gentle agitation. Slides were

extensively washed and coverslips mounted. Slides were viewed using a Zeiss Axioskop

Microscope (Germany) using the appropriate filters.

Synchronizing Cell Experiments

The human prostate cancer cell line PC-3 was plated onto two-well Lab-Tec II glass

chamber slides (Nalge Nunc Int, Naperville, IL) in RPMI 1640, 10% FBS, and 1%

antibiotic/antimycotic and incubated for 24 hours at 37°C in 5% CO_2. Media was removed

and replaced with media containing 2.5mM thymidine (Sigma, St. Louis, MO). After 16

hours, the thymidine containing media was removed and the slides were rinsed with fresh

media to ensure the complete removal of the thymidine. Cells were incubated with fresh

media (containing no thymidine) for nine hours followed by an additional incubation with

media containing 2.5mM thymidine for 14 hours. Cells were rinsed with fresh media and

released by incubation with media containing no thymidine. Slides were fixed with a 50/50

solution of methanol and acetic acid at various timepoints. Slides were incubated in a

1:5,000 dilution of KP3A terminal bleed antibody or the KP3A pre-bleed control diluted in

1X PBS with 1% (w/v) BSA and developed using the Oncogene Science UniTect

Immunohistochemistry Detection Systems (Uniondale, NY) and viewed under light microscopy as previously described.

Results

In order to begin the characterization process, MCF10A cells were grown and nuclear matrix proteins were isolated. In order to visualize the individual nuclear matrix proteins, high resolution two-dimensional gels were run, silver stained, and analyzed. When the MCF10A gels were compared, it was found that there were several proteins that were reproducible from gel to gel. The reproducible nuclear matrix proteins that were selected for further study were protein 1 (15kD, pI 7.2), protein 2 (32kD, pI 6.5), protein 3 (33kD, pI 6.3), protein 4 (15kD, pI 6.2), and protein 5 (10kD, pI 6.5) (Figure 12). These five proteins were low in their molecular weights, therefore, increasing the success rate of obtaining microsequencing information. When other two-dimensional gels from other cells and tissues were analyzed, it was noticed that these five proteins were also present (data not shown). Specifically, these five proteins were present in the nuclear matrix of human prostate cancer cells, human lung carcinoma gels, normal human breast tissue, and human breast carcinoma tissue lending to the notion that these nuclear matrix proteins may belong to the common set of nuclear matrix proteins that have been previously observed by many investigators. Over 200 high resolution two-dimensional gels were run in order to accumulate adequate amounts of protein for microsequencing analysis. Gels used for this purpose were visualized using a technique referred to as reverse staining. This method was selected because it is well known that the commonly used methods for protein staining, such as Coomassie Blue, dramatically reduce protein recovery from gels. In contrast, reverse staining has been shown to allow efficient recovery of proteins along with successful acquisition of microsequencing information (Fernandez-Patron et al., 1992). Reverse staining utilizes imidazole-zinc staining which causes the gels to turn opaque while the protein spots remain clear. Using the silver stained MCF10A two-
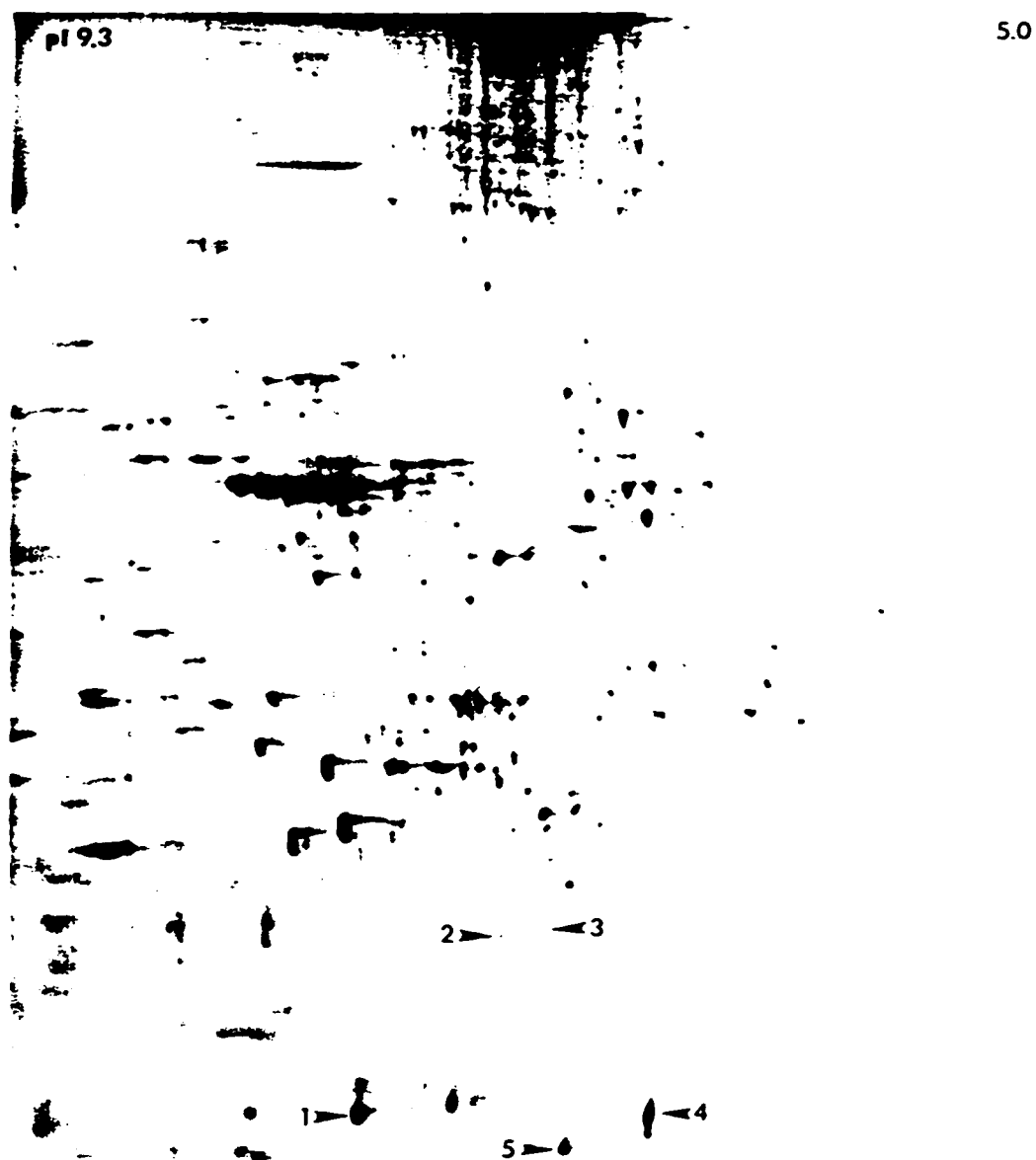
Figure 12. Two-dimensional gel of the MCF10A nuclear matrix proteins. The common nuclear matrix proteins that were selected for further characterization were labeled 1-5.

dimensional gels as guides, proteins 1–5 were excised from gels. These protein spots were concentrated using a one-dimensional electrophoresis system and blotted onto membrane. The protein bands were excised and sent for microsequencing analysis at The Michigan State University Microsequencing Core Facility.

Unfortunately, when the microsequencing analysis was complete, amino acid sequence was only available for two of the five proteins. Specifically, protein 2 (KP2) contained the seven amino acid sequence: Val/Gly/Ile/Met/Ser/Thr/Gly, while protein 3 (KP3) contained the eleven amino acid sequence:

Ala/Ala/Ser/Phe/Asp/Thr/Val/Pro/Leu/Asp/Lys.

Several explanations for the microsequencing failure of proteins 1, 4, and 5 include the possibility that the proteins were N-terminally blocked or that there was not enough protein for the analysis. The KP2 and KP3 amino acid sequences were analyzed using GENBANK, however, due to the small size of the sequences, this information was of little use. In order to verify the validity of these sequences, Northern analysis was utilized. A Northern blot containing MCF10A mRNA was hybridized with the KP2 and KP3 peptide fragments and the results are shown in Figure 13. Several bands (approximately 1 and 7Kb) were observed in the blot hybridized with the KP3 peptide fragment. In addition, it also appears that the KP3A fragments are also hybridizing to a ribosomal band (18S) as well. No bands were seen in the blots incubated with the KP2A peptide fragment (data not shown).

Next, these amino acid sequences were used to generate the best possible degenerate oligonucleotide for each protein and used to screen cDNA libraries in order to isolate the DNA sequences responsible for the production of the KP2 and KP3 proteins. In addition, the amino acid sequences were also used to generate peptide fragments from The University of Michigan Protein Core Facility. In order to continue to characterize the nature of these unknown nuclear matrix proteins, polyclonal antibodies were generated in
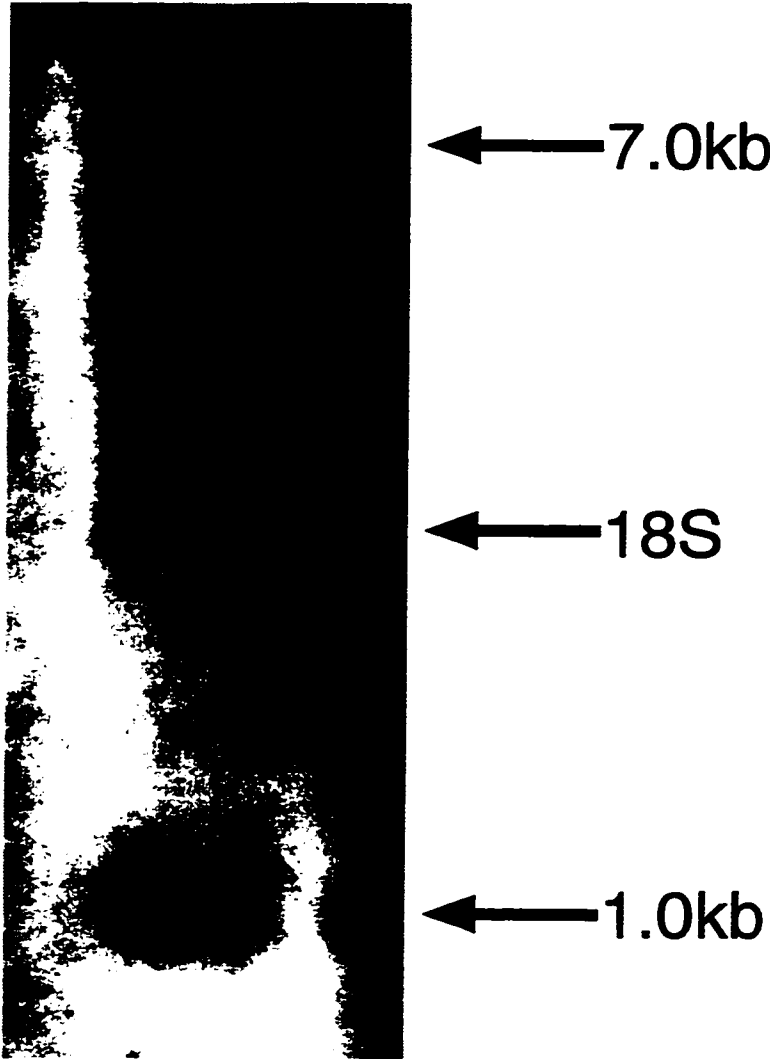
Figure 13. MCF10A mRNA Northern analysis using the KP3
degenerate oligonucleotide probe.

rabbits using the peptide fragments (KP2A and KP3A), as well as the whole proteins that were excised from the two-dimensional gels (KP2 and KP3). An additional 200 two-dimensional gels were run in order to provide enough KP2 and KP3 proteins for antibody production. Immunizations and blood collection were accomplished using standard protocols used by Bethyl Laboratories. The immunoglobulins from the rabbit sera were isolated and stored at 4°C according to the manufacturers' instructions.

Initially, our main goal was to clone the genes responsible for the nuclear matrix proteins KP2 and KP3. MCF10A unamplified and amplified libraries were generated and screened using the degenerate oligonucleotides for several years. Control membranes were probed with λgt11 oligonucleotides which were the same length and approximately the same Tm values of the KP2 and KP3 oligonucleotides to ensure that the screening conditions were consistent with successful identification of positive phage clones. Several tertiary clones from the libraries were isolated, however, Southern analysis which was used to verify the validity of the clones revealed that these clones were indeed false positives (i.e. no bands seen). Hence, screening of the cDNA libraries proved to be unsuccessful.

Therefore, the polyclonal antibodies were used in several different experiments to further characterize the unknown nuclear matrix proteins. One-dimensional Western blots were performed using these antibodies in order to determine if the rabbits generated an immune response to the KP2 and KP3 nuclear matrix proteins. Figure 14 shows the Western blot of this initial analysis using the immunoglobulins generated against the KP3 peptide fragment (KP3A). Several bands can be seen in the MCF10A KP3A TB lanes (representing both rabbits immunized for the KP3A peptide fragment, lanes 2 and 4), while no bands are seen in the control non immunized sera lanes (KP3A prebleed, lanes 1 and 3). Specifically, several faint bands can be seen in the 28–40kD range, while the strongest band was seen at approximately 55kD in both rabbit TB lanes. The KP3A TB antibodies were the only antibodies that showed any specificity toward nuclear matrix proteins using Western analysis. In addition, one of the rabbits injected with the KP3A peptide fragment

appeared to produce a stronger immunologic response. Specifically, the KP3A TB antibodies used in lane 2 produced stronger signals when compared to the KP3A TB antibodies used in lane 4. Unfortunately, the other antibodies that were generated by Bethyl Laboratories, specifically the KP2 and KP3 antibodies (antibodies generated against the whole proteins) and the KP2A antibody (antibodies generated against the KP2 peptide fragment), showed negative results on all Western analyses that were done (i.e., no bands seen in any lanes). Therefore, these antibodies were not used in any further analyses and all further studies utilized the KP3A TB antibodies that gave the highest immunologic response (lane 2). In addition, nuclear matrix proteins from a human dura metastatic lesion and normal human liver tissue underwent one-dimensional Western analysis using the same conditions and antibody dilutions used previously (Figure 14). A human metastatic lesion in the dura, a specific tissue between the skull and brain, revealed only one band which was seen at approximately 55kD (lane 5) while the normal human liver tissue revealed bands at approximately 35kD and 55kD (lane 6). No bands were observed in the dura or liver tissue using the non-immunized PB sera (data not shown).

Next, immunocytology experiments using various cell lines were done. First, MCF10A cells were grown on chamber slides and incubated with KP3A TB or the KP3A PB antibodies (Figure 15). The KP3A antibody appears to darkly stain MCF10A cells undergoing mitosis (Figure 15A). Specifically, it appears that the antibody is binding to the nucleus with specific affinity for the chromosomes. Interphase cells show a much lighter staining which is specific for the nucleus with very little to no cytoskeletal staining.

The nonimmune prebleed antibodies showed no such staining in interphase or mitotic cells (Figure 15B). In addition, other cell lines exhibited a similar intense nuclear staining of mitotic cells including the human prostate carcinoma cell line DU–145 (Figure 16A), the human colon carcinoma cell line WiDr (Figure 16B), the human lung carcinoma cell line H661 (Figure 16C), and the human renal carcinoma cell line 769–P (Figure 16D). The specific chromosomal staining by the KP3A TB antibodies can be further demonstrated in
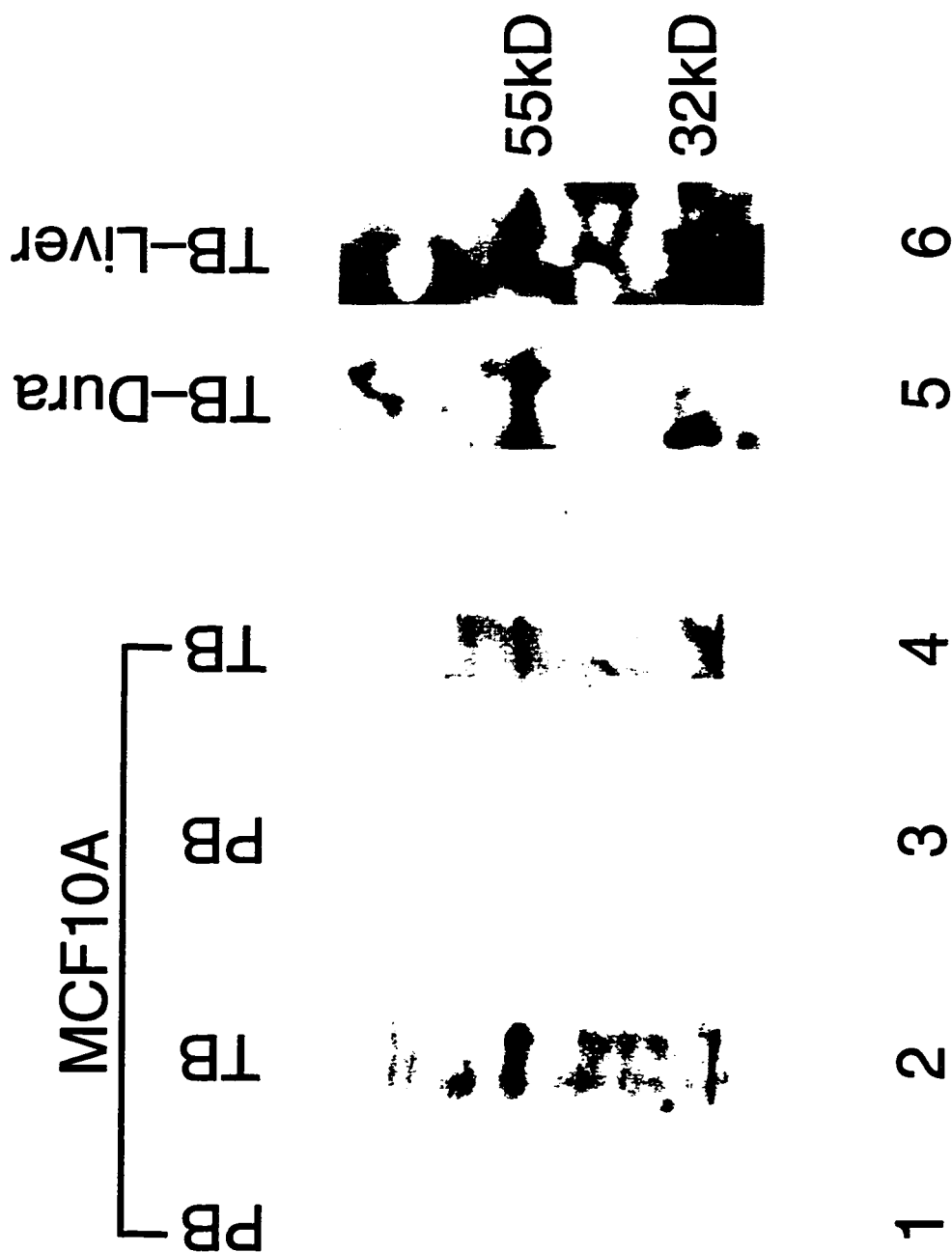
Figure 14. KP3A Western analyses of the human breast cancer cell line MCF10A (Lanes 1–4), human dura tissue (Lane 5), and human liver tissue (Lane 6). [PB=pre-bleed nonimmune sera, TB=immunized terminal bleed sera]
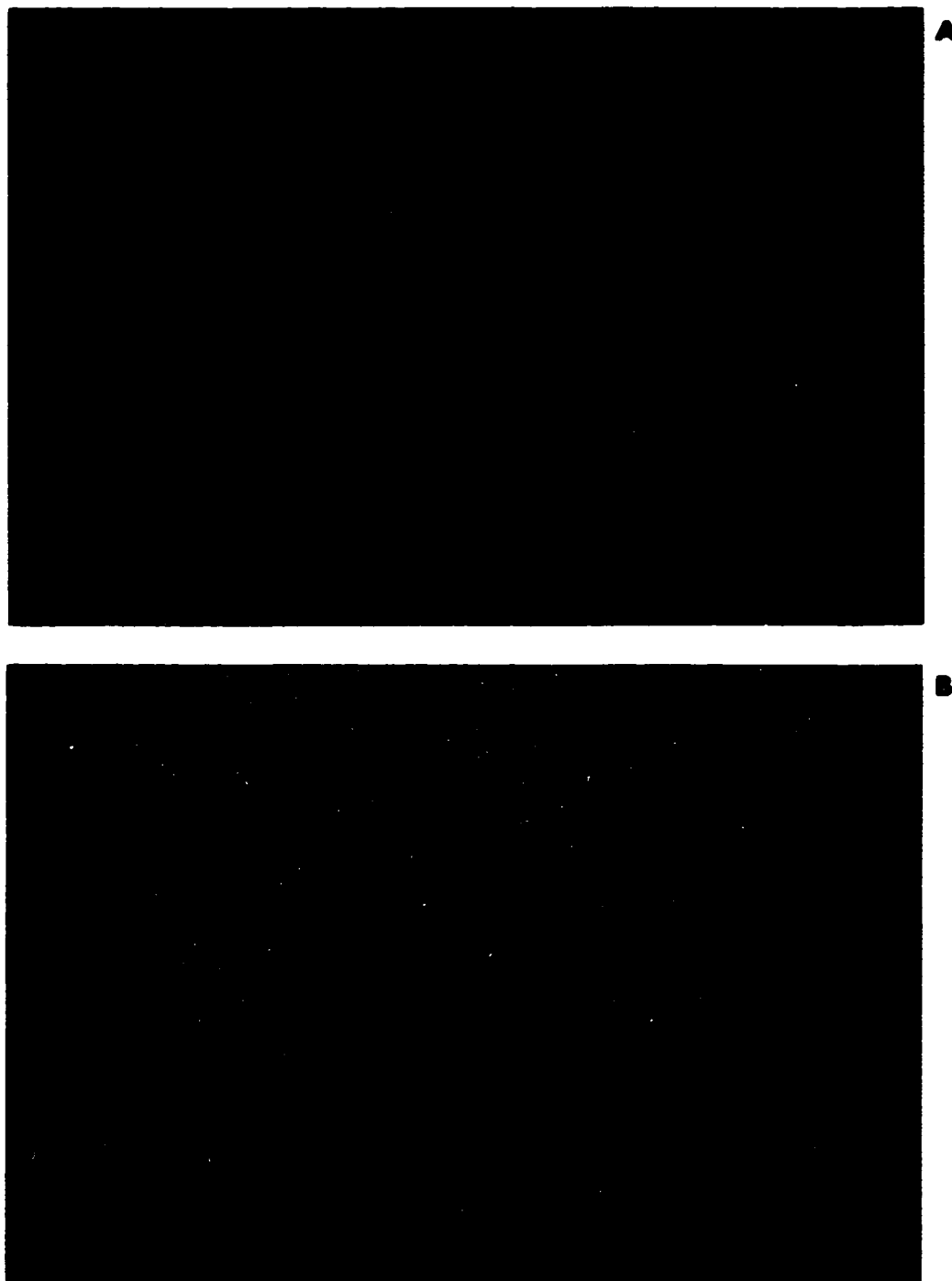
Figure 15. (A) Immunocytochemical analysis of the human breast cell line MCF10A stained with the KP3A antibody (terminal bleed). (B) Immunocytochemical analysis of the human breast cell line MCF10A stained with the non-immunized control sera.
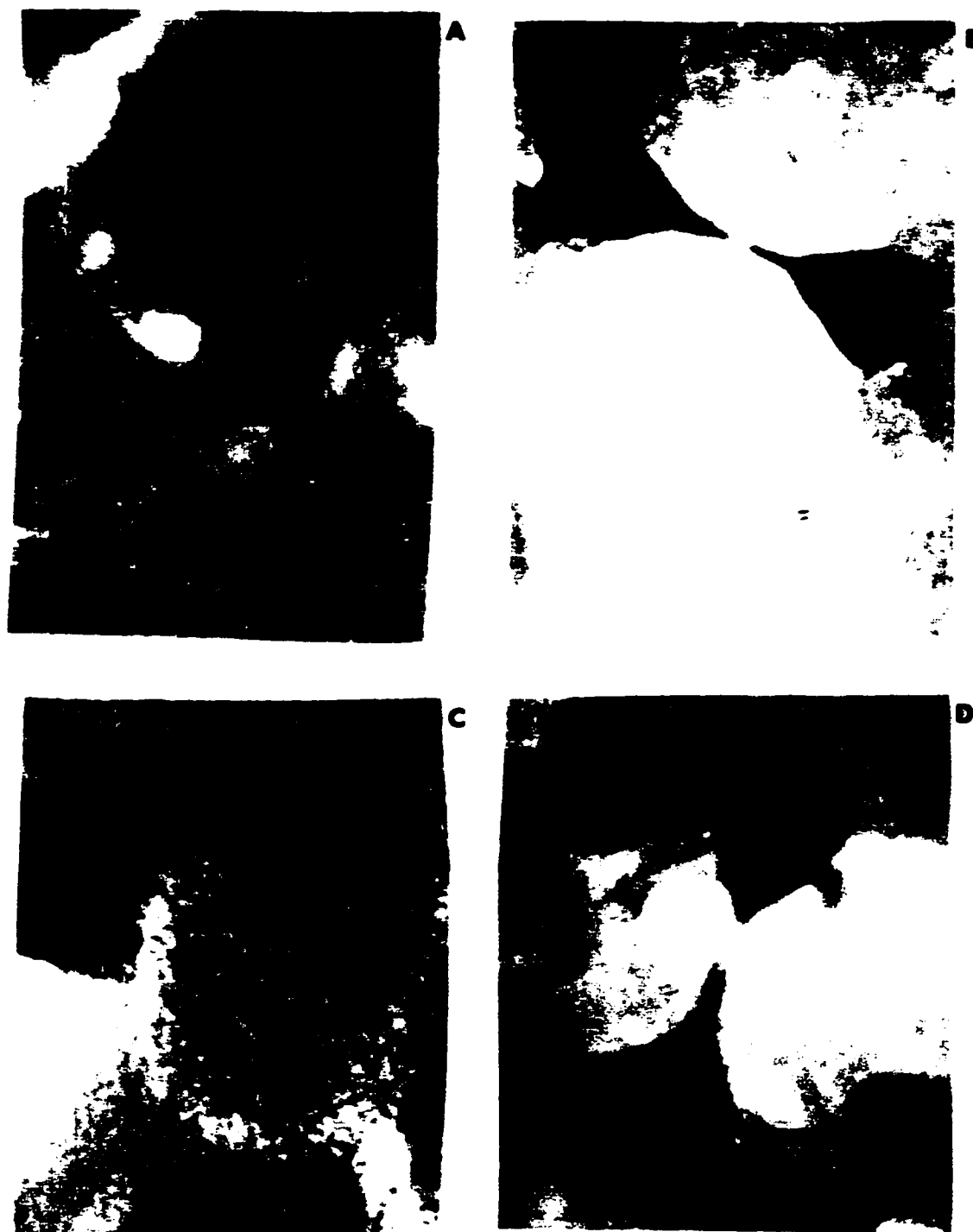
Figure 16. (A) Immunocytochemical analysis of the human prostate cell line DU-145 stained with the KP3A antibody (terminal bleed). (B) Immunocytochemical analysis of the human colon cell line WiDr stained with the KP3A antibody (terminal bleed). (C) Immunocytochemical analysis of the human lung cell line H661 stained with the KP3A antibody (terminal bleed). (D) Immunocytochemical analysis of the renal cell line 769-p stained with the KP3A antibody (terminal bleed).

Figures 16A and 16C. The nonimmune prebleed antibodies did not demonstrate any nuclear staining in any of the cell lines that were used (data not shown).

In order to more fully characterize the mitotic staining of the KP3A antibody, dual fluorescence studies were performed using the MCF10A cell line. This involved the coincubations of two primary antibodies (KP3A TB antibody in conjunction with one of the following antibodies: PCNA, Ki-67, or NuMA). PCNA and Ki-67 were selected because these antibodies are specific for cells undergoing division. The NuMA antibody is one of the few commercially available nuclear matrix antibodies which is specific for a 240kD nuclear matrix protein. During mitosis, this protein is concentrated at the polar regions of the mitotic apparatus while in interphase cells, it is restricted to the nucleus. When the MCF10A cells are coincubated with these antibodies, it was shown that the KP3A antibody appears to colocalize with the PCNA (Figure 17), Ki-67 (Figure 18), and the NuMA (Figure 19) antibodies. These data provide further evidence to the notion that the KP3A antibody is binding to a protein(s) that may play an active role in the process of mitosis.

Lastly, investigations specifically analyzing the binding of the KP3A TB antibody at the various stages of the cell cycle were done. The human prostate cancer cell line (PC-3) was synchronized by utilizing a double thymidine block. After the cells were released, cells were fixed at various timepoints and analyzed using the KP3A TB antibody. Once again, it appears that the KP3A TB antibodies are specific for the nucleus of cells that are actively undergoing mitosis (Figure 20). Initially, the KP3A TB antibodies demonstrate binding at the nuclear level. Specifically, the entire nucleus is stained while there is no staining of the cytoskeleton which has previously been shown. Specifically, at the six hour timepoint, the KP3 TB antibody appears to be binding to the two sets of chromosomes within a dividing cell (Figure 20A). At the 14 hour timepoint, the mitotic phase of the cell cycle is well underway with both cells demonstrating dark staining using the KP3A TB antibodies (Figure 20B). At 18 hours, the process of cell division is almost complete with
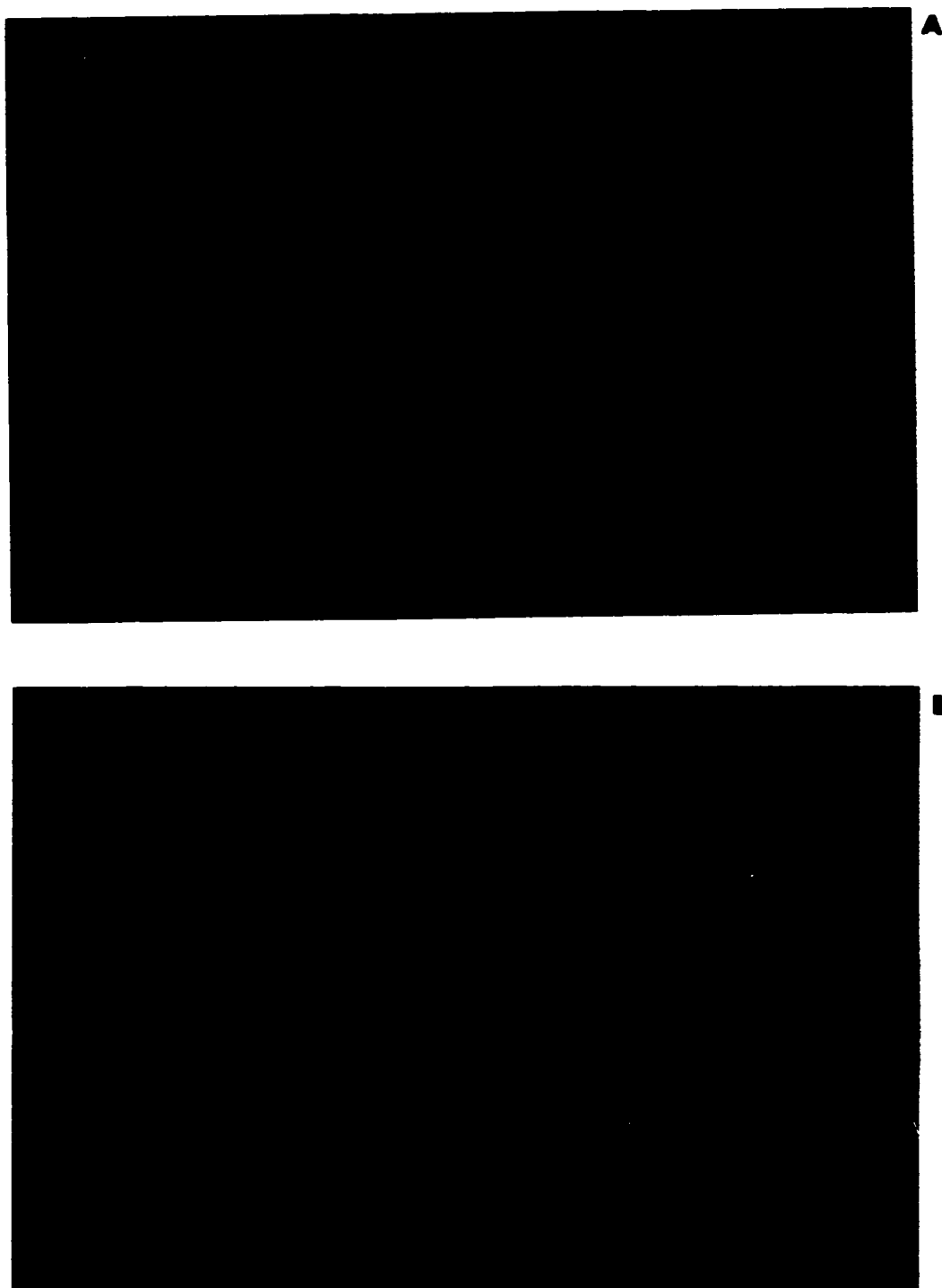
Figure 17. Dual fluorescence studies using the MCF10A cell line. (A) KP3A antibody (terminal bleed) (B) PCNA antibody.
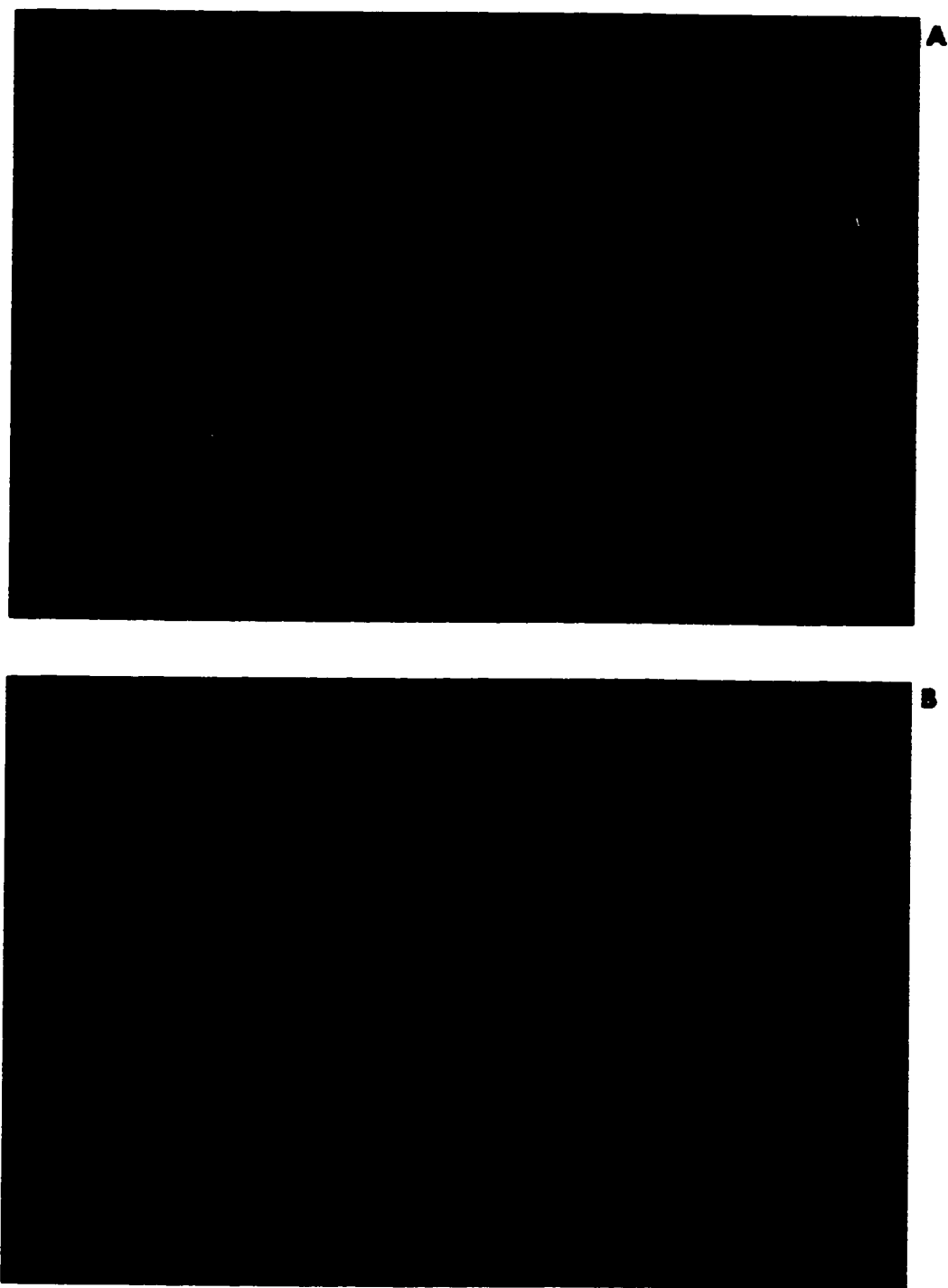
Figure 18: Dual fluorescence studies using the MCF10A cell line. (A) KP3A antibody (terminal bleed) (B) Ki-67 antibody.
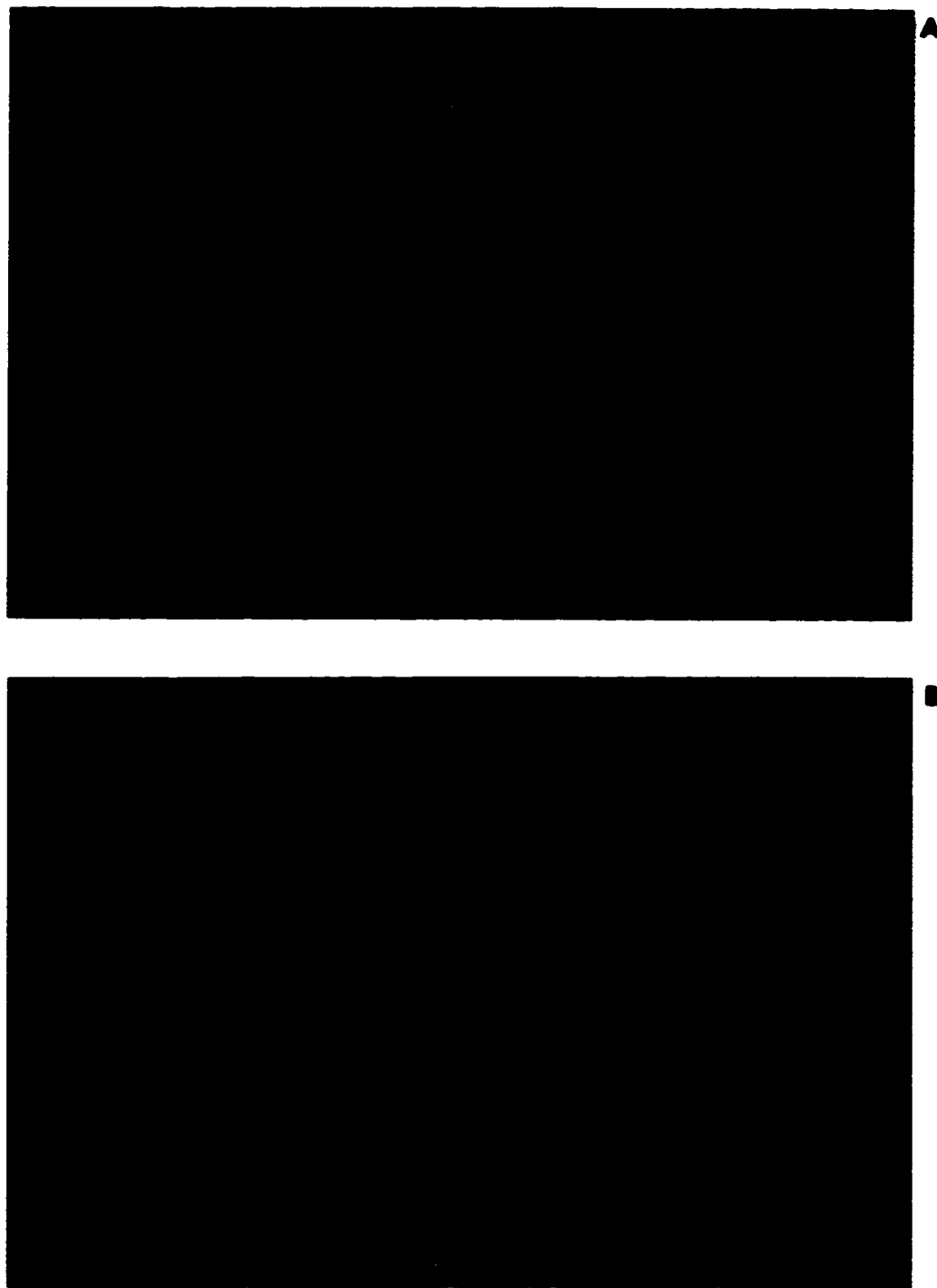
Figure 19: Dual fluorescence studies using the MCF10A cell line. (A) KP3A antibody (terminal bleed) (B) NuMA antibody.
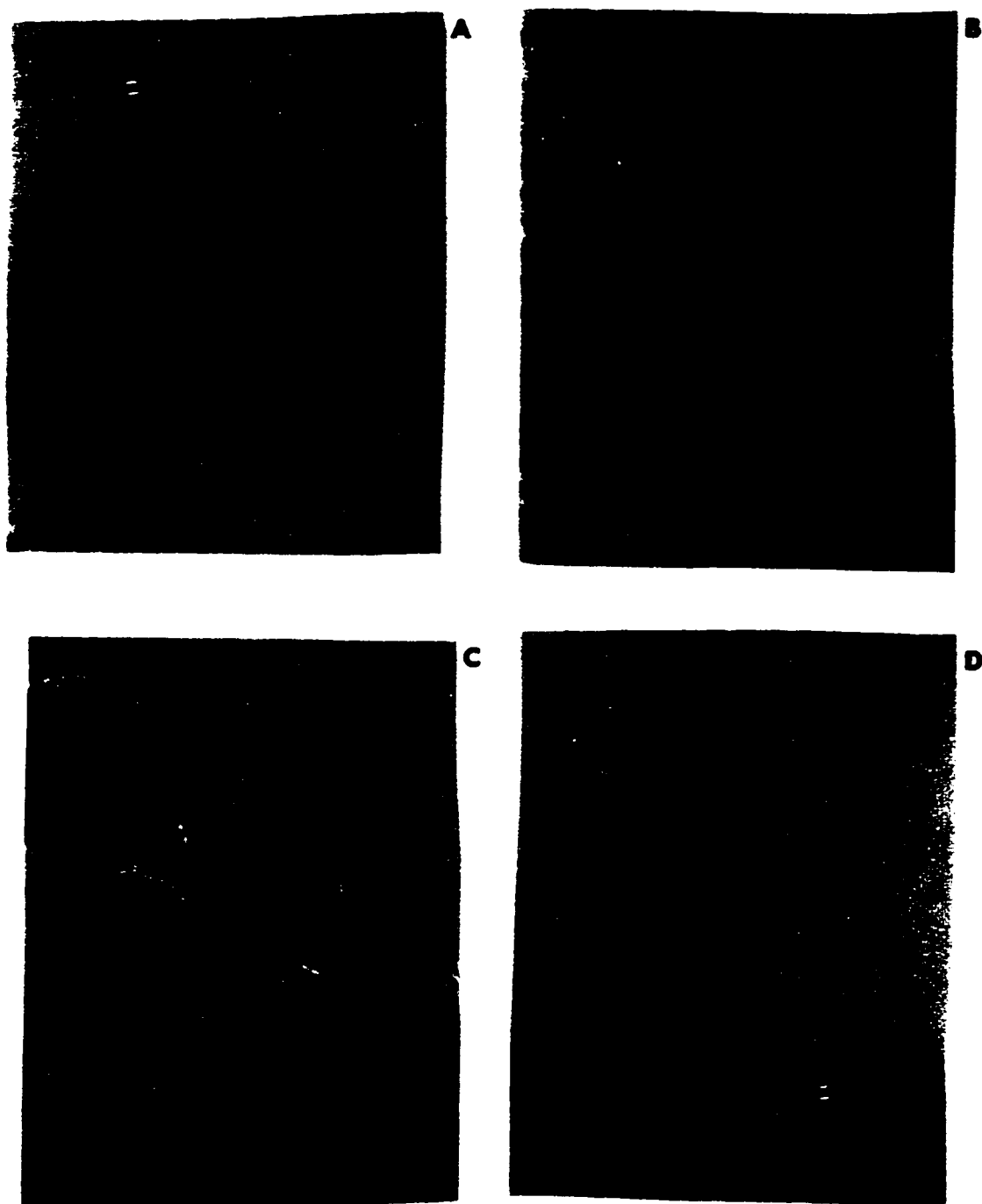
Figure 20. PC-3 synchronizing cell experiments using the KP3A PB and TB antibodies. (A) 6 hour time point with the KP3A TB antibody (B) 14 hour time point with the KP3A TB antibody (C) 18 hour time point with the KP3A TB antibody (D) 14 hour time point with the KP3A PB antibody.

both cells staining darkly (Figure 20C). The prebleed antibodies did not produce any nuclear staining of the cells during any stage of mitosis. For example, Figure 20D shows the 14 hour timepoint of PC-3 cells stained with the KP3A PB control antibodies which demonstrated no nuclear staining of the cells. Taken together, these experiments demonstrate that the KP3A TB antibodies are specific for the nucleus and appear to bind to a nuclear matrix protein(s) that may play a role(s) in the active phases of the cell cycle.

Chapter Five

Discussion of Chapters 2 through 4

Cancer is the second leading cause of death in the United States, accounting for 22% of all deaths (Fraumeni et al., 1993). In order to lower the morbidity and mortality of cancer, many investigators have concentrated on delineating more effective diagnostic techniques, as well as better therapies. The discovery of new cancer biomarkers has been the focus in many studies which could improve the diagnosis, staging, prognosis, and the earlier detection of recurrence of cancer. Therefore, with more sophisticated biomarkers at the clinicians disposal, better treatment decisions could be utilized, therefore, increasing the survival rate of cancer patients. The importance of tumor markers has been recognized for many years. In 1847, Sir Henry Bence Jones described a protein found in the urine which is currently used as a biomarker in myeloma patients (Kahn, 1991). Tumor markers are usually measured quantitatively by biochemical or immunochemical techniques and include tumor-associated antigens, enzymes, specific proteins, metabolites, and oncogenes and their products. In addition, tumor markers could be used to screen the general population for high-risk groups. Many markers are currently recognized and utilized to some extent within the clinical setting. Alpha-fetoprotein (AFP), which is usually undetectable after the first year of life, has been shown to be useful in screening for hepatocellular carcinoma (Tatarinov, 1964; Sell, 1990). Human chronic gondotropin (hCG) has been used for diagnosis and monitoring of gestational trophoblastic diseases (Bagshawe, 1965). In addition, AFP and hCG have also proved to be essential markers in patients with germ cell tumors such as embryonal malignant teratoblastomas of the testes and ovary (Schwartz, 1987A). Elevations of the glycoprotein carcinoembryonic antigen (CEA) have been observed in patients with cancer of the lung, liver, pancreas, breast, colon, head or neck, bladder, cervix, and prostate (Schwartz, 1987B). Prostate specific antigen (PSA) is

76

currently used to evaluate patients with prostate cancer (Livingston et al., 1988). Although tumor markers have proven useful in the clinical setting, as well as adding to our understanding of the natural history of cancer, they are by no means accurate and sensitive in every case. Several problems associated with the currently used tumor markers include the diagnosis of false positives, as well as problems associated with nonspecificity and low sensitivity. In addition, the analyses and usefulness of some tumor markers, such as PSA, remain controversial. Therefore, the development of novel tumor markers that possess greater specificity as well as greater sensitivity could prove extremely useful. One possible candidate for novel tumor markers are the nuclear matrix proteins. Nuclear matrix proteins are a relatively untapped resource for clinically useful cancer diagnostic and prognostic cancer biomarkers. As stated previously, many investigators have reported that the nuclear matrix protein compositions expressed by normal and malignant cells are different. By utilizing these differentially expressed nuclear matrix proteins, earlier markers for cell differentiation as well as indicators of malignancy in borderline or atypical lesions could aid clinicians in diagnosis and prognosis.

The nuclear matrix is the RNA-protein skeleton of the nucleus which contributes to the structural and functional organization of DNA. The nuclear matrix has been demonstrated to play various roles within the cell including DNA organization and replication, RNA synthesis and transport, and the regulation of gene expression. These general functions of the nuclear matrix have been previously discussed in detail in Chapter One.

Nuclear matrix proteins came under consideration as potential biomarkers through the investigations of autoantibodies. Autoantibodies have been utilized as diagnostic markers in the clinic for a variety of diseases including systemic lupus erythematosus, mixed connective tissue disease, Sjogren's syndrome, dermatomyositis, and scleroderma (Tan, 1989). A common feature of an autoimmune disease is an antibody immune response manifested against cellular proteins and nucleic acids that play the role of the

antigens. Every autoimmune disease usually has a characteristic spectrum of autoantibodies that bind against multiple intracellular antigens. Autoantibodies have supplied investigators with insights into important cellular processes such as DNA replication and supercoiling, transcription, and splicing, as well as being utilized to screen cDNA expression libraries. In fact, experiments using autoantibodies led to the initial discovery of the PCNA antibody (Miyachi et al., 1978) which has increased our knowledge of cell cycle processes.

Autoimmune sera have also been reported to detect novel nuclear proteins, including proteins of the nuclear matrix. Sera from a patient with a functioning adrenal tumor was used to characterize a novel protein with a molecular mass of 53kD which was found to be associated with the nuclear matrix (Zuber et al., 1995). This protein is observed in interphase nuclei in a variety of cell lines including human, mouse, hamster lines, as well as peripheral blood lymphocytes, and mouse and rat tissues. The 53kD protein (NDP53) varied in intensity between samples and colocalized with a multiprotein complex known as the PML oncogenic domain, which is known to be translocated in acute promyelocytic leukemia patients. Autoimmune sera from a 54-year old female breast cancer patient was utilized to identify the nuclear autoantigen p330d/CENP-F which was found to be associated with the nuclear matrix, as well as cell cycle specific (Casiano et al., 1995). In a later study, Landberg et al. used p330d/CENP-F to examine different human hematopoietic malignancies, as well as breast cancer samples, and demonstrated that this autoantigen may be a potentially valuable proliferation marker which can be used to assess a variety of tumors using flow cytomety (Landberg et al., 1996).

Antibodies generated by hybridomas in mice to specific nuclear matrix proteins have also been reported to have potential clinical advantages. Wen and Chiu developed monoclonal antibodies by immunizing mice to human colon tumor-associated nuclear matrix (Wen and Chiu, 1987). Sera from the animals were collected, screened, and analyzed. Several of these monoclonal antibodies were found to be highly specific for human colon adenocarcinoma nuclear matrix and chromatin, while showing no or little

cross reactivity with normal human colon epithelial cell matrix and chromatin. Philipova et al. isolated a monoclonal antibody (N9-D2) recognizing a nuclear antigen p125/6.5 associated with the nuclear matrix and was specifically found to be present in proliferating cells (Philipova et al., 1987). The p125/6.5 antigen has been reported to be present in nuclei of malignant tumor cells, but not detected in adjacent normal cells in solid primary tumors or their corresponding metastatic disease (Yankulov et al., 1989). Weidner et al. using the nuclear matrix associated monoclonal antibody NM-200.4 reported that breast carcinoma nuclei revealed the highest and most reliable level of immunoreactivity when compared to benign and malignant nuclei from other organ sites (Weidner et al., 1991). Monoclonal antibodies specific for nuclear matrix proteins in human prostate cancer, but absent from benign prostatic hyperplasia (BPH) or normal prostate tissue have also been reported (Partin et al., 1993; Partin et al., 1997).

Nuclear matrix proteins have not only been detected in tissues, but in body fluids as well. Nuclear matrix antibodies have been found in the urine and blood of cancer patients using several nuclear matrix antibodies in order to diagnose and monitor cancer patients. Using several nuclear matrix-specific antibodies, Miller et al. demonstrated that nuclear matrix proteins were detected in sera of bladder, breast, colon, endrometrial, lung, ovarian, prostate, and rectal cancer patients (Miller et al., 1992). Antibodies toward the nuclear matrix protein NuMA have also been reported to be elevated in the serum of colorectal cancer patients (Bromely et al., 1996). Shelfo and Soloway demonstrated that the urinary level of the nuclear matrix protein, NMP22, was elevated in patients with bladder carcinoma (Shelfo and Soloway, 1997). A commercially available NMP22 immunoassay test kit is currently available from Matritech Inc. (Newton, MA). These studies demonstrate that nuclear matrix proteins are released from dying cells and measured in a quantitative fashion in urine or sera. Hence, nuclear matrix proteins may provide clinicians with better prognostic and diagnostic tools that could eventually increase patient survival.

The majority of my thesis investigated nuclear matrix compositions in various

experimental conditions. Specifically, the majority of experiments were undertaken in response to many investigators who have reported that nuclear matrix proteins have distinct differences when cancer and normal cells are compared.

Chapter Two investigated the response of cells to differing extracellular matrices (ECMs). Cells contain extensive three-dimensional interactive skeletal networks that form the integral structural components of the plasma membrane, cytoplasm, and nucleus. Taken together, this entire system has been named the "tissue matrix" (Isaacs et al., 1981; Bissel et al., 1982; Fey et al., 1984; Pienta and Coffey, 1991). The tissue matrix system forms a structural and functional bridge from the cell periphery to the DNA linking the nuclear matrix to the cytoskeleton and the ECM (Pienta and Coffey, 1991). Hence, extracellular signals (i.e. growth factors and hormones etc.) can transverse into the cell and eventually have an effect on components of the nucleus. Many investigators have demonstrated that cells grown on different ECMs have altered morphologic and phenotypic characteristics (Folkman and Moscona, 1978; Hay, 1977; Ben-Ze'ev, 1980; Wittelsberger et al., 1981; Ingber, 1990; Pienta et al., 1991). Specifically, Pienta et al. reported on the effect of ECMs secreted from both normal and tumor cells on the structure of normal rat kidney epithelial cells (Pienta et al., 1991). Normal rat kidney cells, plated on matrigel (a basement membrane secreted by tumor cells) adopted a morphology and phenotype which closely resembles a Kirsten-ras transformed normal rat kidney cell. This morphologic transformation was not observed for cells plated on individual ECMs (such as lamin and collagen IV) or on a basement membrane secreted by normal placenta cells. These results suggest that tumor derived basement membrane has unique characteristics which may cause morphologic transformation of normal rat kidney cells. The nuclear matrix proteins from cells grown on various ECMs were isolated and analyzed revealed distinct differences between normal rat kidney cells and their rat-transformed counterparts (Getzenberg et al., 1991A). This was the first report to demonstrate that the ECM can have an effect on the nuclear matrix protein composition.

Therefore, based on these reports, we wanted to investigate the role on the ECM in an in vivo system. The MAT-LyLu (MLL) rat prostate cancer cell line was utilized for injections into various organ sites within the rat. One million MLL cells were injected into the prostate, lung, heart, intramuscular, and tail vein of rats for tumor development. Tumors were excised and nuclear matrix proteins isolated and analyzed by high resolution two-dimensional electrophoresis. Upon silver staining of the gels, several distinct populations of nuclear matrix proteins were found. The majority of the nuclear matrix proteins were found to be common in that they appeared in the gels of every organ site analyzed. This finding is in agreement with the reports of many other laboratories who have also observed common nuclear matrix proteins in different cells or tissues being analyzed (Stuurman et al., 1990; Partin et al., 1993; Pienta and Lehr, 1993; Getzenberg et al., 1996; Chew et al., 1997; Korosec et al., 1977; Mattern et al., 1997). However, distinct differences in the nuclear matrix protein composition were also observed between the various organ sites. Specifically, fourteen proteins (L1 through L14) were identified in the lung two-dimensional gel and not observed at the other organ sites. Six proteins (IM-1 through IM-6) were found only in the intramuscular two-dimensional gel, seventeen proteins (H-1 through H-17) were found only in the heart two-dimensional gel, and five proteins (TV-1 through TV-5) were observed only in the tail vein two-dimensional gel. Therefore, distinct nuclear matrix protein differences were seen in all of the sites upon comparison to the orthotopic prostate two-dimensional gel. The highest level of nuclear matrix proteins differences were noticed in the heart tissue, the smallest differences were seen in the tail vein tumor tissue, while the remaining organ sites fell in between these two tissues. These data add further evidence to the observation that the ECM can have profound effects on a cell's structure and function. The MLL rat prostate cancer cells, when injected into other organ sites, were able to grow and produce tumors in which nuclear matrix proteins could be isolated. Hence, these prostate cells were able to survive and grow in environments that were different from the prostate. Differing environmental conditions could include differences in hormones, growth factors, and the ECMs etc.

These factors alone, or in conjunction, could directly affect the cell by either activating cellular receptors on the plasma membrane or directly interacting with nuclear receptors. These signals could then be linked to processes within the cell that directly affect DNA synthesis which can lead to the production of different nuclear matrix proteins. In conclusion, this study demonstrates the significant role(s) that the environment can play by altering the cells' structure and functional status.

Chapter Three investigated the nuclear matrix protein composition of various human lung carcinoma cell lines. As previously discussed, nuclear matrix protein differences have been reported in many different cell types, as well as tissues from various species. However, investigations into nuclear matrix protein compositions in lung cancer had never been reported. Therefore, human carcinoma lung cell lines were selected representing the four major classes of lung cancer: large cell carcinoma, small cell lung carcinoma (SCLC), squamous cell carcinoma, and adenocarcinoma. The human lung cell lines were grown and nuclear matrix proteins were isolated. The two-dimensional gels were analyzed according to the lung classification to which the sample belonged. Once again it was noticed that within each lung cancer category, the majority of the nuclear matrix proteins were found to be common. This observation is in agreement with other investigators which has been stated previously. Ten common proteins within each category, were selected and identified in the two-dimensional gels. The common proteins were of low molecular weight (12-30kD), while the pIs ranged from 4.9-9.5. As expected, distinct protein differences were observed in each of the four lung carcinoma categories. For example, SK-LU-1 contained four nuclear matrix proteins (A-D) that were not present in the A-427 and Calu-3 cell lines. Different nuclear matrix proteins were observed in every cell line analyzed. These data are in agreement with other investigators who have reported differences in nuclear matrix protein composition in cell lines derived from the same organ which has been previously discussed. Many organs have the ability to develop distinctly different tumor types. Several reasons which can cause such differences can be due to the cell type which gave rise to the tumor and/or the different environmental conditions to which the cells were

exposed. Therefore, one would expect to see differences within each lung classification and this was indeed observed. In conclusion, nuclear matrix protein compositions of the four lung carcinoma classifications were found to be different. These protein differences could be due to several factors, including the initial cell type that produced the tumor and the environment. The nuclear matrix protein differences between the lung cancer classifications could be further characterized, possibly producing novel lung cancer biomarkers that could be useful in various diagnostic and therapeutic situations.

Lastly, Chapter Four detailed the identification and characterization of common nuclear matrix proteins found in the MCF10A human breast cell line, as well as a variety of other tissues and cell lines. Five reproducible common nuclear matrix proteins in the MCF10A cell line were selected for further analyses. Microsequencing information was acquired for two of the proteins (KP2 and KP3). A Northern analysis was done in order to verify the validity of the probes that will be used for cDNA library screening. The KP3 peptide fragment produced several bands in the MCF10 mRNA lane. One of these bands (1 or 7kb) may be the transcript responsible for producing the KP3 nuclear matrix protein. In addition to these two bands, the KP3 peptide fragment was also binding to one of the ribosomal band 18S. Even though the Northern analysis used purified mRNA, the preparation will still contain rRNA contamination. The KP2 peptide fragment did not appear to bind to any bands in the Northern analysis. This may be due to several reasons, such as the smaller size of this probe and the hybridization and washing conditions. Even though this peptide showed negative results, we decided to go ahead and use this probe in conjunction with the KP3 probes. My major intent of my thesis was to identify the genes responsible for the production of the KP2 and KP3 proteins. In order to attain this goal, unamplified and amplified MCF10A cDNA libraries were screened using radiolabled degenerate oliogonucleotides as probes. Unfortunately, the cDNA library screening proved unsuccessful.

There are several possible explanations for the unsuccessful screening of the cDNA

libraries, several of which will be mentioned here. First, the decision to use only the best possible degenerate oligonucleotide for screening could have played a role in the failure of the screening process. In this process, the highest probable codon was selected in each case for every amino acid. Therefore, several incorrect codons could have been unknowingly incorporated into the degenerate oligonucleotide sequences which would have detrimental effects on the screening process. Other investigators when posed with the huge task of library screening have tried to overcome this problem by using every possible degenerate oligonucleotide proposed by the amino acid sequence to ensure that the correct sequence is represented. In other cases, investigators have utilized only the top candidates for use in library screening. In deciding what probes I should use to screen with, I consulted Dr. Robert H. Getzenberg at The University of Pittsburgh for his suggestions. Dr. Getzenberg is a well known leader in the nuclear matrix protein field and has successfully cloned several prostate nuclear matrix proteins by cDNA library screening. Although the use of more than one possible degenerate oligonucleotide in screening libraries does increase the chance of success, nevertheless, the problems that arise in doing so must be taken into consideration. The most problematic situation which arises when degenerate oligonucleotides are used is the increased frequency of false positives. Much more time and effort will be expended trying to "weed through" all of the clones which will be selected. Dr. Getzenberg has successfully cloned several nuclear matrix proteins by using only the best possible degenerate oligonucleotide. Therefore, the decision was made to use only the best possible degenerate oligonucleotide for screening of the cDNA libraries. In order to increase my chances of success, I screened the libraries with two degenerate oligonucleotides representing two different nuclear matrix proteins (KP2 and KP3) in the hopes that I could pull out the clones responsible for at least one of these proteins.

Second, the screening conditions (i.e. prehybridization and hybridization temperatures and washing conditions etc.) could have also played a role in the unsuccessful screening of the libraries. The prehybridization and hybridization temperatures used were

based on the Tm values for the degenerate oligonucleotides. The temperatures selected may not have been the optimal conditions that were needed to allow proper and efficient binding of the probes to the appropriate cDNA sequences. In addition, the washing stringencies may have proven to be too harsh. Washing conditions must be carefully monitored when one is working with very small probes in that they may be removed from the DNA very easily when compared to larger probes. In order to circumvent this concern, control membranes were probed with λgt11 sequences that were similar in length and Tm values as the degenerate oligonucleotides. The λgt11 probes did indeed hybridize with the cDNA/phage plaques which provided a useful positive control. Nevertheless, these λgt11 probes were based on the Tm values of the degenerate oligonucleotides which as stated previously, could have been incorrect.

Other potential problems could have arised from the cDNA libraries themselves. The RNA transcripts responsible for the KP2 and KP3 proteins could be rare in the RNA pool within the cell. Based on the silver staining of the two dimensional gels, it is known that the protein levels of the KP2 and KP3 proteins were at least in the nanogram range. However, how this translates into the amount of RNA expression is of course unclear. Rare transcripts in turn will lead to a lower amount of clones containing the corresponding cDNA causing a decreased chance of locating these few positive clones.

Lastly, the construction of the libraries could have also aided in the unsuccessful identification of positive clones. The integrity and purification of the mRNA used in making the library may not have been optimal. Hence, the mRNA responsible for the KP2 and KP3 nuclear matrix proteins may not have been represented with the libraries. Even if the RNA was present, there may have been a chance that the cDNA may not have been packaged within the phage heads. With these problems in mind, every possible effort was taken to ensure that the screening process would produce positive clones. One or more of these explanations could have produced the negative results.

Due to the unsuccessful identification of the cDNA sequences, polyclonal antibodies toward the peptide fragments (KP2 and KP3), as well as antibodies against the whole proteins (KP2 and KP3) were generated and utilized in further characterization of these unknown nuclear matrix proteins.

The first series of experiments involved one dimensional Western analyses. Western analysis using the KP3A TB antibodies demonstrated several bands in the MCF10A nuclear matrix protein lane. Unfortunately, only the rabbits injected with the KP3A peptide fragments produced an immunological response. When using the KP3A TB polyclonal antibodies, it was observed that the antibodies are detecting more than one nuclear matrix protein. Although the appearance of one band located at the appropriate molecular weight would have been preferred, the presence of more than one band is not unexpected. The nature of polyclonal antibodies may account for these results. Polyclonal antibodies contain antibodies that react with many different epitopes, thereby increasing the chance of nonspecific binding. In addition, the polyclonal antibodies could be detecting several nuclear matrix proteins that contain similar amino acid sequences that could be recognized by the nuclear matrix antibodies. In either case, it is clear that the KP3A antibodies can specifically react with several nuclear matrix proteins.

Other Western analyses revealed that the KP3A antibody was detecting nuclear matrix proteins in human tissues such as normal liver, as well as dura metastatic tissue from a patient with prostate cancer. When one compares the MCF10A, dura, and the liver lanes, it appears that the KP3A TB antibody is detecting an identical nuclear matrix protein at 55kD. In addition, other bands are seen around 30-40kD in the MCF10A and liver lanes. Immunocytology experiments revealed that the KP3 antibody could be detected in the MCF10A cell lines as well as in various other human cell lines. Interestingly, the KP3A antibody binding appeared to be specific for cells currently undergoing mitosis. Mitotic cells revealed an intense staining of the nuclei, while the cytoskeleton remained unstained. In addition, dual fluorescence studies demonstrated that the KP3A antibody

binding of the MCF10A cells colocalized with the staining of three specific nuclear antibodies: Ki-67, PCNA, and NuMA. PCNA is a commonly used marker for DNA synthesis while the Ki-67 antigen is expressed during all active stages of the cell cycle. NuMA is one of the very few commercially available antibodies that specifically recognizes a nuclear matrix protein. NuMA is a 240kDa protein and is concentrated during mitosis at the polar regions of the mitotic apparatus while in interphase, it is restricted to the nucleus itself (Lynderson and Pettijohn, 1980). Lastly, synchronizing cell experiments using the PC-3 cells demonstrated specific binding to the nucleus at various timepoints. It appears that the KP3A TB antibodies are binding to nuclear matrix proteins that are associated with the chromosomes. The data demonstrate that the KP3A antibody recognized a protein(s) that may play a role during cell division.

In conclusion, a nuclear matrix protein(s) was identified that appears to be present in a variety of tissues and cell lines, suggesting that this protein belongs to the common set of nuclear matrix proteins. Since this protein was found in cancer and normal cells, its usefulness as a novel cancer biomarker will probably not be investigated. Nevertheless, this nuclear matrix protein could provide investigators with additional information regarding the process of mitosis.

Chapter Six

The Multidrug Resistant Characterization of Various Human and Rat Prostate Cancer Cell Lines and the Development and Initial Characterization of Several Doxorubicin Resistant Rat Prostate Cancer Cell Lines

Introduction

Historically, metastatic prostate cancer has not been responsive to chemotherapeutic agents. The mechanisms for this lack of response have not been defined. One possible explanation is the presence of the multidrug resistance (MDR) phenotype which allow cells to protect themselves from the toxic effect of drugs. MDR mechanisms enable cells to be resistant to several structurally unrelated agents. Such agents include anthracyclines, vinca alkaloids, and anthracyclines. Some cancers initially respond to these agents, but tumor cells that are resistant to chemotherapeutic agents are selected, grow, and eventually prove fatal. In order to study the MDR phenomenon, many investigators have developed MDR cell lines by culturing cells grown in increasing concentrations of a toxic agent producing resistant clones. Analysis of the proteins present in these MDR cell lines revealed differences when compared to the parental sensitive lines (Pastan and Gottensman, 1987). One possible mechanism of the MDR phenotype is mediated by an overexpression of a 170 kDa membrane glycoprotein which has been named P-glycoprotein (Tiirikainen and Krusius, 1991). P-glycoprotein was first described in colchicine resistant Chinese hamster ovary cells by Juliano and Ling and functions as an energy dependent membrane efflux pump that is able to pump out cytotoxic agents before any damage is done to the cell (Juliano and Ling, 1976). It was shown that one particular gene (mdr1) is found to be overexpressed in resistant cells and in 1986, this gene was confirmed as producing P-glycoprotein (Ueda et al., 1986). Mdr1 has been shown to be abundant in many normal human organs such as kidney, liver, and adrenal glands (Isaacs et al., 1986; Krishan,

1990), as well as in tumor cells and tissue (Riordan et al., 1985; Deffie et al., 1988; Weinstein et al., 1990; Tiirikainen and Krusius, 1991). Overexpression of mdr-1 gene or P-glycoprotein has been reported in various malignant tumors but it is still unclear how much of a role the mdr-1 gene and P-glycoprotein play in prostate cancer.

The purpose of the first half of this project was to characterize the expression of P-glycoprotein as well as the possible role P-glycoprotein plays in drug resistance in human and rat prostate cancer cell lines. The second half of this chapter details the development and initial characterization of several doxorubicin resistant rat prostate cancer cell lines.

A.   P-Glycoprotein Expression and Daunomycin Retention in Human and Rat Prostate Cancer Cell Lines

Materials and Methods

P-glycoprotein specific monoclonal antibody C219 was purchased from Signet (Dedham, MA). Vectastain Elite ABC Kit was obtained from Vector Laboratories (Burlingame, CA). All other antibodies, cell culture reagents, and other chemicals were obtained from Sigma (St. Louis, MO).

Cell Culture

The Dunning rat prostate cell lines (AT.1, AT2.1, AT3, MAT-LyLu, Mat-Lu, and GP9F3) and the human prostate cell lines (DU–145, PC–3, TSU-1000, and TSU-parent) were used in the present study. The TSU cells were a gift from William G. Nelson at John's Hopkins Oncology Center (Baltimore, MD). TSU-1000 is an adriamycin-resistant cell line derived by growing the TSU-parent line in increasing concentrations of adriamycin. Cell lines used for controls were the murine leukemic cell lines P388S (parental sensitive line) and P388R (resistant to doxorubicin) and the parental Chinese hamster cell line AUXB1, and its MDR subline CHRC5. All cells lines were grown as monolayers except for P388S and P388R which grew in suspension. AUXB1 and

CHRC5 were grown as monolayers in MEM supplemented with 10% FBS and 1% antibiotics (penicillin/streptomycin), while the TSU-1000 cell line was grown in RPMI-1640 supplemented with 10% FBS, 1% antibiotic, and $1\mu M$ doxorubicin. A 10mM stock of doxorubicin was made in DMSO and stored at $-20^\circ C$. The remaining cell lines were grown in RPMI-1640 supplemented with 10% FBS and 1% antibiotic (penicillin/ streptomycin).

Drug Efflux Studies

Cells were trypsinized and counted using Trypan blue exclusion on a hemacytometer producing solutions of 10^6 cells/mL. $800\mu L$ of each cell line divided into the following five groups: control (no drug), daunomycin (DNR) at a final concentration of 2ng/mL, daunomycin and compazine at final concentrations of 2ng/mL and $25\mu M$ respectively, daunomycin and verapamil at final concentrations of 2ng/mL and $10\mu g/mL$ respectively, and daunomycin and persantine at final concentrations of 2ng/mL and $10\mu g/mL$ respectively. All drugs were added as $100\mu L$ aliquots to give the final concentrations stated above. 1X phosphate buffered saline pH 7.4 (PBS) was to give a final volume of 1mL in each case. Tubes were mixed and placed at $37^\circ C$ with 5% CO_2 for 30 minutes. After the incubation, cells were analyzed on a FACScan flow cytometer (Becton Dickinson, San Jose, CA) to measure cellular DNR fluorescence. Electronic gates were set to exclude dead cells in data analysis. P388S and P388R cells were used as the negative and positive controls respectively.

Immunocytochemistry

Cells were trypsinized and counted using Trypan blue exclusion on a hemacytometer. A stock solution of 10^6 cells/mL of each cell line was cytospinned onto two specific areas on a glass slide. The cells were fixed with ice cold acetone and placed at

4°C for ten minutes. Slides were allowed to come to room temperature and air dried. The immunohistochemistry procedure of the Vectastain Elite ABC Kit, which employs a biotin/avidin system, was followed. Slides were dried and a few drops of 1% H_2O_2 in 1X PBS were placed onto each concentrated cell spot and incubated for ten minutes. Slides were washed three times with 1X PBS for three minutes. Slides were incubated with 1.5% normal horse serum in 1X PBS for 30 minutes to block nonspecific binding. Horse serum was blotted off of the slides and approximately 40μL of 10μg/mL of C-219 antibody in 1X PBS was placed onto one side of the slide while an IgG isotype antibody was placed on the other side. Slides were incubated overnight at 4°C. Slides were washed three times with 1X PBS. 50μL of a 1:200 dilution of the biotinylated secondary antibody was placed onto the cells and incubated for one hour at room temperature. Excess antibody was removed and a few drops of the avidin/biotinylated horseradish peroxidase complex was incubated on the cells for one hour at room temperature. Slides were washed three times using 1X PBS followed by incubation in a peroxidase substrate solution [0.01% H_2O_2, 0.5μg/mL 3,3-diaminobenzidine tetrahydrochloride (DAB), and 0.05M Tris-HCl] for five minutes. Slides were washed with distilled water and stained with hematoxylin for five minutes. Slides were washed with an acid-alcohol solution for five minutes and washed with 1X PBS. Once the slides were air dried, slides were mounted and viewed. Slides were analyzed by three viewers who were blinded to the identification of the slides. Slides were then placed into different categories based on the intensity of staining. The positive control CHRC5 was given the designation ++++ while the negative control AUXB1 was given +.

Quantitative analysis of P-glycoprotein expression by flow cytometry

One million cells/mL were centrifuged, media removed, followed by the addition of 5mL of ice cold 70% ethanol on ice for 15 minutes with intermittent shaking to fix the cells. Cells were centrifuged and the ethanol was removed. Cells were washed with 5mL of 0.3% PBS-T (1X PBS + 0.3% Tween-20), centrifuged, and the PBS-T removed. Cells

were resuspended in 200µL of 0.3% PBS-T and split into two tubes. 10% normal goat serum for blocking the non-specific binding of immunoglobulin was added to each tube and incubated for one hour on ice. Tubes were centrifuged and all the serum except 100µL was removed. C219 antibody (0.5µg/mL) was added to one tube while the same concentration of the IgG isotype antibody was added to the other tube. Tubes were mixed and incubated for 30 minutes on ice. Cells were washed with 0.3% PBS-T and the liquid removed. Cells were incubated with the FITC-conjugated F(ab')2 fragment of a sheep anti-mouse immunoglobulin (3.3µg/mL) for 30 minutes on ice. Cells were washed with 0.3% PBS-T, centrifuged, and the PBS-T removed. Cells were resuspended in 1X PBS and analyzed on the flow cytometer. Electronic gates were set to exclude 99% of fluorescent cells in the isotype controls and C219-treated samples as well as to ensure that no signal could originate from dead cells. Cells with fluorescence more than that of the isotype gated population were counted as positive.

Results

Drug Efflux Studies

Efflux studies are a technique used to examine cellular accumulation of drugs within the cell. Autoflourescence (i.e., normal fluorescence of the cells with no drug added) of each cell line was first determined. Next, cells incubated with daunomycin alone were analyzed. Daunomycin is a commonly used chemotherapeutic agent and is a convenient drug to use for these studies because it fluoresces. Cells with florescence higher than that of the gated population were counted as positive. Daunomycin shown to enter all of the cell lines studied. The next three samples contained compazine, persantine, and verapamil which are known drug modulators in that they are able to overcome the MDR phenotype response by competitively blocking the P-glycoprotein pump. Figure 21 shows this phenomenon with the P388R cell line by exhibiting a shift in their histogram when the three

modulators are added while the P388S cell line does not. The shift in the histograms

represents the blockage of the P-glycoprotein pump causing the drug daunomycin to

accumulate within the cells producing a higher fluorescence reading. The remaining cell

lines were analyzed in the same manner. Figure 21 also shows the histograms for the

human line PC-3 and the rat cell line MAT-LyLu (MLL). PC-3 and the MAT-LyLu cell

lines exhibited a shift in their histograms demonstrating some drug efflux capacity,

although not as strong as P388R. The remaining rat cell lines (AT3, AT.1, GP9F3, MAT-

Lu, and AT2.1) and the human line TSU-1000 demonstrated this MDR drug efflux

phenomenon. Specifically, several rodent cell lines (AT.1, GP9F3, MAT-LyLu, and

MAT-Lu) demonstrated the lowest level of drug efflux capacity, while the rat line AT3

revealed the highest efflux ability. The cell lines that did not exhibit the drug efflux

phenomenon were DU-145 and TSU-parent. Table 5 shows all of the drug efflux data as

ratios of DNR fluorescence for all of the cell lines that were tested.

Table 5. Results of Drug Efflux Studies

Cell Line	Modulation of DNR Retention*
Controls	
P388S	0.90
P388R	3.40
Human	
DU-145	0.87
TSU-parent	1.08
PC-3	1.68
TSU-1000	1.85
Rodent	
AT.1	1.20
GP9F3	1.27
MAT-LyLu	1.27
MAT-Lu	1.31
AT2.1	1.69
AT3	2.06

* Ratio of DNR fluorescence (mean log channel number) of cells incubated with DNR and efflux blocker (persantine) vs. cells incubated with DNR alone.

Immunocytochemistry

Cells were stained with C-219 antibody which is specific for P-glycoprotein. Cells

expressing P-glycoprotein express a rust colored plasma membrane whereas the IgG

isotype shows no such staining (data not shown). Figure 22 shows staining of four of the cell lines. CHRC5 and AUXB1 were used as the positive and negative controls respectively. CHRC5 stains darkly for P-glycoprotein in contrast to AUXB1 (Figure 22A and 22B). The human line PC-3 (Figure 22C) showed darker staining while TSU-parent and DU-145 cell lines did not (data not shown). The rat cell line MAT-LyLu had a higher staining intensity when compared to AUXB1 (Figure 22D). All of the remaining Dunning rat lines (except MAT-Lu) expressed positive staining. Table 6 lists the results of the immunocytochemical analysis of all of the cell lines ranging from the darkest staining (++++) to very minimal staining (+)

Table 6.   Results of Immunocytochemical Staining

Cell Line	Staining
Controls	
CHR	++++
AUX	+
Human	
TSU-R	+++
TSU-S	+
PC-3	++
DU-145	+
Rodent	
MAT-LyLu	++
GP9F3	++
AT.1	+++
AT2.1	+++
AT3	+++
MAT-Lu	+

Quantitative Flow-FITC Studies

Table 7 shows the flow cytometry data of P-glycoprotein expression in several of the cell lines expressed as the percentage of cells bound to the C219 antibody or to the IgG isotype negative control antibody. Figure 23 shows an example of the C219 antibody histograms for several of the cell lines while Table 7 shows all of the data in tabular format. Almost all of the CHRC5 cells (97.75%) were bound to the C219 antibody while AUXB1
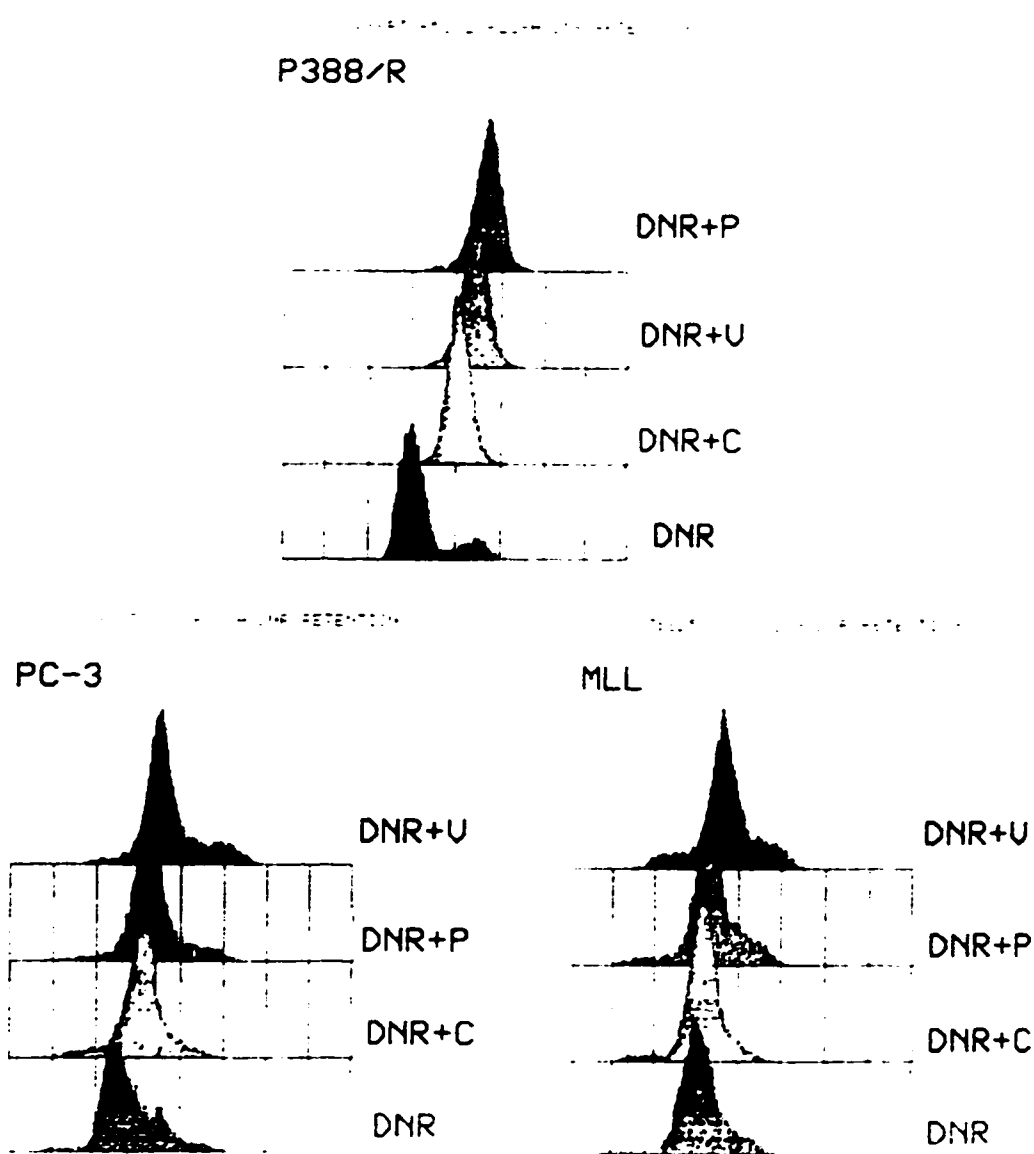
Figure 21. Drug efflux results of the P388/R (positive control), human prostate cancer cell line PC-3, and the rat prostate cancer cell line MLL. (DNR, daunomycin alone; v, verapamil; p, persantine; and c, compazine).
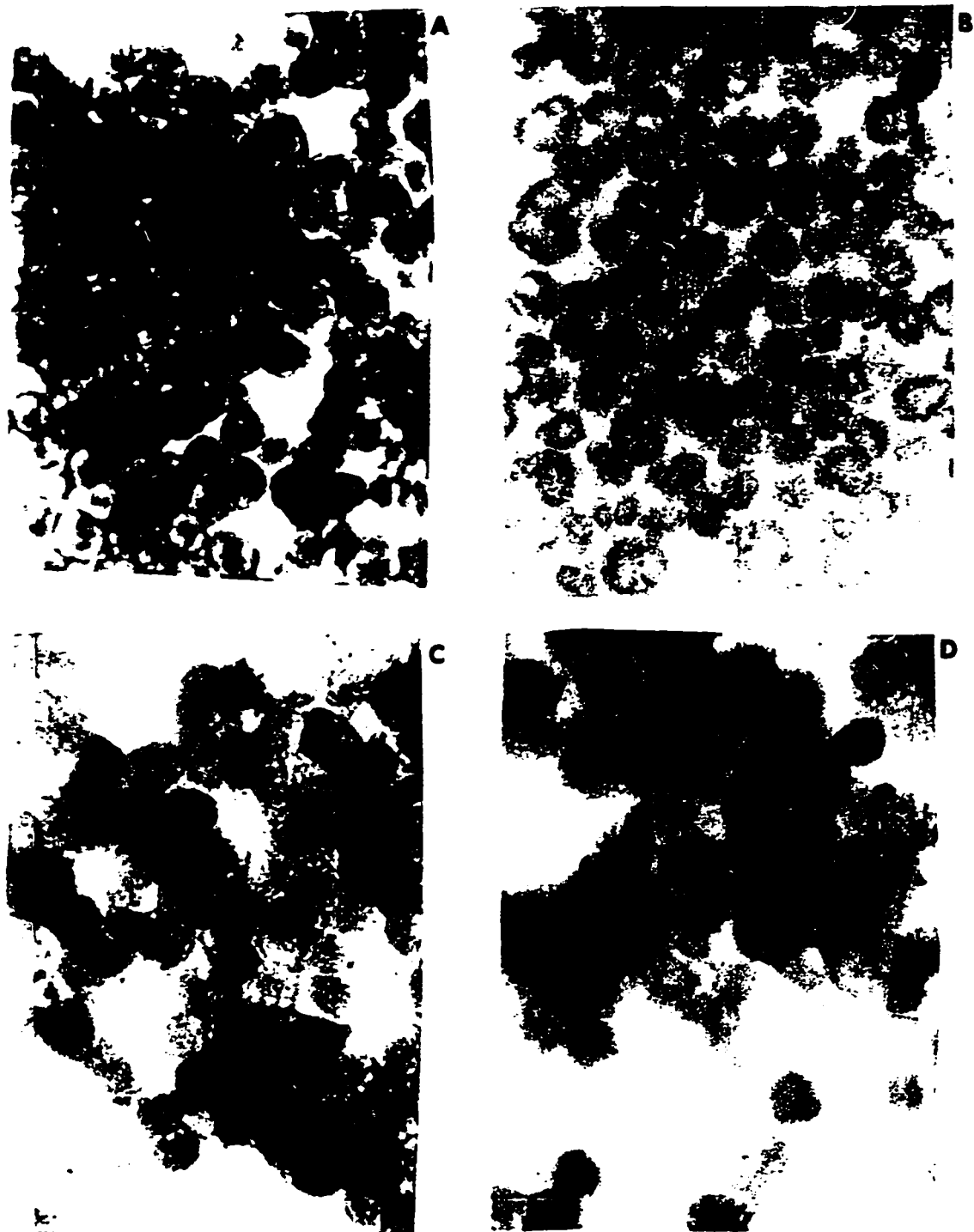
Figure 22. Immunocytochemical C219 analysis of various cell lines. (A) CHR cell line
(positive control). (B) AUX cell line (negative control). (C) PC-3. and (D) MLL.

AUX

CHR

IGG

IGG

13.64%
C219

96.8%
C219

PC3

MLL

IGG

IGG

38.81%
C219

30.00%
C219
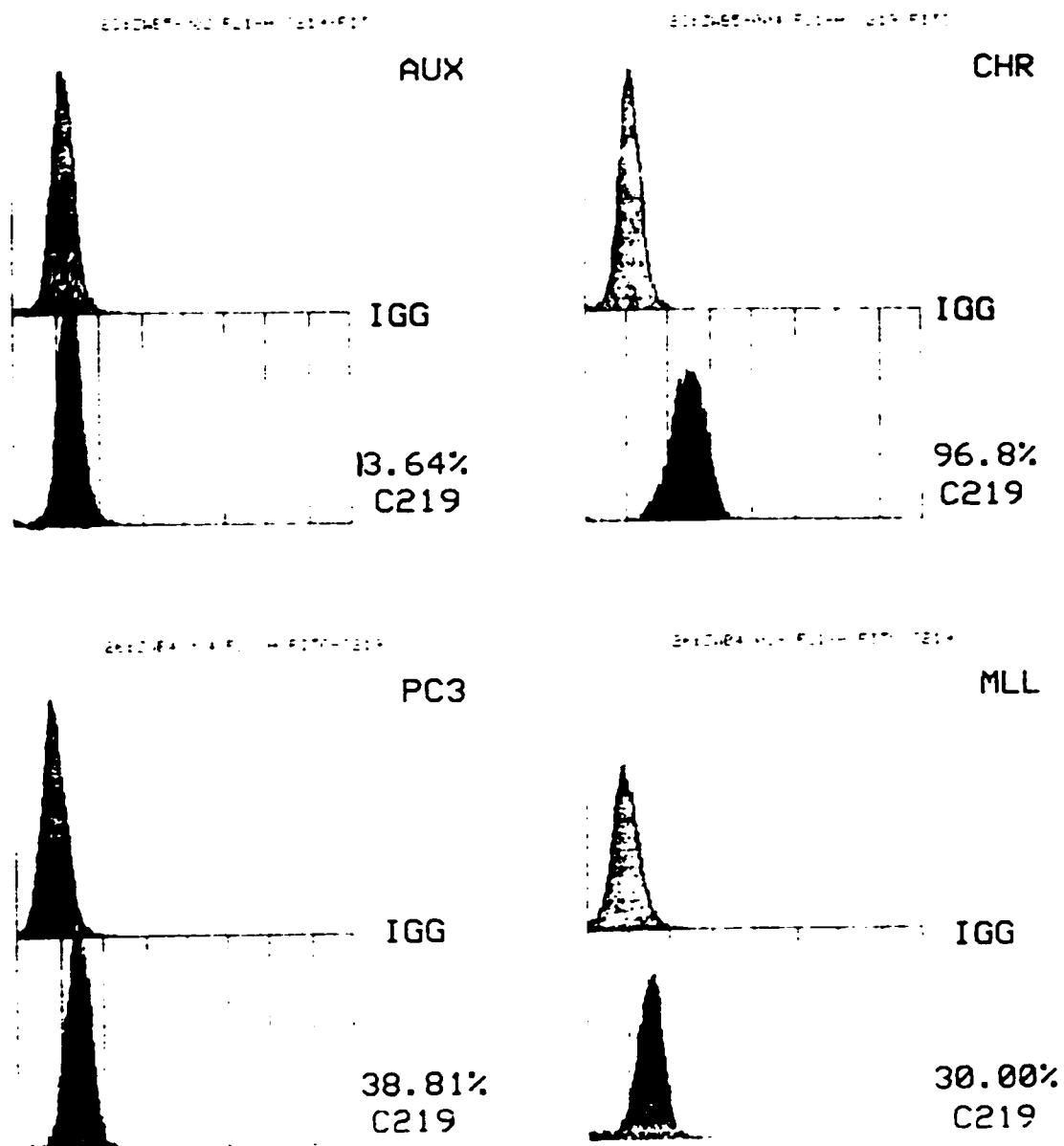
Figure 23. C219 antibody histogram data. IgG, negative control.

revealed only 13.64% binding (Figure 23) . The only human line that demonstrated higher

C-219 binding when compared to AUXB1 was PC-3 (Figure 23). Increased C219

binding was seen in the following rat lines: MAT-LyLu (Figure 23), AT2.1, AT3, and

GP9F3 while no binding was seen in AT.1 and MAT-Lu.

Table 7.   Summary of Flow Cytometry FITC Studies

Cell Line	% Bound to C219	% Bound to IgG Isotype
Controls		
CHRC5	97.75	0.95
AUXB1	13.64	1.14
Human		
TSU-1000	7.20	1.02
TSU-parent	10.74	1.19
PC-3	38.81	1.02
DU-145	0.60	1.09
Rodent		
MAT-LyLu	30.00	1.09
GP9F3	30.93	0.94
AT.1	1.58	0.93
AT2.1	38.30	1.12
AT3	55.82	1.01
MAT-Lu	7.62	0.97

**B.   Development of Doxorubicin Resistant Rat Prostate Cancer Cell
Lines**

Materials and Methods

Cell Culture

The Dunning rat prostate cancer cell lines, AT3 and MAT-LyLu (MLL) were

utilized in the present study (Isaacs et al., 1986). MDR lines (AT3B-1, AT3B-2, MLLB-1,

and MLLB-2) were developed by growing the parental cell lines in increasing

concentrations of doxorubicin (Sigma, St. Louis, MO) in RPMI 1640 media supplemented with 10% fetal bovine serum and 1% antibiotics. Doxorubicin was maintained as a 10mM stock solution in DMSO and stored in small aliquots at $-20°C$. The concentration of doxorubicin was gradually increased until the final concentration of $1\mu M$ was achieved over the course of several years. The MDR lines were maintained at $1\mu M$ doxorubicin for over one year.

Vinblastine Cytotoxicity

200,000 cells of each cell line were seeded into a T-25 culture flask. Culture media supplemented with 100nM, 500nM, and $1\mu M$ vinblastine were added to AT3B-1, AT3B-2, MLLB-1, and MLLB-2 lines, as well as the parental cell lines, and incubated for 48 hours at 37°C in 5% CO_2. All drug concentrations were done in triplicate. After 48 hours, the flasks were rinsed with 1X PBS followed by the addition of 5mLs of hypotonic solution (0.01M Hepes and 0.015 $MgCl_2$). Nuclei were released upon the addition of $200\mu L$ lysis buffer (0.13M c-ethylhexadecyldimethylammonium bromide and 3% acetic acid). Nuclei were counted using a Coulter Counter (Coulter, Miami, Fl).

Drug Efflux Studies

The drug efflux protocol used in this study has been previously discussed. Briefly, one million cells of the MDR lines and the parental cell lines were suspended in culture media containing no doxorubicin. Cells received either 2ug/mL daunomycin alone or in combination with either verapamil (20ug/mL) or cyclosporin A (2ug/mL). Cells were incubated for 30 minutes at 37°C with 5% CO_2 and analyzed using a Coulter EPICS XL cytometer (Coulter, Miami, Fl).

In vivo Rat Studies

One million cells of each MDR line, as well as the parental cell lines, were injected

subcutaneously into the flank of male Copenhagen rats (day 0). Rats received either DMSO, 0.9mg, or 1.2mg doxorubicin on days 3, 6, 9, and 12 and were sacrificed on day 14. Treatment of the rats were within the guidelines of The Guiding Principles in the Care and Use of Animals. Tumors were excised and the tumor weights recorded.

Results

MDR resistant cell lines were developed by growing the parental AT3 and MAT-LyLu cell lines in increasing concentrations of doxorubicin. The MDR lines were then maintained in $1\mu M$ doxorubicin for over one year.

AT3B-1, AT3B-2, MLLB-1, and MLLB-2, as well as the AT3 and MLL parental cell lines, were exposed to various concentrations of vinblastine for 48 hours to examine the presence of cross resistance. In Figure 24, the AT3 parental cell viability was 27%, 16.5%, and 17.4% when cells were exposed to 100nM, 500nM, and $1\mu M$ vinblastine respectively. In contrast, AT3B-1 and AT3B-2 cells were better able to withstand vinblastine treatment. Specifically, AT3B-1 cell viability was 100%, 73%, and 64% when cells were treated with 100nM, 500nM, and $1\mu M$ vinblastine respectively. AT3B-2 cell viability was 97%, 57.4%, and 62% when the cells were grown in 100nM, 500nM, and $1\mu M$ vinblastine respectively. In Figure 25, MLL parental cell viability was 9.9%, 6.7%, and 6.1% in 100nM, 500nM, and $1\mu M$ vinblastine respectively while MLLB-1 viability was 87.8%, 60%, and 85% for the same concentrations. Lastly, the MLLB-2 viability was 92%, 59%, and 29% for 100nM, 500nM, and $1\mu M$ vinblastine.

Drug efflux pumping ability of the various cell lines was tested by measuring the accumulation of the fluorescent drug daunomycin in the absence or presence of the P-glycoprotein blockers verapamil and cyclosporin A (Table 8). Cells were exposed to

daunomycin alone (D) and the concentrations of drug were compared to the

autoflourescence (AF) in which the cells were not exposed to any drug (D/AF ratio). The

parental AT3 and MLL cell lines were shown to retain higher concentrations of daunomycin

when compared to their corresponding MDR cell lines. Specifically, the relative mean

fluorescent intensities of the AT3 parental line was 4.67 while AT3B-1 and AT3B-2 values

were 1.80 and 1.45 respectively. The MLL parental line had a value of 2.60 compared to

1.53 for MLLB-1 and 1.80 for MLLB-2. The AT3 parental lines, when treated with

verapamil or cyclosporin A, had a lower accumulation of daunomycin compared to the AT3

MDR lines. Specifically, verapamil and cyclosporin A caused a very similar level of

accumulation of daunomycin in AT3B-1 cells with D&V/D and D&C/D ratios of 2.16 and

2.13 respectively. AT3B-2 cells also demonstrated an even higher accumulation of

daunomycin with verapamil or cyclosporin A with D&V/D and D&C/D ratios of 2.50 and

2.79 respectively. MLLB-1 and MLLB-2 demonstrated lower accumulations of

daunomycin compared to the MLL parental line. Specifically, MLLB-1 had accumulations

of 1.87 and 2.11, while MLLB-2 ratios were 1.45 and 1.27 when treated with verapamil

(D&V/D ratio) and cyclosporin A (D&C/D ratio) respectively (Table 8).

Table 8. Drug Efflux Data

Cell Line	AF[1]	D[2]	D/AF[3]	D&V[4]	D&V/D[5]	D&C[6]	D&C/D[7]
AT3 Parent	0.48	2.24	4.67	3.47	1.55	3.83	1.71
AT3 B-1	0.64	1.15	1.80	2.48	2.16	2.45	2.13
AT3 B-2	0.58	0.84	1.45	2.10	2.50	2.34	2.79
MLL Parent	0.50	1.30	2.60	3.12	2.40	4.04	3.11
MLL B-1	1.18	1.81	1.53	3.38	1.87	3.82	2.11
MLL B-2	0.92	1.66	1.80	2.40	1.45	2.11	1.27

[1]AF = Autoflourescence

[2]D = Daunomycin

[3]D/AF = Daunomycin /Autoflourescence

[4]D&V = Daunomycin & Verapamil

[5]D&V/D = Daunomycin&Verapamil /Daunomycin

[6]D&C = Daunomycin & Cyclosporin A

[7]D&C/D = Daunomycin & Cyclosporin A/Daunomycin
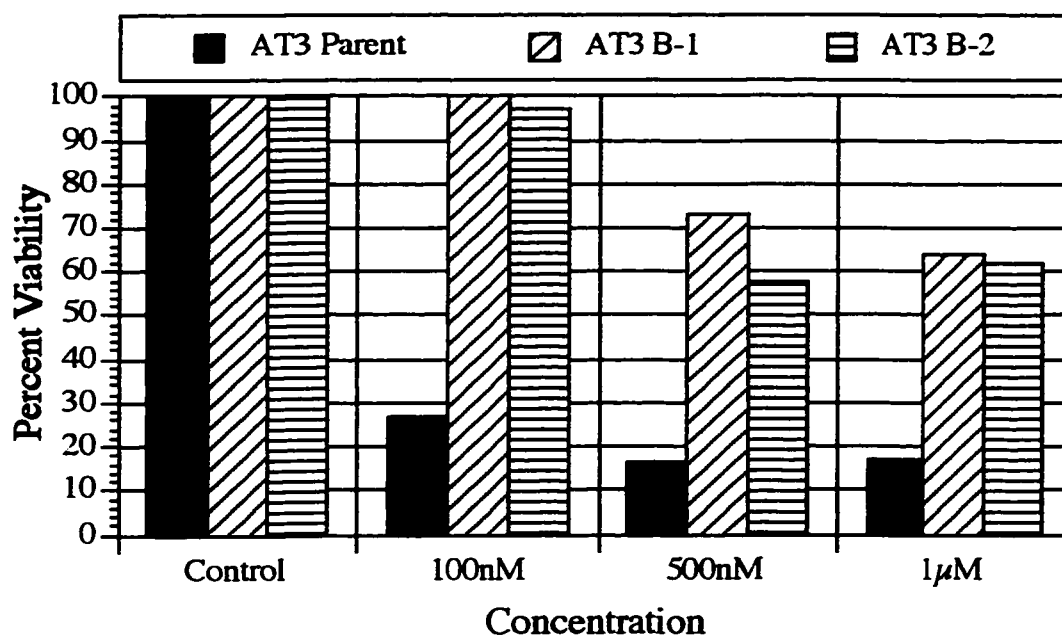
Figure 24.   AT3 Vinblastine Cytotoxicity Data
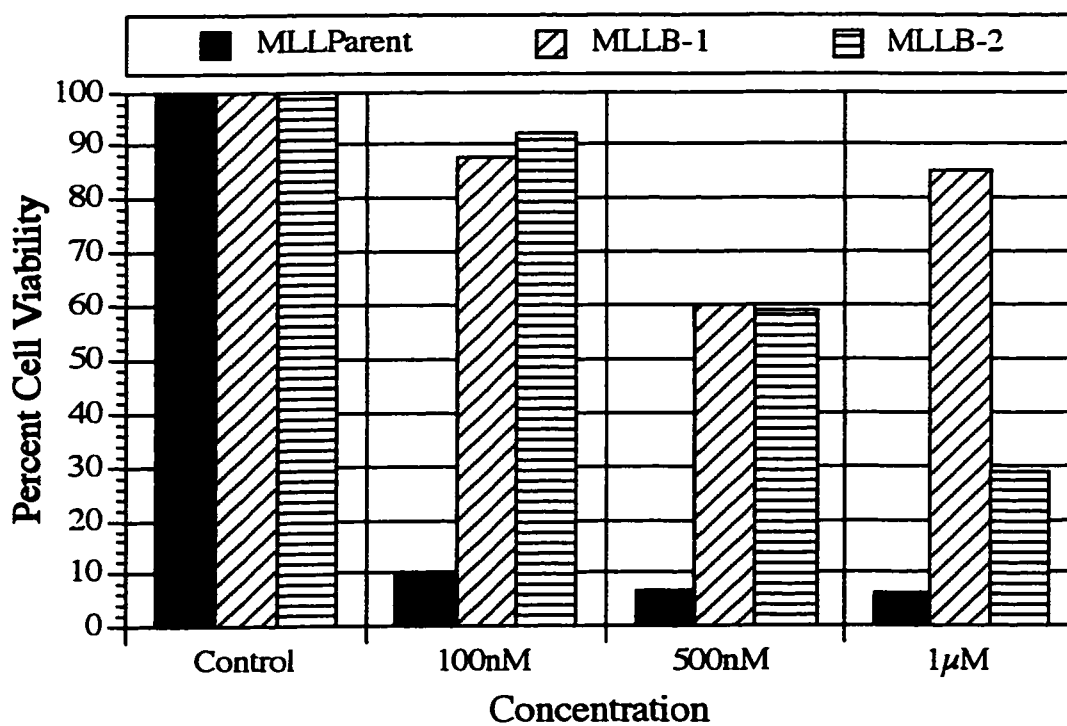
Figure 25.   MAT-LyLu Vinblastine Cytotoxicity Data.

To investigate the *in vivo* sensitivity of these cell lines, male Copenhagen rats were

injected with one million cells of AT3 parent, AT3B-1, or AT3B-2 on day 0. Rats received

either 0.9mg or 1.2mg doxorubicin or DMSO intrapertineally on days 3, 6, 9, and 12. On

day 14, the rats were sacrificed and tumor weights were measured (Figure 26). The

tumors produced by the AT3 parent cells showed a decrease in tumor weights of 63.3%

and 76% by treatment with 0.9mg and 1.2mg doxorubicin respectively. Tumors produced

by AT3B-1 cells were decreased by 53.7% and 63.6% by 0.9mg or 1.2mg doxorubicin

respectively while AT3B-2 tumors decreased in weight by 53% and 48% with 0.9mg and

1.2mg doxorubicin treatment respectively.

Discussion

One of the possible reasons of chemotherapeutic drug failure is the multidrug

resistance phenotype. In such instances, the cells appear to be immune to the toxic actions

of the chemotherapeutic agents. The P-glycoprotein pump has come under a great deal of

study as a possible cause of this phenotype, pumping the cytotoxic agent out of the cell
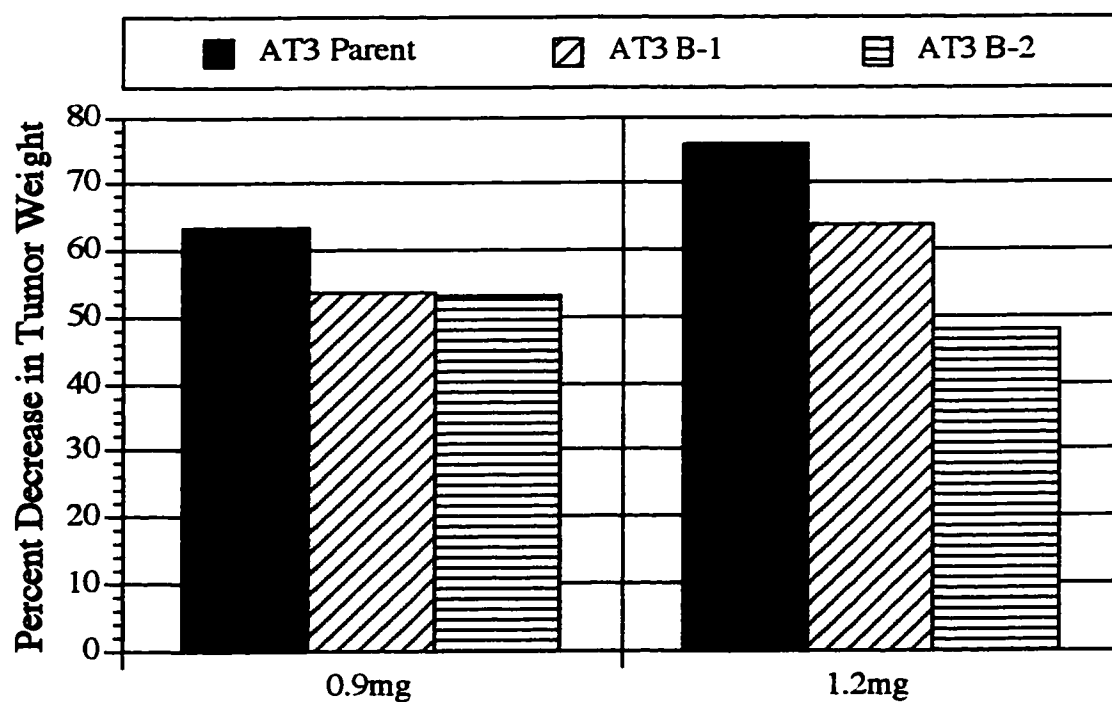
Figure 26.   *In vivo* Doxorubicin Rat Data

before any damage is able to occur. The goal of the first part of this study was to

investigate the P-glycoprotein expression and its mediated efflux function in human and the

Dunning rat prostate cell lines and to speculate if P-glycoprotein plays a role in drug

resistance in various prostate cancer cell lines.

The first series of experiments were the drug efflux studies which examined the

ability of cells to excrete DNR through a P-glycoprotein mediated efflux which could be

blocked by various modulators. Drug efflux analysis using flow cytometry was developed

by Krishan (Krishan, 1990). Cell lines that were able to pump out the drug were shown to

have a increase in fluorescence in the presence of a drug modulator. The drug modulators

used were verapamil, persantine, and compazine all of which have been demonstrated to

overcome the MDR phenotype (Begleiter et al., 1988; Chao et al., 1988). The Dunning rat

cell lines that had this ability were MAT-LyLu, MAT-Lu, AT.1, AT2.1, AT3, and GP9F3

while the positive human lines were PC-3 and TSU-1000, demonstrating the ability of

these prostate cancer cell lines to pump drug out. The two human lines (DU-145 and

TSU-parent) and the P388S cell lines did not show any drug efflux capability. Correlation

between P-glycoprotein/mdr-1 expression and drug efflux has been so far controversial.

Nooter et al. reported that increased DNR accumulation by cyclosporin A was correlated

with mdr-1 expression in acute myelogenous leukemia (Nooter et al., 1990). On the

contrary, lack of correlation has been reported in not only cell lines (Ramachandran et al.,

1993), but also clinical samples (Marie et al., 1993).

P-glycoprotein expression was then investigated by two methods,

immunocytochemistry and flow cytometry. The use of monoclonal antibodies to screen for

P-glycoprotein came about due to the work of Katner et al. who produced several P-

glycoprotein specific monoclonal antibodies (Katner et al., 1985). One of these antibodies,

C219, recognizes a conservative intracellular epitope of P-glycoprotein. C219 is one of the

most frequently used antibodies for immunohistochemical detection of P-glycoprotein

expression. C219 is able to recognize P-glycoproteins from various species including

human and rat which were used in this study. Other antibodies used in other studies

include MRK16, JSB-1, HYB241, and HYB612. JSB-1, like C219, detects am intracellular epitope while MRK16 detects an extracellular epitope. HYB241 and HYB612 detect a conformation dependent extracellular epitope (Tiirikainen et al., 1991). The C219 antibody has come under some scrutiny due to the fact that it has been reported to cross react with some myosin isoforms (Thiebaut et al., 1989). Immunocytochemical analyses demonstrated that the human lines PC-3 and TSU-1000 showed higher intensities of staining when compared to a negative control (AUXB1) while DU-145 and TSU-parent did not. In contrast, all of the Dunning rat lines showed higher intensities of staining. These data correlated well to the drug efflux data reported earlier, except for the rat line MAT-LyLu. In this case, drug efflux was demonstrated for the MAT-Lu cell line while immunocytochemical staining was negative for P-glycoprotein. Possible explanations include difficulty in immunocytochemical staining of P-glycoprotein in these cells or the accumulation of DNR within the cell by some other mechanisms. The MAT-Lu studies were repeated yielding similar results.

Lastly, the C219 antibody binding experiments analyzed by flow cytometry revealed some unexpected results. The PC-3 human cell line demonstrated an increased C219 binding when compared to the AUXB1 control, while TSU-parent, TSU-1000, and DU-145 did not. The TSU-1000 data was in contrast to the drug efflux and immunocytochemical data. The majority of the rat lines revealed a high percentage of C219 binding, while AT.1 and MAT-Lu did not. Once again, the C219 flow cytometry data for the AT.1 and MAT-Lu rat cell lines did not agree with the previous studies. The discrepancies of the C219 binding in the immunocytochemical and flow cytometry analyses are still unknown. Different fixing procedures were first thought to be the problem, although this was eventually ruled out. These studies were repeated with similar results.

In conclusion, most of the cell lines studied did show increased expression of the P-glycoprotein pump. This multidrug resistance phenotype may be one possible reason why cancer chemotherapy has traditionally failed in the past.

The last part of the study involved the development of doxorubicin resistant rat prostate cell lines. By developing these lines, chemotherapeutic studies using these resistant clones could yield more information regarding the MDR phenomenon.

The Dunning cell lines, which include AT3 and MAT-LyLu (MLL), are a well characterized and commonly used model system for prostate cancer. We have previously demonstrated that the Dunning model can be used to predict activity of chemotherapeutic drugs in men with hormone refractory prostate cancer (Pienta and Lehr, 1993). To date, there are currently no human model systems for prostate cancer available. Therefore, the rat Dunning cell lines were utilized in these studies.

Understanding the mechanisms of multidrug resistance is crucial for improving upon the current chemotherapeutic therapies. Specifically, cells with the MDR phenotype are resistant to several structurally unrelated compounds which could lead to patient treatment failure. In order to better understand this process, MDR lines of the rat prostate cancer cell lines AT3 and MLL were developed by growing the parental cell lines in increasing concentrations of doxorubicin. The MDR cell lines were established and maintained in $1\mu M$ doxorubicin, followed by examination for the presence of the P-glycoprotein pump.

AT3B-1, AT3B-2, MLLB-1, and MLLB-2 cells, along with the parental cell lines, were exposed to varying concentrations of vinblastine. After 48 hours, it was found that all of the MDR clones were able to survive vinblastine treatment at a significantly higher level when compared to the AT3 and MLL parental controls. These data appear to be consistent with a MDR phenomenon in the AT3B-1, AT3B-2, MLLB-1, and MLLB-2 cells in which cells become resistant to more than one compound. In any case, it is clear that the MDR clones are better equipped to handle vinblastine treatment when compared to their parental counterparts.

In order to further determine the presence of the P-glycoprotein pump within the MDR lines, functional drug efflux studies were done. Cells containing P-glycoprotein are

able to withstand exposure to drug treatment by pumping the drug out of the cell before any damage can be sustained. Thus, drug efflux studies using the fluorescent drug daunomycin were used to examine the pumping capability of AT3B-1, AT3B-2, MLLB-1, and MLLB-2 cells compared to their corresponding parental controls. The AT3 and MLL parental cell lines exhibited a higher accumulation of daunomycin (D/AF ratio) when compared to AT3B-1, AT3B-2, MLLB-1, and MLLB-2 cells (Table 8). Verapamil and cyclosporin A, which are blockers of the P-glycoprotein pump, were added to the reactions. If the P-glycoprotein pump becomes blocked by the addition of these compounds, then a corresponding increase in cellular accumulation of daunomycin should be observed. When AT3B-1 and AT3B-2 cells were given daunomycin and verapamil, an increase in the accumulation of daunomycin (D&V/D ratio) was observed suggesting that the P-glycoprotein pump activity had been blocked. In contrast, the MLLB-1 and MLLB-2 cells, upon receiving verapamil or cyclosporin A, showed no such accumulation of daunomycin within the cells. Several possible explanations could account for the MLLB-1 and MLLB-2 drug efflux data. First, it is possible that the verapamil and cyclosporin A blockers used were not able to completely abolish the P-glycoprotein pumping ability in the MLL MDR lines. Second, other MDR mechanisms could be responsible for the MDR phenotype. For example, increased glutathione S-transferase (GST) activity has also been implicated in producing the MDR phenotype (Sridar et al., 1993; Krishan and Sauerteig, 1991; Katner et al., 1985). Increased GST could account for the MDR phenotype in cells that may not have abnormally high levels of P-glycoprotein expression.

In vivo studies involved the injection of one million cells of the MDR lines, as well as the parental cell lines, into male Copenhagen rats followed by treatment of 0.9mg or 1.2mg doxorubicin, or DMSO. The tumors produced by AT3B-1 and AT3B-2 cells were larger when compared to the AT3 parental cell lines after 0.9mg or 1.2mg doxorubicin treatment. Suprisingly, when the MLLB-1 and MLLB-2 cells were injected subcutaneously into the rats, no tumor growth was observed. Repeated injections of the MLL MDR clones into different animals produced the same results. By unknown

mechanisms, the drug exposure of the parental cells altered their ability to produce tumors.

In summary, doxorubicin induced MDR clones of parental AT3 and MLL cell lines were developed. Increased P-glycoprotein expression does seem to account for part of the MDR phenotype of these cells.

References

Abulafia R, Ben-Zeev A, Hay N, Aloni Y. (1984): Control of late simian virus 40 transcription by the attenuation mechanism and transcriptionaly active ternary complexes are associated with the nuclear matrix. J Mol Biol. 172: 467-487.

Bagshawe KD. (1965): Clinical application of hCG. Adv Exp Med Biol. 76: 313-324.

Barrack ER, Coffey DS. (1980): The specific binding of estrogens and androgens to the nuclear matrix of sex hormone responsive tissues. JBC. 255: 7265-7275.

Barrack ER. (1983): The nuclear matrix of the prostate contains acceptor sites for androgen receptors. Endocrinology. 113: 430-432.

Begleiter A, Leith MK, McClarty G, Beeken S, Goldberg GJ, Wright JA. (1988): Characterization of L5178Y murine lymphoblasts resistant to quinone antitumor agents. Cancer Res. 48: 1727-1735.

Ben-Zeev A. (1980): Protein synthesis requires cell-surface contact while nuclear events respond to cell shape in anchorage-dependent fibroblasts. Cell 21: 365-372.

Ben-Zeev A, Aloni Y. (1983): Processing of SV40 RNA is associated with the nuclear matrix and is not followed by the accumulation of low-molecular-weight RNA products. Virology. 125: 475-479.

Berezney R, Coffey DS. (1974): Identification of a nuclear protein matrix. Biochem Biophys Res Comm. 60: 1410-1417.

Berezney R, Coffey DS. (1975): Nuclear protein matrix: Association with newly synthesized DNA. Science. 189: 291-292.

Berezney R, Coffey DS. (1977): Nuclear matrix: isolation and characterization of a framework structure from rat liver nuclei. J Cell Biol. 73: 616-637.

Berezney R, Basler J, Hughes BB, Kaplan SC. (1979): Isolation and characterization of the nuclear matrix from Zajdela ascites hepatoma cells. Cancer Res. 39: 3031-3039.

Berezney R, Buchholtz, LA. (1981): Dynamic association of replicating DNA fragments with the nuclear matrix of regenerating liver. Exp Cell Res. 132: 1-13 .

Bidwell JP, Van Wijen AJ, Fey EG, Dworetzky S, Penman S, Stein JL, Lian JB, Stein GS. (1993): Osteocalcin gene promoter-binding factors are tissue-specific nuclear matrix components. PNAS USA. 90: 3162-3166.

Bissell MJ, Hall MG, Parry G. (1982): How does the ECM direct gene expression? J Theor. Biol. 99: 31-68.

Bromley SE, Camara C, Genduso RA. (1996): Detection of elevated levels of a nuclear matrix protein in serum of colorectal cancer patients. Proc Am Assoc Cancer Res. (#3146). Wash. D.C.

Buckler-White A, Humphrey GW, Pigiet J. (1980): Association of polyoma T antigen and DNA with the nuclear matrix from lytically infected 376 cells. Cell. 22: 37-46

Casiano CA, Humbel RL, Peebles C, Covini G, Tan EM. (1995): Autoimmunity to the

cell-cycle dependent centromere protein p330d/CENP-F in disorders associated with cell proliferation ratio. J. Autoimmun. 8: 575-586.

Chao CCK, Huang Y-T, Ma CM, Chou WY, Lin-Chao S. (1991): Overexpression of glutathione S-transferase and elevation of thiol pools in a multidrug-resistant human colon cancer cell line. Mol Pharm. 41: 69-75.

Chew EC, Liew CT, Wu S, Yang L, Yam HF, Wang SW, Lee SM, Wang ZH, Chew-Cheng SB. (1997): Electrophoretic analysis of nuclear matrix proteins in human hepatocellular carcinoma. Anticancer Res. 17: 3581-3585.

Chin JE, Soffir R, Noonan KE. (1989): Structure and expression of the human mdr (p-glycoprotein) gene family. Mol Cell Biol. 9: 3808-3820.

Ciejek EM, Nordstrom JL, Tsai MJ, O'Malley BW. (1982): Ribonucleic acid precursors are associated with the chick oviduct nuclear matrix. Biochemistry. 21: 4945-4953.

Ciejek EM, Tsai MJ, O'Malley BW. (1983): Actively transcribed genes are associated with the nuclear matrix. Nature. 306: 607-609.

Compton DA, Szilak I, Cleveland DW. (1992): Primary structure of NuMA, an intranuclear protein that defines a novel pathway for segregation of proteins at mitosis. J Cell Bio. 116: 1395-1408.

Cook PR, Lang J, Hayday A, Lania L, Fried M, Chiswell DJ, Wyke JA. (1982): Active viral genes in transformed cells lie close to the nuclear cage. EMBO J. 1: 447-452.

Cunha GR, Reese BA, Sekkingstad MN. (1980): Induction of a nuclear androgen-binding sites in epithelium of the embryonic urinary bladder by mesenchyme of the urogential sinus of embryonic mice. Endocrinology. 107: 1767-1770.

Deffie AM, Alam T, Seneviratne C, Beenken SW, Batra JK, Shea TC, Henner WD, Goldenberg GJ. (1988): Multifactorial resistance to adriamycin: relationship of DNA repair, glutathione transferase activity, drug efflux, and P-glycoprotein in cloned cell lines of adriamycin-sensitive and -resistant P388 leukemia. Cancer Res. 48: 3595-3602.

Dickinson LA, Joh T, Kohwi Y, Kohwi-Shigematsu T. (1992): A tissue-specific MAR/SAR DNA-binding protein with unusual binding site recognition. Cell. 70: 631-645.

Donat TL, Sakr W, Lehr JE, Pienta KJ. (1996): Nuclear matrix protein alteration in intermediate biomarkers in squamous cell carcinoma of the head and neck. Otolaryn-Head Neck Surg. 114: 387-393.

Durfee T, Mancini MA, Jones D, Elledge SJ, Lew WH. (1994): The amino-terminal region of the retinoblastoma gene product binds a novel nuclear matrix protein that co-localizes to centers for RNA processing. J Cell Bio. 127: 609-622.

Earnshaw WC, Heck MM. (1985): Localization of topoisomerase I in mitotic chromosomes. J Cell Biol. 100: 1716-1725.

Fernandez-Patron C, Castellanos-Serra L, Rodriguez P. (1992): Reverse staining of sodium dodecyl sulfate polyacrylamide gels by imidazole-zinc salts: sensitive detection of unmodified proteins. Biotech. 12: 564-573.

Feuerstein N, Mond JJ. (1987): "Numatrin," a nuclear matrix protein associated with

induction of proliferation in B lymphocytes. JBC. 262: 11389-11397.

Feuerstein N, Chan PK, Mond JJ. (1988): Identification of Numatrin, the nuclear matrix protein associated with induction of mitogenesis, as the nucleolar protein B23. JBC. 263: 10608-10612.

Feuerstein N, Mond JJ, Kinchington PR, Hickey R, Lindsberg MLK, Hay I, Ruyechan WT. (1990): Evidence for DNA binding activity of numatrin (B23), a cell cycle-regulated nuclear matrix protein. Biochem Biophys Acta 1087: 127-136.

Fraumeni J, Hoover R, Devesa S, Kinlen L. (1993): Epidemiology of cancer. In Cancer: principles and practice of oncology. Devita, Hellman, Rosenburg (Eds): Philadelphia: JB Lippincott Co.

Fey EG, Wan KM, Penman SP (1984): Epithelial cytoskeletal framework and nuclear matrix-intermediate scaffold: three-dimensional organization and protein composition. J Cell Biol 98: 1973-1984.

Fey EG, Penman S. (1988): Nuclear matrix proteins reflect cell type of origin in cultured human cells. PNAS USA. 85: 121-125.

Fojo AT, Veda K, Slaman DJ. (1987): Expression of a multidrug-resistance gene in human tumors and tissues. PNAS USA. 84: 265-269.

Folkman J, Moscona A. (1978): Role of cell shape in growth control. Nature 273: 345-349.

Getzenberg RH, Pienta KJ, Coffey DS (1990): The tissue matrix: cell dynamics and hormone action. Endocrine Rev. 11: 399-417.

Getzenberg RH, Pienta KJ, Huang EYW, Murphy BC, Coffey DS. (1991A): Modifications of the intermediate filament and nuclear matrix networks by the extracellular matrix. Biochem Biophys Res Comm. 179: 340-344.

Getzenberg RH, Pienta KJ, Huang, E.Y.W., Coffey, D.S. (1991B): Identification of nuclear matrix proteins in the cancer and normal rat prostate. Cancer Res. 51: 6514-6520., 1991.

Getzenberg RH, Konety BR, Oeler TA, Quigley MM, Hakam A, Becich MJ, Bahnson RR. (1996): Bladder cancer associated nuclear matrix proteins. Cancer Res. 56: 1690-1694.

Gordon JN, Shu WP, Schlussel RN, Droller MJ, Liu BCS. (1993): Altered extracellular matrices influence cellular processes and nuclear matrix organizations of overlying human bladder urothelial cells. Cancer Res. 53: 4971-4977.

Gospodarowicz D, Greenburg G, Birdwell CR. (1978): Determination of cellular shape by the extracellular matrix and its correlation with the control of cellular growth. Cancer Res. 38: 4155-4171.

Gubler U, Hoffman BJ. (1986): A simple and very efficient method for generating cDNA libraries. Gene. 25: 263-269.

Hakes DJ, Berezney R. (1991): DNA binding properties of the nuclear matrix and individual nuclear matrix proteins. JBC. 266:11131-11140.

Hancock R, Boulikas T. (1982): Functional organization in the nucleus. Int. Rev. Cytology. 79: 165-214.

Hansen LK, Mooney DJ, Vacanti JP, Ingber DE. (1994): Integrin binding and cell spreading on extracellular matrix act at different points in the cell cycle to promote hepatocyte growth. Mol Biol Cell. 5: 967-975.

Hay ED. (1977): Cell matrix interaction in embryonic induction. In International Cell Biology. (Brinkley BR, Porter KR eds.) Rockfeller University Press, New York: 50-57.

Henry SM, Hodge LD. (1983): Nuclear matrix: a cell-cycle-dependent site of increased intranuclear protein phosphorylation. Eur J Biochem. 133: 23-29.

Hentzen PC, Rho JH, Bekhor I. (1984): Nuclear matrix DNA from chicken erythrocytes contains B-globin gene sequences. PNAS USA. 81: 304-307.

Herlan G, Eckert WA, Kaffenberger W, Wunderlich F. (1979): Isolation and characterization of a RNA-containing nuclear matrix from *Tetrahymena* macronuclei. Biochemistry. 18: 1782-1788.

Herman R, Weymouth L, Penman S. (1978): Heterogeneous nuclear RNA-protein fibers in chromatin-depleted nuclei. J Cell Biol. 78: 663-674.

Ingber DE. (1980): Fibronectin controls capillary endothelial cell growth by modulating cell shape. PNAS USA. 87: 3579-3583.

Ingber DE, Madri JA, Folkman J. (1987): Endothelial growth factors and extracellular matrix regulate DNA synthesis through modulation of cell and nuclear expansion. In vitro Cell Devel Bio. 23: 387-394

Isaacs JT, Barrack ER, Isaacs WB, Coffey DS. (1981): The relationship of cellular structure and function: the tissue matrix system. Prog Clin Biol Res. 75A: 1-24.

Isaacs JT, Isaacs WB, Feitz WFJ, Scheres J. (1986): Establishment and characterization of seven Dunning rat prostatic cancer cell lines and their use in developing methods for predicting metastatic abilities of prostatic cancers. Prostate. 9: 261-281.

Jackson DA, McCready SJ, Cook PR. (1981): RNA is synthesized at the nuclear cage. Nature. 292: 552-555.

Jost JP, Seldran M. (1984): Association of transcriptionally active vitellogenin II gene with the nuclear matrix of chicken liver. EMBO J. 3: 2005-2008.

Juliano RL, Ling V. (1976): A surface glycoprotein modulating drug permeability in Chinese hamster ovary cell mutants. Biophys. Acta. 455: 152-162.

Kahn SN. (1991): Dear Dr. Bence Jones. Clin Chem. 37: 1557-1558.

Katner N, Evernden-Porelle D, Bradely G, Ling V. (1985): Detection of P-glycoprotein in multidrug resistant cell lines by monoclonal antibodies. Nature. 316: 820-823.

Keesee SK, Meneghini MD, Szaro RP, Wu YJ. (1994): Nuclear matrix proteins in human colon cancer. PNAS USA. 91: 1913-1916.

Khanuja PS, Lehr JE, Soule HD, Gehani S K, Noto AC, Choudhury S, Chen R, Pienta

KJ. (1993): Nuclear matrix proteins in normal and breast cancer cells. Cancer Res. 53: 3394-3398.

Kim MK, Lesoon-Wood LA, Weintraub BD, Chung JM. (1996): A soluble transcription factor, Oct-1, is also found in the insoluble nuclear matrix and possesses silencing activity in its alanine-rich domain. Mol. Cell Biol. 6: 4366-4377.

Korosec T, Gerner C, Sauermann G. (1997): Common nuclear matrix proteins in rat tissues. Electrophoresis. 18: 2109-2115.

Krishan A. (1990): Rapid determination of cellular resistance-related drug efflux in tumor cells. Meth Cell Bio. 33: 491-500.

Krishan A, Sauerteig A. (1991): Flow cytometric monitoring of cellular resistance to cancer chemotherapy. In "Flow Cytometry: Principle and Clinical Application." Bauer KD, Duque RE, Shankey TV (eds): Williams and Wilkins. 1991.

Krishan A. (1990): Rapid determination of cellular resistance-related drug efflux in tumor cells. Meth Cell Bio. 33: 491-496.

Kumara-Siri MH, Shapiro LE, Surks MI. (1986): Association of the 3, 5, 3'-triiodo-L-thyronine nuclear receptor with the nuclear matrix of cultured growth hormone-producing rat pituitary tumor cells (GC cells). JBC. 271: 2844-2852.

Landberg G, Erlanson M, Roos G, Tan EM, Casiano CA. (1996): Nuclear autoantigen p330d/CENP-F: a marker for cell proliferation in human malignancies. Cytometry. 25: 90-98.

Livingston RB, Bartolocci A, Becker JA. (1988): The management of clinically localized prostate cancer. JAMA. 258: 2727-2730.

Long BH, Ochs RL. (1983A): Nuclear matrix, hnRNA, and snRNA in Friend erythroleukemia nuclei depleted of chromatin by low ionic strength EDTA. Biol Cell 48: 89-98.

Long BH, Schrier WH. (1983B): Isolation from Friend erythroleukemia cells of an RNase-sensitive nuclear matrix fibril fraction containing hnRNA and snRNA. Biol Cell 48: 99-108.

Ludérus MEE, de Graaf A, Mattia E, den Balen JL, Grande MA, de Jong L, Van Driel R. (1992): Binding of matrix attachment regions to Lamin B_1. Cell 70: 949-959.

Lydersen BK, Pettijohn DE. (1980): Human-specific nuclear protein that associates with the polar region of the mitotic apparatus: distribution in a human/hamster hybrid cell. Cell. 22: 489-499.

Marie JB, Faussat-Suberville AM, Zhou D, Zittoun R. (1993): Daunorubicin uptake by leukemic cells: correlations with treatment outcome and mdr1 expression. Leukemia 7: 825-831.

Marimam ECM, Van Eekelen CAG, Reinders RJ, Berns AJM, Van Venrooij WJ. (1982): Adenoviral heterogeneous nuclear RNA is associated with the host nuclear matrix during splicing. J Mol Biol. 154: 103-119.

Mattem KA, van Goethem REM, de Jong L, van Driel R. (1997): Major internal nuclear

matrix proteins are common to different human cell types. J Cell Biochem. 65: 42-52.

Mayer DT, Gulick A. (1942): The nature of the proteins of cellular nuclei. JBC. 146: 433-440.

Merriman HL, van Wijnen AJ, Hieberts A, Bidwell JP, Fey E, Lian J, Stein J, Stein GS. (1995): The tissue-specific nuclear matrix protein, NMP-2, is a member of the AML/CBF/PEBP2/runt domain transcription factor family: interactions with the osteocalcian gene promoter. Biochem. 34: 13125-13132.

Miller TE, Huang CY, Pogo AO. (1978): Rat liver nuclei skeleton and ribonucleoprotein complexes containing hnRNA. J Cell Biol 76: 675-691.

Miller TE, Beausang LA, Winchell LF, Lidgard GP. (1992): Detection of nuclear matrix proteins in serum from cancer patients. Cancer Res. 52: 422-427.

Minna JD, Pass, H, Glatstein E, and Ihde DC.(1989): Cancer of the Lung. In: Cancer: Principles and Practice of Oncology. DeVita VT, Hellman S, and Rosenberg SA (eds.) Philadelphia, PA. J.B. Lippincott Co. 591-705.

Miyachi K, Fritzler MJ, Tan EM. (1978): Autoantibody to a nuclear antigen in proliferating cells. J Immunol. 121: 2228-2234.

Muschel R, Khoury G, Reid LM. (1986): Regulation of insulin mRNA abundance and adenylation; dependence on hormones and matrix substrate. Mol Cell Biol. 6: 337-341.

Nakayasu H, Mori H, Ueda K. (1982): Association of small nuclear RNA-protein complex with the nuclear matrix from bovine lymphocytes. Cell Struc Funct. 7: 253-262.

Nardozza TA, Quigley MM, Getzenberg RH. (1996): Association of transcription factors with the nuclear matrix J. Cell. Biochem. 61: 467-477.

Nickerson JA, Krochmalnic G, Wan KM, Penman S. (1989): Chromatin architecture and nuclear RNA. PNAS USA 86: 177-181.

Nooter K, Sonneveld P, Oostrum R, Herweijer H, Hagenbeck T, Valerio D. (1990): Overexpression of the mdr1 gene in blast cells from patients with acute myelocytic leukemia is associated with decreased anthracycline accumulation that can be restored by cyclosporin-A. Int. J Cancer 45: 263-268.

Pardoll DM, Vogelstein B, Coffey DS. (1980): A fixed site of DNA replication in eukaryotic cells. Cell. 19: 527-536.

Partin AW, Getzenberg RH, CarMichael MJ, Vindivich D, Yoo J, Epstein JI, Coffey DS. (1993): Nuclear matrix protein patterns in human benign prostatic hyperplasia and prostate cancer. Cancer Res. 53: 744-746.

Partin AW, Briggman JV, Subong ENP, Szaro R, Oreper A, Wiesbrock S, Meyer J, Coffey DS, Epstein JI. (1997): Preliminary immunohistochemical characterization of a monoclonal antibody (PRO:4-216) prepared from human prostate cancer nuclear matrix proteins. Urology 50: 800-808.

Paston I, Gottesman M (1987): Multiple-drug resistance in human cancer. N. Engl. J. Med.: 316: 1388-1393.

Philipova RN, Zhelev NZ, Todorov IT, Hadjiolov AA. (1987): Monoclonal antibodies against a nuclear matrix antigen in proliferating human cells. Biol Cell. 60: 1-8.

Pienta KJ, Coffey DS. (1991): Cellular harmonic information transfer through a tissue-tensegrity matrix system. Med. Hyp. 34: 88-95.

Pienta KJ, Murphy BC, Getzenberg RH, Coffey DS. (1991): The effect of extracellular matrix interactions on morphologic transformation in vitro. Biochem Biophys Res Comm 179: 333-339.

Pienta KJ, Murphy BC, Getzenberg RH, Coffey DS. (1993A): The tissue matrix and the regulation of gene expression in cancer cells. Adv Mol Cell Biol 7: 131-156.

Pienta KJ, Lehr JE (1993B): Inhibition of prostate cancer growth by estramustine and etoposide: Evidence for interaction at the nuclear matrix. J. Urol. 149: 1622-1625.

Pienta KJ, Lehr JE. (1993C): A common set of nuclear matrix proteins in prostate cancer cells. Prostate. 23: 61-67.

Ramachandran C, Yuan ZK, Huang XL, Krishan A. (1993): Doxorubicin resistance in human melanoma cells: MDR-1 and glutathione S-transferase pi gene expression. Biochem. Pharm. 45: 743-751, 1993.

Reddi AM, Anderson WA. (1976): Collageous bone matrix induced endochondral ossification and hemopoieses. J. Cell. Biol. 69: 557-572.

Reddy GPV, Pardee AB. (1980): Multienzyme complex for metabolic channeling in mammalian DNA replication. PNAS USA. 77: 3312-3316.

Replogle-Schwab TS, Pienta KJ, Getzenberg RH. (1996A): The utilization of nuclear matrix proteins for cancer diagnosis. In: Critical Reviews of Gene Expression (Stein GS, Stein JL, Lian TB, eds.). 6(2&3): 103-113.

Replogle-Schwab TS, Getzenberg RH, Donat TL, Pienta KJ. (1996B). Effect of organ site on nuclear matrix protein composition. J Cell. Biochem. 62: 132-141.

Riordan JR, Deuchars, Kartner N, Alon N, Trent J, Ling V. (1985): Amplification of P-glycoprotein genes in multidrug-resistant mammalian cell lines. Nature. 316: 817-819.

Robinson SI, Small D, Idzerda R, McKnight GS, Vogelstein B. (1983): The association of transcriptionally active genes with the nuclear matrix of the chick oviduct. Nuc Acids Res. 11: 5113-5130.

Romig H, Fackelmayer F, Renz A, Ramsperger U, Richter A. (1992): Characterization of SAF-A, a novel nuclear DNA binding protein from HeLa cells with high affinity for nuclear matrix/scaffold attachment DNA elements. EMBO J. 11: 3431-3440.

Saredi A, Howard L, Compton DA. (1996): NuMA assembles into an extensive filamentous structure when expressed in the cell cytoplasm. J Cell Sci. 109: 619-630.

Schwartz MK. (1987A): Biochemical and immunological diagnosis of cancer. Germ cell tumors. Tumor Biol. 8: 106-108.

Schwartz MK (1978B): Tumor markers in diagnosis and screening. In Human Tumor Markers. Ting SW, Chen JS, Schwartz MK (Eds). Amsterdam: Elsevier Science 3-16.

Sell S. (1990): Cancer markers of the 1990s. Clin Lab Med. 10: 1-37.

Shelfo SW, Soloway MS. (1997): The role of nuclear matrix protein NMP22 in the detection of persistent or recurrent transitional-cell cancer of the bladder . World J Urol 15: 107-111.

Shen D-W, Cardarelli C, Hwnag J, Cornwell M, Richert N, Ishii S, Pastan I, Gottesman MM. (1986): Multidrug drug resistant human KB carcinoma cells independently selected for high-level resistance to colchicine, adriamycin or vinblastine show changes in expression of specific proteins. JBC. 261: 7762-7768.

Smetana K, Steele, WJ, Busch H. (1963): A nuclear ribonucleoprotein network. Exp Cell Res. 31: 198-201.

Smith HC, Berezney R. (1980): DNA polymerase α is tightly bound to the nuclear matrix of actively replicating liver. Biochem Biophys Res Comm. 97: 1541-1547.

Smith HC, Harris SG, Zillman M, Berget SM. (1989): Evidence that a nuclear matrix protein participates in premessenger RNA splicing. Exp Cell Res. 182: 521-533.

Sridar M, Krishan A, Ocar A, Gamy S, Elie-Auguste M, Sauerteig A, McPhee G, Ramachandran C, Benedetto P, Garcia J. (1993): Phase 1 clinical and pharmocokinetic study of escalating doses of dipyridamole and a fixed dose of Doxorubicin. Proc. of ASCO 12: 164.

Stuurman N, van Driel R, DeJong L, Meijne AML. (1989): The protein composition of the nuclear matrix of murine P19 embroyonal carcinoma cells is differentiation-stage dependent. Exp Cell Res. 180: 460-466.

Stuurman N, Meijne AML, van der Pol AJ, deJong L, van Driel R, van Renswoude J. (1990): The nuclear matrix from cells of different origin: evidence for a common set of matrix proteins. JBC. 265: 5460-5465.

Tan EM. (1989): Antinuclear antibodies: diagnostic markers for autoimmune diseases and probes for cell biology. 44: 93-151.

Tatarinov YS. (1964): Detections of embryonic-specific globulin in the blood serum of patients with primary liver tumor. Vopr Med Khim. 10: 90-91.

Thiebaut F, Tsuruo T, Hamada H, Gottesman MM, Pastan I, Willingham MC. (1989): Immunohistochemical epitopes in the multidrug transporter protein P-170. J Histochem Cytochem. 37: 159-164.

Tiirikainen MI, Krusius M. (1991): Multidrug resistance. Ann. Med. 23: 509-590.

Tubo RA, Smith HC, Berezney R. (1985): The nuclear matrix continues DNA synthesis at in vivo replicational forks. Biochem Biophys Acta. 825: 326-334.

Ueda K, Cornwell MM, Gottesman MM (1986): The mdr1 gene, responsible for multidrug-resistance, codes for P-glycoprotein. Biochem Biophys Res Comm. 141: 956-962.

Valenzuela MS, Mueller GC, Dasgupta S. (1983): Nuclear matrix-DNA complex resulting from EcoRI digestion of HeLa nucleoids is enriched for DNA replicating forks. Nuc Acids Res. 11: 2155-2164.

Van der Velden HMU, Van Willigen G, Wetzels RHW, Wanka F. (1984): Attachment of origin of replication to the nuclear matrix and the chromosome scaffold. FEBS. 171: 13-16.

Van Eekelen CAG, Van Venrooij WJ. (1981): hnRNA and its attachment to a nuclear protein matrix. J Cell Bio. 88: 554-563.

Verheijen R, Van Venrooij W, Ramaekers F. (1988): The nuclear matrix: structure and composition. J. Cell Sci. 90: 11-36.

Verheijen R, Kuijpers HJH, Schlingemann RO, Boehmer ALM, Van Driel R, Brakenhoff GJ, Ramaekers FCS. (1989): Ki-67 detects a nuclear matrix-associated proliferation-related antigen. I. Intracellular localization during interphase. J Cell Sci. 92: 123-130.

Vogelstein B, Pardoll D, Coffey DS. (1980): Supercoiled loops and eukaryotic DNA replication. Cell. 22: 79-85.

Weidner N, Weinberg DS, Hardy SC, Hollister KA, Lidgard GP. (1991): Localization of nuclear matrix proteins (NMPs) in multiple tissue types with NM-200.4 (an antibody strongly reactive with NMPs found in breast carcinoma. Am J Path. 138: 1293-1298.

Weinstein RS, Kuszak JR, Kluskens LF, Coon JS. (1990): P-glycoproteins in pathology: the multidrug resistance gene family in humans. Hum Path. 21: 34-48.

Wen BG, Chiu JF. (1987): Monoclonal antibodies to nonhistone proteins associated with human colon cancer nuclear matrix. Int J Biochem. 19: 1-328.

Wittelsberger SC, Kleene K, Penman S. (1981): Progressive loss of shape-responsive metabolic controls in cells with increasingly transformed phenotype. Cell. 24: 859-866.

Wray W, Boulikas T, Wray V, Hancock R. (1981): Silver staining of proteins in polyacrylamide gels. Anal Biochem. 118: 197-203.

Yamazaki K, Replogle-Schwab TS, Pienta KJ. (1996). Nuclear matrix protein composition of human lung carcinoma cell lines. Oncology Reports 3: 737-741.

Yankulov KY, Hadjiolova KV, Kounev KV, Getov C, Hadjiolov AA. (1989): The use of a monoclonal antibody against a proliferating cell nuclear matrix antigen in the study of solid human tumors. Int J Cancer. 43: 800-804.

Younghusband HB. (1985): An association between replicating adenovirus DNA and the nuclear matrix of infected HeLa cells. Can J Biochem Cell Biol. 63: 654-660.

Zuber M, Heyden TS, Lajous-Petter AM. (1995): A human autoantigen recognizes nuclear matrix-associated nuclear protein localized in dot structures. Biol. Cell. 85: 77-86.

Abstract

ISOLATION AND CHARACTERIZATION OF A COMMON NUCLEAR MATRIX PROTEIN AND OTHER STUDIES

by

TRACY SUE SCHWAB

December 1998

Advisor: Dr. Kenneth J. Pienta

Major: Cancer Biology

Degree: Doctor of Philosophy

The nuclear matrix, the RNA-protein skeleton of the nucleus, is known to play functional and structural roles within the cell. My thesis investigated the roles of the nuclear matrix proteins under various circumstances. First, the rat prostate cancer cell line (MLL) was injected into various sites within the rat. Tumors were isolated and nuclear matrix proteins isolated and analyzed by two-dimensional electrophoresis. Upon comparison, distinct nuclear matrix protein differences were observed in all of the organ sites that were investigated suggesting that the extracellular matrix, as well as growth factors and hormones, may be important in directing the production of nuclear matrix proteins. Second, nuclear matrix proteins from various cell lines representing the four classes of human lung carcinoma were analyzed. Upon comparison, it was observed that there were at least two classes of nuclear matrix proteins present. The majority of the nuclear matrix proteins were common within each lung cancer category, while other nuclear matrix proteins were found to be different. These nuclear matrix protein differences may be due to the various classes of phenotypic and genotypic distinct classes of lung cancer. Lastly, several reproducible nuclear matrix proteins isolated from the human breast MCF10A cell line were characterized. Although cDNA library screening proved unsuccessful, antibodies toward one of these proteins (KP3) provided further information into the function of this protein. Western and immunocytochemical analyses provided

evidence to suggest that this protein was common and could be found in all cell lines and tissues that were analyzed. In addition, further analyses suggested that this protein could play an important role(s) in mitosis.

Multidrug resistance (MDR) was also investigated in various human and rat prostate cancer cell lines. The majority of the cell lines analyzed did express an increased MDR phenotype when compared to the MDR negative controls. Two rat prostate cell lines (MLL and AT3) where selected and grown in increasing concentrations of doxorubicin to enhance the MDR phenomenon. MLL and AT3 MDR cell lines had an increased MDR phenotype when compared to their normal counterparts.

Autobiographical Statement

TRACY SUE SCHWAB

University of Michigan, 1500 East Medical Center , 7431 CCGC, Ann Arbor, MI 48109

Phone: (734) 647-3411   Fax: (734) 647-9480   e-mail: treplog1@umich.edu

EDUCATION

May 1989	B.S.-Chemistry, Walsh College, North Canton, Ohio
August 1989–May 1992	University of Akron, Ohio
May 1992–1998	Ph.D., Wayne State University, Dept. of Cancer Biology, Detroit, MI

PUBLICATIONS

Papers

Fakih M, Yagoda A, Replogle T, Lehr JE, and Pienta KJ. Inhibition of Prostate Cancer Growth by Estramustine and Colchicine. Prostate 26: 310-315, 1995.

Naik H, Lehr J, Pilat MJ, Donat T, Yamazaki K, Replogle T, Raz A, and Pienta KJ. Inhibition of Spontaneous Metastasis in a Rat Prostate Cancer Model by Oral Administration of Modified   Citrus Pectin. Journal of the National Cancer Institute 87: 384-353, 1995.

Pienta KJ, Replogle T, and Lehr JE. Inhibition of Prostate Cancer Growth by Vinblastine and Tamoxifen. Prostate 26(5): 270-274, 1995.

Replogle-Schwab TS, Getzenberg RH, Donat TL, and Pienta KJ. The Effect of Organ Site on Nuclear Matrix Protein Composition. Journal of Cellular Biochemistry. 62: 132-141, 1996.

Yamazaki K, Replogle-Schwab TS, and Pienta KJ. Nuclear Matrix Protein Composition of Human Lung Carcinoma Cell Lines. Oncology Reports. Vol. 3: 737-741, 1996.

Replogle-Schwab TS, Schwab ED, and Pienta KJ. Development of Doxorubicin Resistant Rat Prostate Cancer Cell Lines. Anticancer Research Vol. 12: 4535-4538, 1997.

Book Chapters

Replogle TS, and Pienta KJ. The Role of the Nuclear Matrix in Breast Cancer. 1996. In: Mammary Tumor Cell Cycle, Differentiation, and Metastasis. R.B. Dickson and M. E. Lippman Eds. Kluwer Academic Publishers, Norwell, MA, pg. 127-140.

Replogle-Schwab TS, Pienta KJ, and Getzenberg RH. The Utilization of Nuclear Matrix Proteins for Cancer Diagnosis. In: Critical Reviews in Eukaryotic Gene Expression. Eds: Stein GS, Stein JL, and Lian JB. 6(2&3): 103-113, 1996.

Abstracts

Replogle-Schwab TS, Getzenberg RH, Donat TL, and Pienta KJ. The Effect of Organ Site on Nuclear Matrix Protein Composition. American Association for Cancer Research. April 20-24, 1996. Abstract #3744.

Replogle-Schwab TS, Schwab ED, and Pienta KJ. Development of Doxorubicin Resistant Rat Prostate Cancer Cell Lines. American Association for Cancer Research. April 12-16, 1997. Abstract #2608.

Replogle-Schwab TS, Quigley MM, and Pienta KJ. Identification and Characterization of Nuclear Matrix Proteins (NMPs) Present in Both Breast Cancer Tissue and MCF10 Cell Lines. March 28-April 1, 1998. Abstract #2407.

Awards

Young Investigator Award September 10, 1994 Meeting of the American Cancer Society. University of Michigan, Ann Arbor, MI.